

***Final Project Report
Coupled Biogeochemical Process Evaluation
for Conceptualizing Trichloroethylene
Co-Metabolism: Co-Metabolic Enzyme
Activity Probes and Modeling Co-Metabolism
and Attenuation***

Prepared for:
U.S. Department of Energy



Prepared by:
North Wind, Inc.



February 2010

**Final Project Report
Coupled Biogeochemical Process Evaluation
for Conceptualizing Trichloroethylene Co-Metabolism:
Co-Metabolic Enzyme Activity Probes and Modeling
Co-Metabolism and Attenuation**

**Robert C. Starr, North Wind, Inc.
Brennon R. Orr, North Wind, Inc.
M. Hope Lee, Idaho National Laboratory
Mark Delwiche, Idaho National Laboratory**

February 2010

**Environmental Remediation Science Program
Award Number DE-FG02-06ER64199**

EXECUTIVE SUMMARY

Trichloroethene (TCE) (also known as trichloroethylene) is a common contaminant in groundwater beneath both government and privately-owned facilities. Contributing factors to TCE being a common contaminant include that it was widely used as a solvent or cleaning agent, and that it was released to the subsurface via product usage, waste disposal, and leaks and spills. TCE is regulated in drinking water at a concentration of 5 µg/L, and therefore a small mass of TCE released to the subsurface has the potential to contaminate large volumes of water. The physical and chemical characteristics of TCE allow it to migrate quickly in most subsurface environments, and thus large plumes of contaminated groundwater can form from a single release. The migration and persistence of TCE in groundwater can be limited by biodegradation, in which native soil microorganisms convert TCE into other products. Ideally, the biodegradation products are less hazardous than the initial compounds. TCE can be biodegraded via two different processes that operate under anaerobic or aerobic conditions. Under anaerobic conditions, TCE is reduced as chlorine atoms are sequentially removed from the molecule and replaced by hydrogen atoms; this process is known as anaerobic reductive dechlorination (ARD). The chlorinated intermediate products are themselves hazardous compounds, but the non-chlorinated end products are non-hazardous. ARD is widely recognized as being an important mechanism that contributes to natural or enhanced attenuation of TCE in anaerobic groundwater environments. What is less well recognized is that TCE can also be biodegraded by native microorganisms under aerobic conditions (i.e., in groundwater) that contain appreciable concentrations of dissolved oxygen. Under aerobic conditions, TCE can be oxidized to non-hazardous conditions by enzymes that microorganisms produce to perform some other process, such as oxidizing other organic carbon to obtain energy. This fortuitous reaction with an enzyme synthesized for a different purpose, without benefiting the organism that synthesized the enzyme, is known as cometabolism. Aerobic cometabolism of TCE is the focus of this research.

Earlier studies have shown that TCE is commonly attenuated in aerobic groundwater at rates relevant to environmental regulatory timeframes, and that cometabolic degradation is an operative mechanism in some aerobic, TCE-contaminated groundwater. This suggests that cometabolic degradation may be an environmentally significant mechanism and that further evaluation of TCE biodegradation in aerobic groundwater is warranted. In particular, development of methods to demonstrate that cometabolic degradation occurs and that provide a basis for estimating the in situ degradation rate. Enzyme activity probe (EAP) techniques have been developed to demonstrate that the cometabolic process does occur and to identify the responsible enzymes, and hence the class of substrate utilized by the microorganisms. An EAP is a chemical that reacts with a particular targeted enzyme; it is non-fluorescent when not bound to an enzyme and fluorescent when bound to the targeted enzyme. Hence, the appearance of fluorescence in a sample of bacteria collected from an aquifer indicates that the targeted enzyme is present and active in those bacteria, which then indicates that reactions catalyzed by those enzymes are occurring in the aquifer. EAPs have been developed for several enzymes that cometabolize TCE. In this study, EAPs were used to assay several TCE plumes in aerobic groundwater to evaluate if TCE is being cometabolized. Sites investigated include the Idaho National Laboratory (INL) Test Area North (TAN) TCE plume, plumes at the Savannah River National Laboratory, and at the Paducah Gaseous Diffusion Plant. Providing evidence at the mechanistic level that a biological attenuation mechanism occurs at a site is a very important piece of evidence in building a case that natural attenuation may be an applicable regulatory remedy for a contaminated site. In order to further evaluate the potential applicability of a cometabolism-based natural attenuation remedy, the in situ degradation rate must be determined and used to predict the evolution of the contaminant plume over time. Research focused on developing methods for extrapolating short-term laboratory measurements using the EAP technique, and more conventional microcosm-based methods to quantifying in situ kinetics, was also performed.

A modeling task was performed to evaluate alternative approaches to simulating the transport and fate of TCE in aerobic groundwater while undergoing cometabolic degradation. Two general approaches for describing degradation kinetics were evaluated: (1) competitive inhibition and (2) first order decay.

The competitive inhibition kinetics approach is based on two substrates competing for the same enzyme. One substrate, termed the growth substrate, is the material that a microorganism produced (i.e., an enzyme to oxidize) in order to obtain energy. The other substrate, termed the cometabolic substrate, is a material that also reacts with the enzyme but does not yield energy that can be harvested by the enzyme-synthesizing microorganism. Two substrates compete for the same enzyme, and hence the presence of one substrate interferes with reactions by the other substrate. Hence, the kinetic model is termed “competitive inhibition.” The form of the competitive inhibition model used in this study is applicable to natural attenuation, not enhanced attenuation in an engineered bioremediation system. It is assumed that the portion of a plume where natural attenuation might be applicable has oligotrophic conditions and a stable biomass concentration, and hence no provisions for changes in biomass concentration were included in the kinetic model used. Oligotrophic conditions likely correspond to the aerobic conditions in groundwater in which cometabolic degradation of TCE may occur.

A parametric study of competitive inhibition kinetics in a batch reactor was used to evaluate the effect of each parameter on reaction rates and temporal concentration trends. This study, based on literature values of kinetic parameters and biomass and substrate concentration ranges measured at the INL TAN TCE plume, shows that the range of predicted rates and concentration trends spans several orders of magnitude, due largely to the wide range of literature parameter values, which emphasizes the need for site-specific parameter values.

The competitive inhibition kinetic model is derived from the Michaelis-Menton kinetic model, and preserves the general form of that model in which reaction rates are approximately proportional to substrate concentrations at low concentrations and reach a plateau at higher concentrations. In the low concentration range, reaction kinetics are approximately the same as first-order kinetics, in which reaction rates are proportional to concentration. The parametric study suggests that for the substrate concentrations present throughout much of the TAN plume, and possibly at other aerobic plumes in which TCE is slowly degrading, competitive inhibition reaction kinetics are in the pseudo-first order range. In that case, the greater difficulty in parameterizing the competitive inhibition model relative to a first-order decay model would not be justified.

In order to incorporate competitive inhibition kinetics into groundwater reactive transport codes, new code for competitive inhibition kinetics was developed for the program RT3D (Reactive Transport in Three Dimensions). This kinetics package has been made publically available. An existing groundwater flow and transport model of an aerobic TCE plume was modified to incorporate competitive inhibition kinetics using RT3D, and the evolution of a TCE plume was simulated using a combination of kinetic parameter values from the literature, and biomass and substrate concentrations measured at the TAN TCE plume. The range of literature values used was selected based on batch reactor simulations to yield temporal concentration trends similar to those observed in plumes undergoing slow attenuation. This set of simulations yields credible results and demonstrates that the new kinetic module in RT3D functions properly.

The second modeling approach used in this study is based on the first-order decay kinetic model. An important advantage of the first order decay model is that it requires only one parameter value (degradation half-life), in contrast to five values needed in the competitive inhibition model. Degradation half-life values were estimated for the TAN TCE plume using the tracer-corrected method in which concentration trends along the length of the plume are normalized by concentrations of a conservative co-contaminant, tritium in this case. The estimated half-life value depends on the assumed groundwater

velocity and which, if any, data are excluded from the analysis. A fairly narrow range of half-life values was determined using recent data from the distal portion of the plume, which is downgradient of an area where active remediation has been occurring for about a decade. Although this simulation study was based in part on parameter values derived from the TAN plume, it does not account for on-going remedial activities, and therefore these simulations are not intended to predict the actual evolution of this plume; instead, this flow and transport model is being used simply as a tool to further understanding.

Transport simulations were made using the same groundwater flow model used to evaluate competitive inhibition kinetics, with TCE transport simulated using first order decay kinetics. Simulations based on a range of half-life values estimated in this study, and by others, illustrate that substantial differences in plume evolution could be expected based on a range of credible half-life values.

Modeling studies performed using both the competitive inhibition kinetic model and the first-order decay model clearly demonstrate that the numerical values of the kinetic parameters are critical controls on plume evolution. This indicates that credible and defensible methods for reliably determining in site values for kinetic parameters are needed if reliable predictions of plume evolution are to be made.

The final task of this project was providing financial support to a series of in situ experiments performed by other researchers using a flow-through in situ reactor (FTISR) in order to meet the goals of the overall project and to obtain information on TCE degradation kinetics. A set of six columns filled with basalt chips was suspended in a well in the TAN plume and groundwater was flushed through the columns for approximately 6 months. The six columns provide three replicates of two experimental treatments. During the incubation period, microorganisms suspended in groundwater colonized the basalt chips. The FTISR was retrieved, and cells were harvested and distributed to other researchers for characterization using a variety of methods, including a microcosm study for measuring degradation kinetics. The FTISR was deployed a second time, and equipment failure prevented the planned experiments from being conducted in situ. The FTISR was retrieved and the colonized basalt chips were used to prepare laboratory microcosms for, in part, characterizing degradation kinetics. The first microcosm experiment was not successful; the second microcosm experiment shows that TCE is slowly degraded. The second microcosm experiment will be continued after this project ends using other sources of support.

CONTENTS

EXECUTIVE SUMMARY	iii
ACRONYMS AND ABBREVIATIONS	xi
1. INTRODUCTION	1-1
1.1 Background.....	1-1
1.2 Project Overview	1-5
2. CHARACTERIZATION OF TCE BIODEGRADATION IN AEROBIC GROUNDWATER	2-1
2.1 Evaluation of Microbial Populations along a Transect Through Part of the TAN TCE Plume	2-1
2.2 Microcosm Study to Estimate Aerobic Degradation of TCE.....	2-3
2.2.1 Theory of Enzyme Activity Probes.....	2-3
2.2.2 Theory of Microcosm Study	2-5
2.2.3 Control Studies	2-6
2.2.4 Degradation Rate Determination	2-6
2.3 Deployment of Colonized FTISRs (I).....	2-8
2.4 Deployment of Colonized FTISRs (II)	2-10
2.4.1 On-going Studies at INL: Microcosms	2-11
2.5 Evaluation of Aerobic Cometabolic Degradation of TCE at Other Sites	2-11
3. MODELING COMETABOLISM AND TCE ATTENUATION.....	3-1
3.1 Introduction.....	3-1
3.2 Microbial Degradation Kinetic Models	3-1
3.2.1 Background.....	3-2
3.2.2 Kinetic Models.....	3-2
3.3 Compilation of Cometabolic Degradation Kinetic Parameter Values	3-6
3.3.1 Literature Values for Kinetic Parameters	3-6
3.3.2 Methane Concentrations	3-11
3.3.3 Biomass Concentration	3-11
3.4 Parametric Study of Competitive Inhibition Kinetic Model.....	3-11
3.4.1 Low Dissolved Oxygen Inhibition Term	3-12
3.4.2 Parametric Study of Competitive Inhibition Kinetics in a Batch Reactor	3-13

3.4.3	Batch Reactor Kinetics Based on Literature and Observed Parameter Values	3-15
3.4.4	Conclusions from the Parametric Study	3-26
3.5	Simulation of TCE Transport Using Competitive Inhibition Kinetics	3-27
3.5.1	Development of a Competitive Inhibition Kinetics Module for RT3D	3-27
3.5.2	Numerical Modeling Approach	3-28
3.5.3	Modeling Results	3-28
3.5.4	Conclusions from the Competitive Inhibition Kinetics Simulations	3-35
3.6	Simulation of TCE Transport at TAN Using First-Order Kinetics.....	3-36
3.6.1	Recalculation of TCE Half-Life	3-36
3.6.2	Simulation of TCE Transport with First-Order Decay Kinetics	3-43
3.6.3	First-Order Decay Kinetics Conclusions	3-44
3.7	Summary and Conclusions	3-47
4.	INCIDENTAL SUPPORT OF FLOW-THROUGH IN SITU REACTOR STUDIES.....	4-1
4.1	Construction and Operation	4-1
4.2	Discussion.....	4-2
5.	REFERENCES	5-1

Appendix A – Cometabolic Kinetic Reaction Package for RT3D

FIGURES

Figure 2-1.	Trichloroethene plume at TAN at the INL.....	2-2
Figure 2-2.	Example micrographs of microbial samples assayed via the EAP technique: Left – treated with a stain that highlights living cells; Center – positive response to EAP is indicated by individual cells fluorescing; Right – no response to an EAP indicated by lack of fluorescing cells....	2-5
Figure 2-3.	Results of microcosm with natural cells from the TAN contaminated aquifer, TAN-29. Top: TCE degradation over time. Middle and Bottom: sMMO and toluene oxygenase activity, respectively	2-9
Figure 3-1.	Effect of half-saturation coefficient on low-oxygen inhibition term.....	3-12
Figure 3-2.	Effect of rate parameters and competitive inhibition ratio on reaction rate for 1 mg/L biomass concentration.....	3-14
Figure 3-3.	Effect of half-saturation coefficients and maximum growth rate coefficient k_g on substrate concentrations as a function of time.	3-16
Figure 3-4.	Effect of half-saturation coefficients and maximum cometabolic rate coefficient k_c on substrate concentrations as a function of time.	3-17

Figure 3-5. Summary of trends in individual concentration versus time plots and in composite figures.	3-18
Figure 3-6. Growth substrate utilization rate versus concentration for maximum and minimum rate cases.	3-19
Figure 3-7. Growth substrate utilization rate for maximum (upper) and minimum (lower) rate cases.	3-20
Figure 3-8. Cometabolic substrate utilization rate versus concentration for maximum and minimum rate cases.	3-21
Figure 3-9. Cometabolic substrate utilization rate for maximum (upper) and minimum (lower) rate cases.	3-22
Figure 3-10. Growth and cometabolic substrate concentration trends for maximum (upper) and minimum (lower) rate cases.	3-24
Figure 3-11. Growth (upper) and cometabolic (lower) substrate utilization rate for intermediate rate case.....	3-25
Figure 3-12. Growth and cometabolic substrate concentration trends for intermediate rate case.	3-26
Figure 3-13. Comparison of the extent of TCE and conservative tracer in stress period 15 following addition of identical pulses of TCE and tracer in stress period 7.	3-30
Figure 3-14. Comparison of breakthrough curves for cell row 23, column 34, layer 15 for TCE (blue) and conservative tracer (red).	3-31
Figure 3-15. Ratio of TCE to conservative tracer concentrations.....	3-31
Figure 3-16. Mass of TCE and conservative tracer added to the RT3D model in stress period 7 and simulated TCE and tracer masses with time.	3-32
Figure 3-17. Simulated changes with time of TCE mass for cometabolic substrate specific rate coefficients of 0.2 and 1.0 mg growth substrate/mg cells-day.....	3-33
Figure 3-18. Ratio of the TCE mass for a k_C of 0.2 to the mass for a k_C of 1.0 for the modeled interval, in days.....	3-33
Figure 3-19. Simulated changes with time of TCE mass for biomass concentration (X) values of 0.001 and 0.01 mg cells/L.	3-34
Figure 3-20. Simulated changes with time of TCE mass for growth substrate half-saturation coefficient (K_{sg}) values of 1 and 5 mg growth substrate/L.	3-34
Figure 3-21. Simulated methane mass for growth substrate specific rate coefficients of 0.2 and 1.0 mg growth substrate/mg cells-day.	3-35
Figure 3-22. Plots of the natural log of the ratio of TCE to tritium concentrations with distance downgradient from the TSF-05 injection well for an assumed groundwater velocity of 0.098 m/d for the complete data set and the data set minus samples with UJ flags.....	3-40

Figure 3-23. Plots of the natural log of the ratio of TCE to tritium concentrations with distance downgradient from the TSF-05 injection well for an assumed groundwater velocity of 0.11 m/d for the complete data set and the data set minus samples with UJ flags.....	3-41
Figure 3-24. Plots of the natural log of the ratio of TCE to tritium concentrations with distance downgradient from the TSF-05 injection well for an assumed groundwater velocity of 0.125 m/d for the complete data set and the data set minus samples with UJ flags.....	3-42
Figure 3-25. Extent of TCE plume in layer 15 after 20 years (SP60), 40 years (SP82), and 60 years (SP97) using 12.3-, 12.7-, and 12.9-year TCE half-lives.	3-45
Figure 3-26. Comparison of the TAN TCE plume extent after 20, 40, and 60 years simulated using 11-, 12.3-, and 17-year TCE half-lives.....	3-46
Figure 4-1. FTISR design and dimensions.....	4-3
Figure 4-2. Schematic of pneumatic pump system used in both years.	4-3
Figure 4-3. Operation schematic for first year system.	4-4
Figure 4-4. Operation schematic for second year system.	4-4

TABLES

Table 2-1. Enzyme activity probe and FISH analysis of groundwater from monitoring wells along the mid-plume flow path, TAN contaminant plume. A positive indicates that the EAP or FISH probe showed a significant response for the targeted group.	2-4
Table 2-2. FISH and EAP analysis of groundwater from monitoring well TAN-35 and reactors filled with colonized basalt chips. A positive indicates that the EAP or FISH probe showed a significant response for the targeted group.	2-10
Table 2-3. Enzyme activity probe applications at various DOD, DOE, and private industry field sites.	2-12
Table 2-4. Sites where laboratory microcosms have been completed; calculated degradation half-life for TCE under field conditions; and relevant geochemical description.	2-13
Table 3-1. Kinetic coefficients for methanotropic cometabolism of TCE.....	3-7
Table 3-2. Kinetic coefficients for TCE cometabolism by aromatic degraders.....	3-8
Table 3-3. Kinetic coefficients for TCE cometabolism by other bacteria.	3-9
Table 3-4. Kinetic parameter values for TCE and methane degradation.....	3-10
Table 3-5. Summary of literature values of kinetic parameters for methane oxidation and TCE cometabolism.	3-11
Table 3-6. Methanotroph biomass concentration.....	3-11
Table 3-7. Summary of effect of increasing parameter values on reaction rates.	3-13

Table 3-8. Parameter values that yield maximum, minimum, and intermediate reaction rates.....3-19

Table 3-9. RT3D Chemical Reaction Package parameters.....3-29

Table 3-10. Determination of the decay-corrected tritium concentration for the range of groundwater velocities, 2009 data set.....3-38

Table 3-11. Computation of the natural log of the ratio of TCE to tritium concentrations, 2009 data set.3-39

Table 3-12. Determination of TCE half-life for the range of acceptable groundwater flow velocities.3-43

ACRONYMS AND ABBREVIATIONS

AFB	Air Force Base
ARD	anaerobic reductive dechlorination
bls	below land surface
CERCLA	Comprehensive Environmental Response, Compensation, and Liability Act
DCE	dichloroethene
DHC	<i>Dehalococcoides</i>
DNA	deoxyribonucleic acid
DO	dissolved oxygen
DOD	Department of Defense
DOE	Department of Energy
EAP	Enzyme Activity Probe
FISH	fluorescence in situ hybridization
ft	foot or feet
FTISR	Flow-Through In Situ Reactor
GC	gas chromatography, gas chromatographic
g/L	grams per liter
GMS	Groundwater Modeling System
in	inch or inches
INL	Idaho National Laboratory
m/d	meters per day
MT3D	Mass Transport in Three Dimensions
MCL	maximum contaminant level
mg/L	milligrams per liter
MNA	monitored natural attenuation
North Wind	North Wind, Inc.

PCE	tetrachloroethene
PCR	polymerase chain reaction
PLFA	phospholipid fatty acid
pMMO	particulate methane monooxygenase
qPCR	quantitative polymerase chain reaction
RNA	ribonucleic acid
ROD	Record of Decision
RT-PCR	real time polymerase chain reaction
RT3D	Reactive Transport in Three Dimensions
SCIA	stable carbon isotope analysis
sMMO	soluble methane monooxygenase
SRNL	Savannah River National Laboratory
TAN	Test Area North
TCE	trichloroethene
TCM	tracer corrected method
µg/L	micrograms per liter
VC	vinyl chloride
VOC	volatile organic compound

1. INTRODUCTION

This document is the final technical report for the portion of the project *Coupled Biogeochemical Process Evaluation for Conceptualizing Trichloroethylene Cometabolism* performed by North Wind, Inc. (North Wind). It addresses Subtask 3.3, “Cometabolic Enzyme Activity Probes (EAPs),” and Task 4 – “Modeling Cometabolism and Attenuation,” identified in Field Work Proposal INL-05-00227, *Coupled Biogeochemical Process Evaluation for Conceptualizing Trichloroethylene Co-metabolism*. In addition, support provided to perform Task 2, “Flow-Through In Situ Reactor (FTISR) Water Chemistry and Flow Rate Analysis” is described. The research described here was supported by the Department of Energy (DOE), Office of Biological and Environmental Research, Office of Science via Grant Number DE-FG02-06ER64199. The research described in this report is part of a larger research project of the same name. Researchers at other institutions (i.e., Idaho National Laboratory [INL], University of Idaho, and Lawrence Berkeley National Laboratory) received separate funding to execute research described in the field work proposal, and hence have separate reporting requirements.

The research described here was performed by a team led by Robert Starr of North Wind, who was also the technical lead for the modeling task (Task 4). He was assisted by Dr. Prabahakar Clement of Auburn University, who developed software used in the modeling study; and Brennon Orr of North Wind, who conducted groundwater flow and transport simulations. EAP studies (Subtask 3.3) were performed under the direction of Hope Lee, who was a North Wind employee during the first part of this study and continued to contribute to this project under subcontract after she transitioned to the INL. FTISR water chemistry and flow rate analysis (Task 2) was performed by the INL. Mark Delwiche (INL) led FTISR activities, but North Wind provided financial support in order to facilitate achieving the objectives of the entire research team, including determining kinetic parameter values needed in the modeling study.

Field activities at the INL Test Area North (TAN) groundwater plume were made possible by agency personnel responsible for the TAN plume remediation project, including Mark Shaw and Nicole Hernandez, Department of Energy – Idaho Operations Office; Matt Wilkening, EPA-Region 10; Mark Jeffers and Gerry Winter, Idaho Department of Environmental Quality; and by Idaho Cleanup Project managers Lee Nelson and Howard Forsyth. Field support was provided by Evan Myler and Riena Carroll of the Idaho Cleanup Project, and by Dana Swift of North Wind. The assistance of these individuals and organizations is acknowledged and appreciated.

This report is organized as follows. The remainder of Section 1 provides background information about aerobic cometabolic degradation of trichloroethene (TCE) in groundwater and an overview of this project. Section 2 describes the research related to EAPs (Subtask 3.3 in the field work proposal). Section 3 describes modeling of aerobic cometabolic degradation of TCE. Section 4 briefly describes the activities supported by North Wind related to the FTISR studies (Task 2) performed by INL.

1.1 Background

Investigation, management, and remediation of groundwater contaminated by human activities is a significant activity at DOE facilities, other government sites, and at private sector properties. Improving the ability to remediate groundwater contamination will reduce the environmental legacy associated with contaminated sites and will allow efforts currently expended for managing these sites to be applied to other purposes. The research described in this report focused on improving our ability to remediate groundwater contaminated with TCE.

TCE is one of the most common groundwater contaminants at industrial and hazardous waste sites. This situation results from a combination of factors, including:

- TCE was commonly used as a solvent for petroleum products in many commercial and industrial processes, and therefore it was used and disposed at numerous locations.
- TCE was often used or disposed in ways that resulted in its migration into groundwater.
- TCE is highly mobile in groundwater in most aquifers, travelling at approximately the same rate as the groundwater itself.
- A small quantity of TCE can contaminate a large volume of water. TCE is hazardous to humans at fairly low concentrations; the maximum contaminant level (MCL) (i.e., the maximum concentration allowed in drinking water) is only 5 µg/L. One gallon of liquid TCE (density 1,464 g/L) released into the subsurface (mass = 5,541 g) could therefore contaminate approximately 300 million gallons (1.1 billion L) of water to the MCL.
- TCE can exist in the subsurface as a dense, non-aqueous phase liquid that slowly dissolves and continues to create dissolved contaminant plumes for decades or longer.

Large plumes of groundwater contaminated with TCE are at many sites in the DOE complex, including the 2-mile long TAN plume at the INL, the 3-mile long Northwest and Northeast plumes at the Paducah Gaseous Diffusion Plant, numerous smaller plumes at the Savannah River National Laboratory (SRNL), the Portsmouth Gaseous Diffusion Plant, the former Rocky Flats site, and elsewhere. TCE is also a common groundwater contaminant at Department of Defense (DOD) sites and private sector sites.

Dissolved contaminants in groundwater are affected by a variety of processes that influence their migration and persistence. They can be added to groundwater by dissolution and removed from it by precipitation, moved with groundwater itself by advection, mixed with surrounding groundwater via dispersion, removed from solution and attached to solid phases in the aquifer by sorption, lost to the atmosphere by volatilization, and affected by a host of chemical transformations – many of which are biologically mediated.

Biologically-mediated transformations of TCE in groundwater are addressed in this research. TCE is readily transformed by bacteria native to groundwater systems; however, different pathways are used under different geochemical conditions. Under anaerobic conditions, TCE is chemically reduced as chlorine atoms in the TCE molecule are sequentially replaced by hydrogen atoms, in a process known as anaerobic reductive dechlorination (ARD). The ARD degradation sequence is:



In the ARD process, bacteria couple reduction of chloroethenes with oxidation of organic carbon to carbon dioxide, and obtain energy from the process. ARD, as a process for biodegradation of TCE and other chloroethenes, is widely recognized and frequently occurs in groundwater at locations where chloroethenes were co-disposed with a source of labile organic carbon such as petroleum, or where natural organic matter in the aquifer is available as a substrate. Hence, in many situations, ARD causes TCE concentrations to decline without active human intervention – a process termed ‘natural attenuation.’

ARD of chloroethenes is well recognized among the hydrogeologic community, and is the basis for both active and passive remediation approaches for chloroethene-contaminated groundwater. ARD is utilized to actively bioremediate contaminated groundwater by adding a source of readily-utilized organic carbon, possibly other nutrients, and in some cases also inoculating the aquifer with chloroethene-degrading microorganisms. ARD is the basis of the paradigm for a formal procedure for evaluating natural attenuation as a remedial technology for chloroethene-contaminated groundwater (Wiedemeier et al.,

1998). That protocol is based on the paradigm that chloroethenes are readily degraded under anaerobic conditions, but not under aerobic conditions. Although tetrachloroethene (PCE) usually does not degrade biologically under aerobic conditions, the less chlorinated ethenes (TCE, dichloroethene [DCE], and vinyl chloride [VC]) can be biologically degraded under aerobic conditions. Hence, natural attenuation may be an appropriate remedial alternative for TCE and the less-chlorinated ethenes under aerobic conditions as well as anaerobic conditions, if the aerobic degradation products are non-hazardous and if the transformation into non-hazardous products occurs quickly enough to meet remedial objectives at a particular site.

In contrast to anaerobic conditions in which bacteria obtain energy by utilizing chloroethenes in respiration, under aerobic conditions, bacteria do not obtain energy by degrading TCE (although bacteria can obtain energy by oxidizing VC). Instead, TCE is oxidized by enzymes that are produced by bacteria to perform other purposes, such as oxidizing other organic or inorganic compounds to obtain energy. Some enzymes that are produced to perform beneficial processes for the organism that synthesized the enzymes also fortuitously oxidize TCE, apparently without benefiting the organism. A primary substrate (organic carbon utilized as a source of energy by the organism) must be available in order for the non-energy yielding oxidation of TCE to occur; without a substrate, the enzymes that fortuitously degrade TCE are not produced. This process, the fortuitous degradation of a compound without benefit to the organism by an enzyme produced to catalyze a beneficial reaction in the obligate presence of an enzyme-inducing substrate, is known as *cometabolism*.

Bacteria that produce enzymes to utilize several types of substrates, including methane, propane, butane, alkenes, toluene, phenols, and ammonia are known to carry out cometabolic transformation of TCE (Arp et al., 2001, and references cited therein). Hence, in aerobic environments where bacteria that utilize these substrates are active, TCE may be degraded via cometabolism. If cometabolic TCE degradation does occur in a particular contaminated aquifer and the rate is sufficiently fast, then this process may make a significant contribution to limiting migration of contaminated groundwater and to remediating the plume of contaminated groundwater. This is particularly important since cometabolic degradation occurs in aerobic groundwater; shallow aquifers that are frequently utilized as drinking water supplies are often aerobic. Hence, cometabolic degradation of TCE in aerobic groundwater may have an important beneficial effect of limiting TCE migration, and hence minimizing the spatial extent of contaminated groundwater, and also be important for remediating contaminated groundwater and returning it to beneficial use. The cometabolic process is important in aerobic groundwater because TCE is not directly utilized as a substrate under aerobic conditions, but it can be degraded via cometabolic processes. Hence, if not for cometabolic processes, TCE would be biologically recalcitrant in aerobic groundwater.

Conceivably, cometabolic degradation of TCE could be applied both for active groundwater remediation and in a natural attenuation remedy. For example, Goltz et al. (2001) describe modeling studies that evaluated various approaches for adding substrate during active remediation, and Semprini and McCarty (1992) describe a field trial of enhanced bioremediation via cometabolism. The focus of this research is the natural attenuation application. If natural attenuation is applied as a groundwater remedy to comply with regulatory requirements, it is termed *monitored natural attenuation* (MNA), in recognition that the remedy includes on-going monitoring of contaminant concentrations in the plume. Evaluation of MNA as a potential remedy typically includes assessment of contaminant trends with distance along a flowpath and over time, identification of the mechanism responsible for attenuation, and defensible predictions of how contaminant concentrations will evolve over time. On-going monitoring of an in-place remedy typically includes tracking contaminant concentration trends in space and time, and comparing observed plume evolution against the predicted behavior. If contaminants migrate farther or faster than predicted as the basis for selecting an MNA remedy, that could be justification for requiring that the MNA remedy be replaced with a more expensive active remedy. Obviously, making more realistic predictions of plume evolution will result in better decisions about the suitability of MNA as a regulatory remedy.

One example of a site where a MNA remedy for aerobic, TCE-contaminated groundwater is being implemented is the TAN plume at the INL. At this site, sanitary wastes, hazardous wastes, and radioactive wastes were disposed from the 1950s through the 1970s by injecting liquids into fractured basalt in the Eastern Snake River Plain aquifer. The hazardous wastes included PCE and TCE, and the radioactive wastes included tritium. By the 1990s, a plume of contaminated groundwater extended approximately 2 miles downgradient from the former waste injection well. TCE extended the farthest downgradient at concentrations above its allowable concentration in drinking water (the MCL), but both PCE and tritium were also present throughout much of the TCE plume.

The TAN plume was addressed via the Comprehensive Environmental Response, Compensation and Liability Act (CERCLA) process, and a Record of Decision (ROD; DOE et al., 1995) was signed that stipulated containing the entire plume using pump-and-treat. The ROD also required evaluation of alternative technologies to enhance or replace pump and treat. These technology evaluations were completed, an Explanation of Significant Differences was prepared, and a ROD amendment (DOE et al., 2001) modified the remedy to include three components: (1) enhanced in situ bioremediation in the hotspot near the former waste disposal well where TCE concentrations were greater than 20,000 $\mu\text{g/L}$; (2) pump-and-treat during an interim period in the medial portion of the plume where TCE concentrations were between 1,000 and 20,000 $\mu\text{g/L}$; and (3) MNA for the remainder of the plume where TCE concentrations were between 5 and 1,000 $\mu\text{g/L}$. The MNA remedy was applied to the majority of the areal extent of the plume, and the cost savings associated with implementing the multi-component remedy in lieu of pump-and-treat was estimated to save \$26M.

Groundwater in the TAN TCE plume is aerobic, except in the immediate vicinity of the former waste injection well, where residual organic matter from sanitary wastewater injected into the aquifer causes redox conditions to be anaerobic. If the conceptual model embodied in Weidemeier et al. (1998) were accepted (i.e., that TCE can be degraded under anaerobic conditions but is recalcitrant under aerobic conditions), then MNA would be eliminated as a potential remedy for the TAN plume. Under this paradigm, TCE would be expected to be transported downgradient of the hotspot without being degraded, and hence the ratio of TCE to conservative co-contaminants would be the constant throughout the plume. In contrast, Sorenson et al. (2000) showed that TCE concentrations declined relative to the concentration of PCE and tritium with increasing distance along the flowpath, which they attributed to biodegradation of TCE, possibly via cometabolism, while PCE and tritium were conservative. Based on the decline in TCE concentrations with distance relative to concentrations of PCE and tritium, a TCE degradation half-life of 13 to 21 years was determined. This demonstration of preferential attenuation of TCE was part of the geochemical evidence of attenuation that provided the basis for the ROD amendment that specified MNA as a remedy. Subsequent investigations at the TAN plume have provided evidence that TCE is being degraded via aerobic cometabolism.

Following applying the tracer corrected method (TCM) at the TAN TCE plume and determining that the rate of aerobic degradation could be fast enough to be significant in a regulatory-remediation context, data for TCE plumes across the DOE complex were screened to determine if there were other plumes in aerobic groundwater where the presence of a conservative co-contaminant would allow application of the TCM. In previous research funded by the Environmental Management Science Program, Starr et al. (2004) screened 127 TCE plumes in aerobic groundwater and identified nine plumes where a conservative co-contaminant was present and where there were sufficient wells distributed throughout the plume for use of the TCM to be feasible. TCE plumes at four DOE sites (Brookhaven National Laboratory, Paducah Gaseous Diffusion Plant, Rocky Flats Environmental Test Site, and SRNL) were determined to exhibit preferential loss of TCE relative to a conservative co-contaminant in aerobic groundwater. Degradation half-lives ranging from 1 to 12 years were calculated. This study suggests that (a) TCE degradation in aerobic groundwater may be a commonplace occurrence, and (b) half-lives for biodegradation under aerobic conditions may be short enough that MNA can be a feasible remedy in some conditions.

However, the study also suggests that a small proportion of aerobic TCE plumes also have data for a conservative co-contaminant, which therefore limits the applicability of the TCM. Furthermore, in all plumes identified in that study, the conservative co-contaminant was itself a hazardous constituent. Thus, even if TCE biodegraded to innocuous concentrations, the conservative co-contaminant would likely remain and therefore would continue to impair water quality. In part, this reflects the data available, in that water samples collected in a regulatory program are analyzed primarily for regulated constituents but not for non-hazardous constituents.

An alternative approach for assessing whether TCE is being cometabolized in aerobic groundwater has also been applied at the TAN TCE plume, in several other aerobic TCE plumes at DOE sites, and elsewhere. That technique, the EAP Method, is an assay for some of the enzymes that are known to be capable of cometabolically degrading TCE in aerobic conditions. The EAP technique uses a series of enzyme-specific chemical probes to determine if enzymes known to be responsible for cometabolic degradation of TCE are active in bacteria harvested from groundwater. The EAPs are non-fluorescent when not bound to an enzyme but fluoresce when bound to an enzyme. Samples of bacteria collected from an aquifer are treated with a series of EAPs that each react one of the enzymes responsible for TCE cometabolism. A fluorescent response in a sample treated with a probe indicates that the targeted enzyme is active in the sampled bacteria. This technique yields a positive/negative response (i.e., the enzyme targeted by a probe either is or is not active in the sample), and thus the bacterial community is or is not capable of cometabolizing TCE.

The appearance of a fluorescent product, when an EAP is applied to a bacterial sample, indicates that the bacteria are capable of cometabolizing TCE. However, it does not provide information about the rate of TCE transformation. EAP data are used to estimate in situ degradation rates from those measured in laboratory microcosms by scaling microcosm-measured rates by the concentration of microorganisms that exhibit a positive EAP response under in situ and laboratory conditions.

EAP studies conducted at over 20 sites where aerobic groundwater is contaminated with TCE show that the bacterial communities in these plumes virtually always exhibit a positive response to at least one EAP that targets enzymes involved in TCE cometabolism (see Section 2.5), which indicates that TCE cometabolism in aerobic groundwater is likely a commonplace occurrence. This is consistent with the study of TCE plumes in aerobic groundwater by Starr et al. (2004) that used the TCM (Sorenson et al., 2000) to examine data from TCE plumes at four DOE sites and reached the same conclusion.

These results suggest that biodegradation of TCE in aerobic groundwater is likely a commonplace occurrence, and therefore that natural attenuation may be an appropriate component of a remedy for TCE in some aerobic groundwater plumes. In order to evaluate the suitability of natural attenuation as a remedy, it would be highly desirable to:

- Apply a technique that demonstrates that a biological degradation mechanism is active,
- Determine degradation rate kinetics using a defensible method, and
- Predict future plume evolution based using a flow and transport model that includes appropriate degradation kinetics and defensible kinetic parameter values.

1.2 Project Overview

The research conducted in this project included the following.

- Further development of the EAP technique, including developing methodology for using it to determine in situ TCE degradation rates from laboratory measurements.
- Application of the EAP method at TCE plumes in aerobic groundwater located at INL TAN, at SRNL, and at the Paducah Gaseous Diffusion Plant.
- Developing a reaction module for the software RT3D (Reactive Transport in Three Dimensions), which is used to simulate transport of contaminants in groundwater with kinetically-controlled degradation; the kinetic module simulates competitive inhibition kinetics, which accounts for the adverse interactions between the primary substrate (the carbon source utilized as an energy source by bacteria) and the cometabolic substrate.
- Supporting an in situ column experiment that was used to develop a microbial culture in the aerobic TCE plume at TAN. The culture was used in microcosm studies to determine reaction kinetics, and in studies performed by researchers at other institutions who performed other Environmental Remediation Sciences Program-funded research on TCE cometabolism.

The objectives of North Wind’s research, identified in Field Work Proposal INL-05-00227, were achieved, as shown in Table 1-1.

Table 1-1. Comparison of research objectives and achievements.

Task	Objective	Results
Subtask 3.3: Co-Metabolic Enzyme Activity Probes	Detect methanotrophic enzyme activity in solids and water from the FTISR.	Methanotrophic activity was investigated using a broader suite of EAPs than anticipated in the proposal; EAP were applied to bacteria harvested from groundwater collected from the INL TAN TCE plume, FTISRs, three TCE plumes at the SRNL, and the northwest TCE plumes at the Paducah Gaseous Diffusion Plant.
	Discriminate between sMMO activity and particulate methane monooxygenase activity.	The coumarin probe only detects the sMMO enzyme, not the particulate form. Thus, activity determined with EAP targets exclusively the soluble form. PCR for these studies targeted a subunit of the sMMO as well. So for the studies completed at the INL, the target was the soluble form.
	Relate enzyme activity results to TCE cometabolism rates determined in Subtask 3.1 (INL, LBNL task) and Subtask 3.4 (INL task).	TCE cometabolism rates were estimated based on (a) groundwater collected from the TAN site and (b) basalt/groundwater incubations from the TAN site. Microcosms studies were also completed for one of the sites located at SRNL. A microcosm study for the northwest plume at the Paducah plant is on-going, as is the second microcosm study specific for this project (basalt chips and groundwater from TAN).

Table 1-1. (continued).

Task	Objective	Results
Task 4: Modeling Co-Metabolism and Attenuation at TAN, Paducah, and Savannah River Site	Develop mathematical expression for TCE degradation.	Modified Michaelis-Menton based competitive inhibition kinetic model to include slowing the reaction rate at low dissolved oxygen concentrations.
	Incorporate mathematical expression in a groundwater flow and transport simulation code.	Developed an Excel spreadsheet for a batch reactor based on the mathematical kinetic model, and developed a kinetic module for the groundwater reactive transport simulation code RT3D.
	Perform sensitivity study.	Completed a detailed parametric study (sensitivity study) for a batch reactor to elucidate the effect of each parameter and interactions between parameters, and demonstrated that the new kinetic model in RT3D functions properly.
	Calibrate to a TCE plume.	Selected parameter values for the competitive inhibition kinetic model in RT3D that yields predicted plume behavior similar to that in a slowly-attenuating TCE plume. Simulated the plume using a simpler first-order kinetic model, and parameterized the model using a range of half-life values calculated for the plume using data sets from different times using the tracer-corrected method.
	Investigate effect of alternative scenarios.	Sensitivity study performed to evaluate the effect of changing parameter values on concentration trends.
EAP = enzyme activity probe FTISR = Flow-Through In Situ Reactor INL = Idaho National Laboratory PCR = polymerase chain reaction sMMO = soluble methane monooxygenase SRNL = Savannah River National Laboratory TAN = Test Area North TCE = trichloroethene		

2. CHARACTERIZATION OF TCE BIODEGRADATION IN AEROBIC GROUNDWATER

This chapter describes the characterization of the indigeneous microbial community that degrade TCE in aerobic groundwater, where cometabolic degradation is thought to be a major contributor to natural attenuation. Molecular techniques were applied to characterize the microbial community and to assay for particular enzyme-mediated processes, primarily in the TCE plume at TAN of the INL (Figure 2-1), and a combination of lab and field experiments were used to measure TCE degradation rates.

The objective of these studies is to establish evidence of natural attenuation of TCE by investigating multiple biogeochemical processes responsible for TCE degradation in aerobic groundwater. The studies are targeted at quantifying TCE cometabolism, characterizing the microbial populations and processes responsible for the degradation, as well as determining rates of degradation. The approaches to achieve this work include the use of fluorescence in situ hybridization (FISH), EAPs, and quantitative polymerase chain reaction (qPCR). In situ studies were performed using a FTISR, which are described in Chapter 4. The details concerning the microbes, the biotic and abiotic characteristics of the subsurface, and the degradation rates can be used to conceptualize the processes responsible for TCE cometabolism. The results of these studies could significantly expand the use and acceptance of MNA at other sites with TCE-contaminated aerobic groundwater across the country.

Molecular work and characterization studies described here include: evaluation of microbial populations in the TAN TCE plume along a transect from near the source area to the leading edge of the medial zone (Section 2.1); a microcosm study to estimate aerobic degradation rates for TCE in groundwater at well TAN-29 (Section 2.2); incubation and subsequent analysis of basalt chips incubated in FTISRs (Section 2.3); a second round of incubations of basalt chips at in FTISRs in well TAN-35 (Section 2.4); and a summary of related studies performed at other sites (Section 2.5).

2.1 Evaluation of Microbial Populations along a Transect Through Part of the TAN TCE Plume

The groundwater microbial community in the TAN TCE plume was characterized along a transect that extends from the anaerobic contaminant source zone (the hotspot; Figure 2-1) that surrounds the well (TSF-05) formerly used for disposing sanitary sewage and industrial wastes into the aquifer, downgradient through the medial zone where TCE concentrations decline and redox conditions are aerobic, to the edge of the distal zone where redox conditions are aerobic and TCE concentrations have historically been below 1,000 µg/L. Bioremediation of TCE in the source zone has been enhanced for approximately a decade by adding soluble organic carbon as an electron donor, which promotes development of strongly reducing conditions and methane production. Downgradient of the enhanced bioremediation zone, redox conditions become aerobic. Due to the variation in redox conditions with increasing distance along the flow path, changes in the metabolic capabilities of the microbial community are expected to occur. In particular, methane production by methanogenic bacteria is expected to occur in the strongly reducing conditions in the contaminant hotspot and the enhanced bioremediation zone; and methane oxidation by methanotrophs is likely in the aerobic conditions that prevail in the medial and distal portions of the plume downgradient of the hotspot.

Bacteria that cometabolize TCE in aerobic conditions synthesize enzymes for other purposes, such as oxidizing methane, aromatic hydrocarbons, or ammonia to obtain energy, and fortuitously those enzymes also oxidize TCE. Characterization techniques were applied that either classify bacteria or that assay for enzymes active in TCE cometabolism.

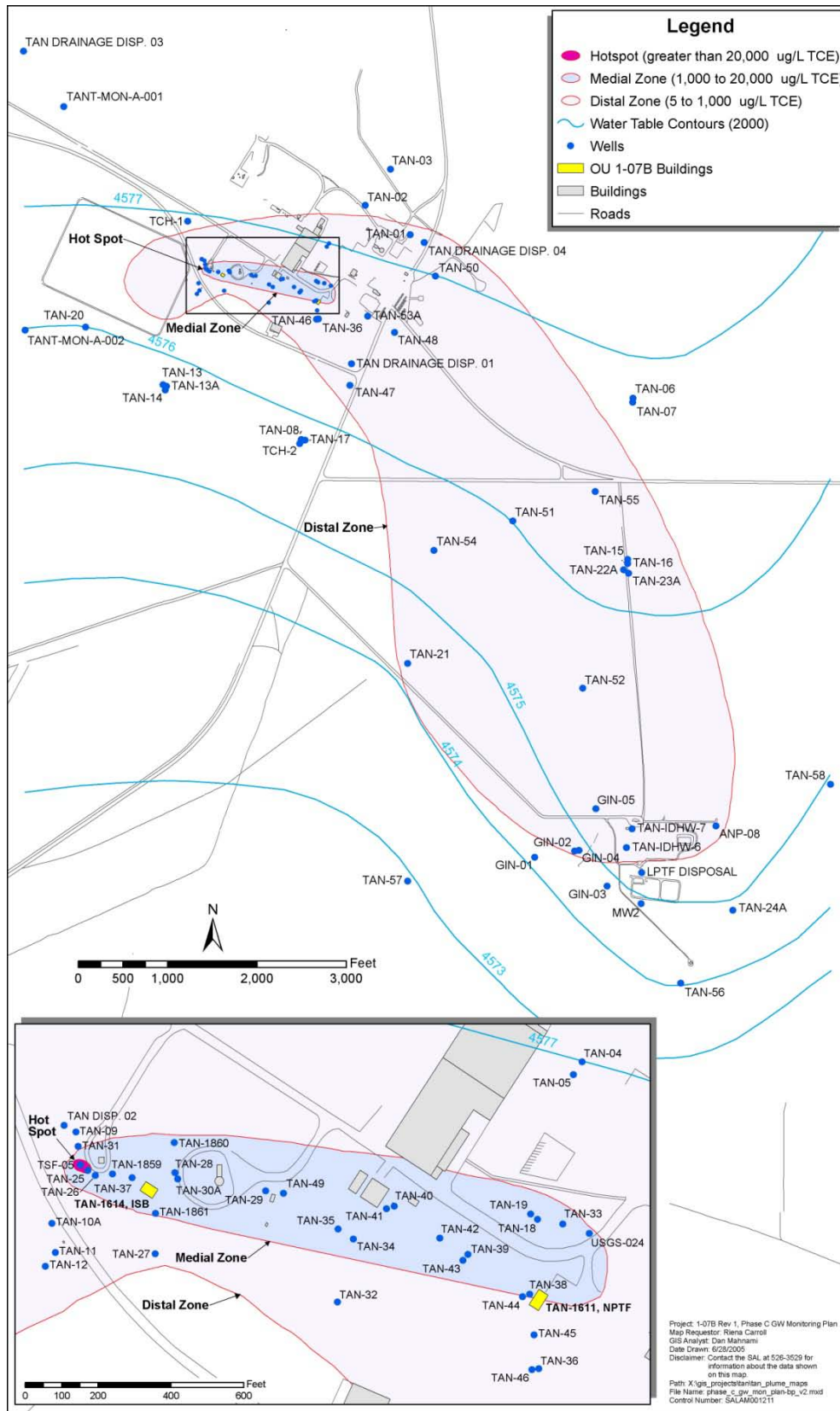


Figure 2-1. Trichloroethene plume at TAN at the INL.

One of the most widely used approaches for examining single-cell activity is FISH, which determines cellular ribosomal content using fluorescently labeled oligonucleotide probes (Howard-Jones et al., 2002). The characterization of the TAN plume for microbial presence and activity involved the application of FISH probes for both anaerobic (methanogens and *Dehalococcoides* [DHC]) and aerobic (oxygenase-carrying and methanotrophic) microorganisms (Table 2-1). Positives in the table show a transition from anaerobic to aerobic microbial population activity along the mid-line of the plume through the medial zone. Furthermore, the data are consistent with geochemical data at the site: anaerobic biodegradation dominates near the source area (well TAN-25), as indicated by the absence of enzymes assayed via EAP responsible for oxidation of methane and toluene, which were detected at other wells. Both methanogenic bacteria and methanotrophic bacteria were detected at all wells examined. Methanogenic bacteria inhabit strongly reducing anaerobic areas, while methanotrophic bacteria inhabit areas where both methane and oxygen are available; detection of both methanogens and methanotrophs suggests that the sample was a mixture of water from different zones. Microbial activity then shifts to aerobic biodegradation, close to monitoring wells TAN-28 and TAN-29, as indicated by EAP detection of oxygenases. Aerobic degradation pathways dominate near the downgradient edge of the medial zone and out to the distal portion of the plume, as indicated by the EAP detection of oxygenases, and detection via FISH of fewer types of methanogens but more methanotrophs. More interestingly, the methane monooxygenase pathway (as opposed to the toluene oxygenase pathway) appears to be the most significant degradation aerobic pathway in and around monitoring wells TAN-28 and TAN-29, which have historically had high concentrations of methane as a result of source area remediation, and the aromatic pathways dominate downgradient of these wells where the concentration of methane is variable and most often <10 mg/L.

2.2 Microcosm Study to Estimate Aerobic Degradation of TCE

Laboratory studies using molecular methods (FISH and EAPs) were used to demonstrate that the TAN groundwater microbial community has the capability to cometabolically degrade TCE. Laboratory microcosm studies provide an independent line of evidence for aerobic TCE degradation capability and kinetics.

2.2.1 Theory of Enzyme Activity Probes

Enzyme activity probes are used to assay microbial communities for activity of particular enzyme-mediated processes. The principal is that transformation of an enzyme activity probe by an enzyme is a clear indication that the enzyme targeted by a probe is active; it can then be inferred that other reactions catalyzed by the same enzyme are also occurring. In this study, EAPs that target enzymes responsible for cometabolizing TCE (i.e., toluene oxygenases and soluble methane monooxygenase) were used to assay microbial samples from groundwater samples collected from the TCE plume at TAN and elsewhere. EAP probes consist of non-fluorescent compounds (substrates) that are transformed by specific oxygenases into strongly fluorescent products. As shown in Figure 2-2, a clear, quantifiable signal (i.e., fluorescence) can be detected only when the targeted enzyme is actively functioning. EAPs have been developed for four separate toluene oxygenases (Keener et al., 1997; 1998; 2001; Kauffman et al., 2003; Clingenpeel et al., 2005) and for soluble methane monooxygenase (sMMO) (Miller et al., 2002). While originally developed specifically for the toluene oxygenase enzymes, these probes have been evaluated and have proven successful against an array of aromatic enzymes, including those for benzene, naphthalene, and phenol (Lee et al., 2005; Lee, 2007). Oxygenase synthesis occurs when the cell responds to the presence of an inducer, which is typically a substrate for the enzyme. In the presence of an appropriate inducer molecule, transcription of the structural genes for the oxygenase is up-regulated, resulting in a significant increase in the synthesis of the oxygenase and/or other enzymes involved in a specific catabolic pathway. Recent studies have found that both naturally occurring humic substances and the chlorinated solvents themselves can act as inducers of the cometabolic enzymes, although the extent of and time for activation, as well as the mechanism for cell energy and growth in these instances, are poorly understood.

Table 2-1. Enzyme activity probe and FISH analysis of groundwater from monitoring wells along the mid-plume flow path, TAN contaminant plume. A positive indicates that the EAP or FISH probe showed a significant response for the targeted group.

Technique	Probe	Target	Plume Zone							
			Source	Medial					Distal	
			TAN 25	TAN 28	TAN 29	TAN 42	TAN 44	TAN 33	TAN 36	
Enzyme Activity Probes	Coumarin	Soluble methanemonooxygenase		+	+	+	+	+	+	
	Phenylacetylene	Toluene-2-monooxygenase; Toluene-3-monooxygenase		+		+	+	+	+	
	trans-cinnamionitrile	Toluene-2,3-dioxygenase				+	+	+	+	
FISH		<i>Archae</i>	+	+	+	+	+	+	+	
		<i>Eubacteria</i>	+	+	+	+	+	+	+	
		<i>Dehalococcoides</i>	+	+	+		+	+		
			Methanogens							
		M825	<i>Methanosaetaceae</i>	+	+	+	+	+	+	+
		M1174	Most <i>Methanobacteriales</i>	+	+	+		+	+	
		M1109	<i>Methanococcales</i>	+	+			+		
		M1200	Most <i>Methanomicrobiales</i>	+	+	+		+	+	
		MSMX 860	<i>Methanosarcina, Methanosaeta</i>	+	+	+	+	+	+	+
			Methanotrophs							
		M450	<i>Methylocystis, Methylosinus</i>	+	+	+	+	+	+	+
		M84	<i>Methylococcus, Methylobacter</i>	+	+	+		+		+
		M705	<i>Methylococcaceae, Methylomonas</i>	+	+		+	+	+	+

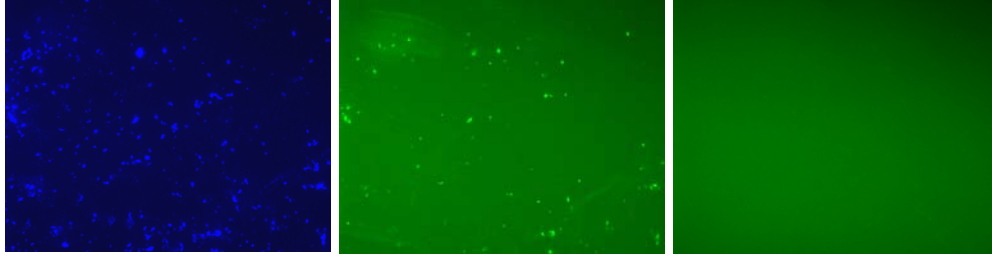


Figure 2-2. Example micrographs of microbial samples assayed via the EAP technique: Left – treated with a stain that highlights living cells; Center – positive response to EAP is indicated by individual cells fluorescing; Right – no response to an EAP indicated by lack of fluorescing cells.

In addition to EAP, a series of molecular probes has been developed or adapted to investigate the potential of oxidizing microbial populations. While EAP measures actual activity of microorganisms, molecular techniques (deoxyribonucleic acid [DNA] analysis) should be used to provide context for the activity probes, i.e., to confirm that the microbial community includes organisms known to carry out a particular process (i.e., methane or toluene oxidation). Microbial DNA can be extracted from water or sediment samples and used in molecular assays. These assays are designed to look for the presence of the genes coding for the biological oxygenases, i.e., to determine if genes responsible for synthesizing oxygenases are present. Coupling EAP measurements with molecular assessment provides direct and supporting evidence of cometabolic enzyme activity toward chlorinated solvents (Lee et al., 2005; Lee, 2007; Wymore et al., 2007). Natural attenuation of TCE through cometabolism can be verified using this type of monitoring technique.

2.2.2 Theory of Microcosm Study

A microcosm study was performed to determine if the microbial community in the TAN TCE plume is capable of cometabolically degrading TCE, and if so, to measure the TCE degradation rate. Each microcosm consisted of ~12 mL of TCE-contaminated groundwater in a ~14-mL crimp-top vial. The headspace in each vial is minimized to (a) simulate in situ conditions and limited availability of oxygen and (b) compensate for stimulation of the aerobic cometabolic pathways, which could be “over stimulated” in the presence of excess oxygen (large headspace would provide more oxygen over time than is available in situ). The treatments are as follows:

- Treatment #1: Whole Groundwater from TAN-29,
- Treatment #2: Concentrated biomass from TAN-29,
- Treatment #3: Kill Control, Sodium Azide 0.01%, and
- Treatment #4: Oxygenase Inhibition, Acetylene 0.5%.

Each treatment included 90 vials, which were sampled destructively over time. All of the vials were incubated at 14°C (while shaking) in the dark for up to 90 days. Sub-samples were taken for gas chromatographic (GC) analysis of volatile organic compounds (VOCs), dissolved oxygen (DO) analysis via Hach kit, and EAP analysis over time. Samples were collected more frequently during the first week of incubation, followed by less frequent sampling over the remaining weeks. DO measurements were taken at each sampling point as a qualitative measurement and recorded as positive or negative; quantitative measurements were not considered necessary for the course of time evaluated (<1 month).

Based on previous studies and a thorough review of the literature, microbial population dynamics and activity assessments tend to vary more over the first few weeks of incubation under laboratory conditions; these changes tend to drop off and populations reach a steady state of growth, death, etc. after 10 to 14 days. While these generalizations commonly hold true in microcosm studies, samples are taken throughout the microcosm study and investigated for contaminant trends via GC analysis; based on the results of each of these sample analyses, time points are determined for full analysis, including microbial activity.

2.2.3 Control Studies

Each set of microcosm treatments is complemented by a series of control studies that include (a) selective irreversible inhibitors of oxygenases in catabolic studies and (b) whole population, cell growth/inhibitors. Abiotic or sterile controls are not performed for these analyses due to the significant changes in geochemistry associated with sterilization of groundwater (VOC's volatilize and overall geochemical changes). However, in sediment/water microcosm studies, some effort was made to include abiotic controls.

Selective inhibitors have been shown (Keener et al., 2001) to preferentially inhibit one or more aromatic oxygenase pathways under controlled conditions. These types of incubations provide a clear line of evidence that the targeted metabolic pathway is being investigated in the microcosm studies. For example, in the inhibitor treatment, if the TCE continues to be degraded and/or the EAP determine there is activity in the sample, then the degradation is not attributable to the aromatic pathways alone and the EAPs are not working properly or are targeting a broader group of oxygenases, respectively. Because the inhibitors differentially influence the mode of action or lack thereof, based on the specific oxygenase (Keener et al., 2001), results from these incubations should be either (1) diminished (depending on which monoxygenase is being expressed and degrading the contaminant) or (2) show a complete lack of activity, as determined by the EAP.

The loss of cellular metabolism through the addition of sodium azide is a second control study that is undertaken in order to isolate the artifacts of microcosm studies, including any abiotic loss, loss due to poor design, and other geochemical, chemical, or physical elements that could produce a loss of the contaminant over the course of the microcosm study. This treatment should result in complete loss of biological degradation; any loss of contaminant in these incubations can and will be attributed in the analysis of the data to loss, not biological transformation.

2.2.4 Degradation Rate Determination

The calculation and assumptions for the degradation rate have previously been described and evaluated (Speitel et al., 1993; for review, Alvarez-Cohen and Speitel, 2001). A pseudo first-order rate model for cometabolism was employed. The rate expression is as follows:

$$r = \frac{dS}{dt} = -k_1 X S \quad \text{Equation 2-1}$$

where:

- r = degradation rate (mg/L-day)
- k_1 = pseudo first-order rate constant (L/mg total suspended solids (TSS)-day)
- X = cell concentration (mg TSS/L)

S = chlorinated solvent concentration (mg/L)
 t = time (days).

The unique attribute of the work described for calculation of a degradation rate in this microcosm is the replacement of the total concentration of cells (X) with a more specific value, the abundance of cells with an active enzyme (i.e., the concentration of cells that exhibited positive response to an EAP). Since the microcosms contained both liquid and gas phases, it was assumed that these phases were in equilibrium. In that case, partitioning between liquid and gas phases is described by Henry's Law, and the following equation then applies (Speitel et al., 1993):

$$S = S_0 \exp\left(\frac{-k_1 X t}{1 + H \frac{V_G}{V_L}}\right) \quad \text{Equation 2-2}$$

where:

S = substrate (TCE) concentration (mg/L)
 S_0 = initial substrate (TCE) concentration (mg/L)
 k_1 = pseudo first-order rate constant (L/active cells-day)
 X = concentration of cells with active enzyme, as measured at each sampling event in the laboratory (active cells/L)
 t = time since the microcosms were built (days)
 H = dimensionless Henry's Law constant (0.415 for TCE; Gossett et al., 1985)
 V_G = volume of the gas in the microcosm (L)
 V_L = volume of the liquid in the microcosm (L).

Equation 2-2 was used to determine the TCE degradation rate constant for each treatment. The rate expression above was then applied to the field by scaling via the concentrations of active cells in the lab and field. The field measurement of the concentration of active cells, X_{field} , was made during the initial screening event in the fall of 2007 (1.5×10^5 cells/mL). The volume of gas in the field is assumed to be negligible; therefore, V_G is assumed to be zero. Thus, the rate expression was simplified to:

$$S = S_0 \exp(-k_1 X_{\text{field}} t) \quad \text{Equation 2-3}$$

where:

S = substrate (TCE) concentration (mg/L)
 S_0 = initial substrate (TCE) concentration (mg/L)
 k_1 = pseudo first-order rate constant (L/active cells-day) from laboratory study

X_{field} = field measurement of concentration of active cells (active cells/L)
 t = time (days).

Groundwater from TAN-29 was used in a microcosm study (Figure 2-3). EAP and GC analyses for VOCs were conducted over time following the initiation of the microcosm study. Activity stayed relatively constant over time, while contaminant concentrations decreased from time 0 to 450 hours (~19 days). Integrating activity, total biomass, and TCE over time allows for an estimation of degradation or attenuation. Control studies supported the finding that aerobic biodegradation contributed to the attenuation of TCE at the TAN site, more importantly in regions of the plume just downgradient of the source area.

2.3 Deployment of Colonized FTISRs (I)

Microorganisms in groundwater systems are either attached to particle surfaces or are not attached to particles but instead move freely in groundwater. Collection of groundwater samples selectively harvests the non-attached (planktonic) microorganisms, and thus laboratory microcosms prepared using groundwater contain a disproportionate amount of planktonic bacteria relative to attached bacteria. In order to obtain samples of the microbial community in the TAN plume, drilled cores of basalt from the aquifer were broken into coarse sand to fine gravel size grains, placed in a permeable bag, and suspended in the open interval of a well in the TAN medial zone. Groundwater actively flows through that part of the well and the basalt chips were exposed to microorganisms transported by groundwater, which inoculated the basalt chips. It is assumed that the microbial community that accumulates on the basalt chips is more representative of the in situ community than the community harvested by conventional groundwater sampling.

Inoculated basalt chips were used to fill FTISRs for subsequent deployment in a well and use in in situ experiments and, after recovery, characterization of the microbial community using various techniques by other researchers. Second, basalt chips and their associated biomass recovered from the FTISRs were used in a microcosm study to measure TCE degradation rates.

Microbial populations were colonized onto the surface of the chips over 3 to 4 months (March-June 2006) of exposure to groundwater by suspending a permeable bag of basalt chips in the screened interval of a well. After being inoculated with the groundwater microbial population, the chips were recovered from the well and used to construct the FTISRs, which were then deployed and remained down hole at TAN-35 for several months while groundwater was slowly pumped through the basalt chips and exposed biomass inside the reactors to hydraulic and geochemical conditions similar to those in the aquifer. Concurrently with the FTISR deployment period, groundwater was collected across the medial zone for geochemical and microbiological analysis (i.e., contaminant trends, stable carbon isotope ratios, microbial potential and activity). Collectively, data collected (groundwater across the medial zone and from the reactors) were used to assess contaminant degradation mechanisms and predict how microbial interactions affect contaminant degradation. Multiple molecular tools (EAP, FISH, and qPCR) demonstrate that microbial populations with oxygenase enzymes were present and active in all six of the FTISRs and in groundwater collected from well TAN-35 (Table 2-2). In general, the results from samples harvested from biomass that accumulated in FTISRs and from TAN-35 groundwater were similar; however, FISH analysis identified three groups of organisms in samples from the FTISRs that were not detected in groundwater samples, suggesting that the groundwater samples do not represent the entire subsurface community. Together with the associated microcosm study results, these data provide direct evidence that microorganisms capable of cometabolically degrading TCE under aerobic conditions are present in the medial zone at TAN, and that TCE is actually being degraded via aerobic cometabolic processes.

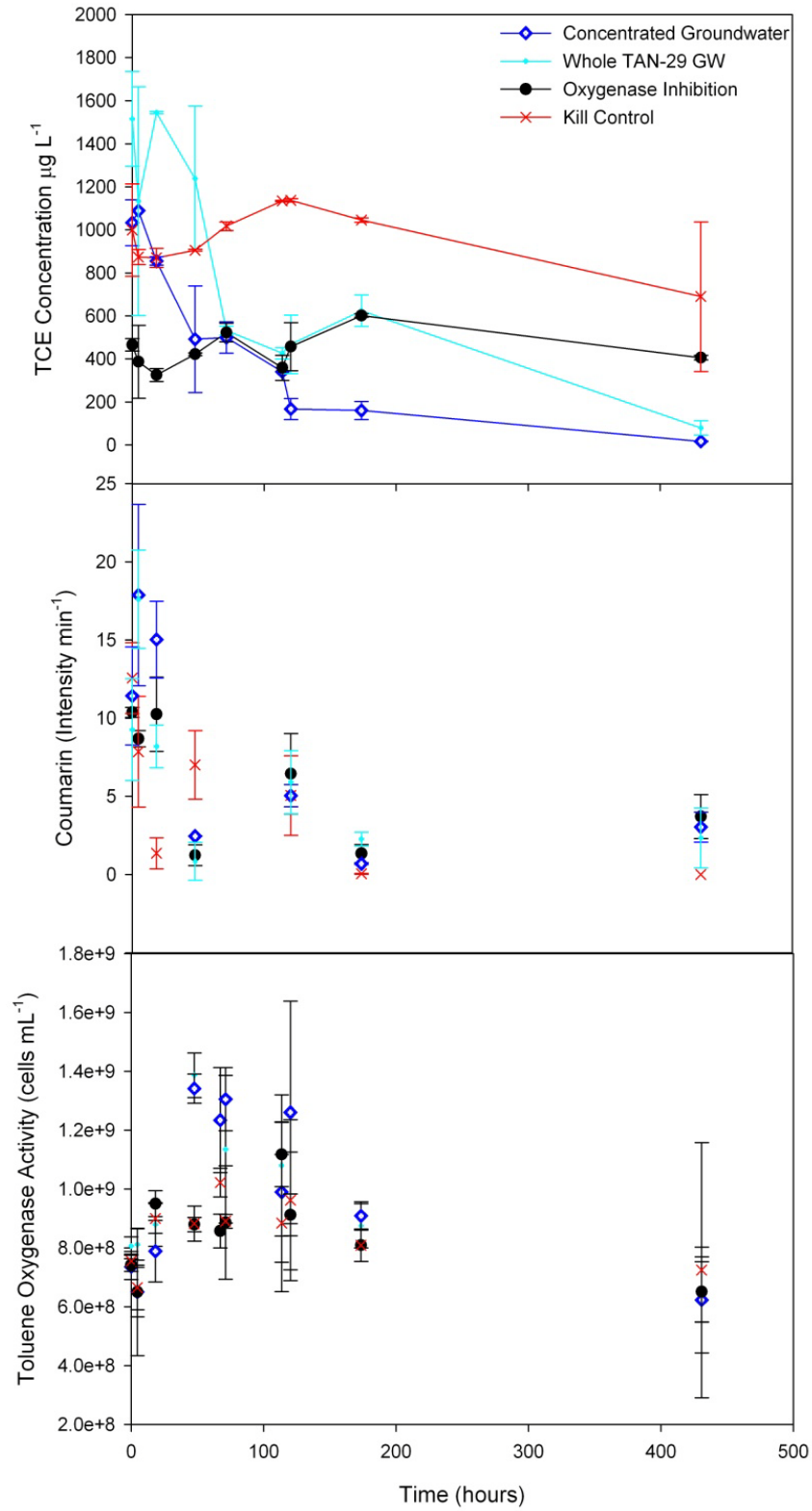


Figure 2-3. Results of microcosm with natural cells from the TAN contaminated aquifer, TAN-29. Top: TCE degradation over time. Middle and Bottom: sMMO and toluene oxygenase activity, respectively.

Table 2-2. FISH and EAP analysis of groundwater from monitoring well TAN-35 and reactors filled with colonized basalt chips. A positive indicates that the EAP or FISH probe showed a significant response for the targeted group.

Technique	Probe	Target	Medium						Ground water from TAN-35	
			Basalt Chips Recovered from Six FTISTRs after Incubation in TAN-35							
			1	2	3	4	5	6		
Enzyme Activity Probes	Coumarin	Soluble methane monooxygenase	+	+	+	+	+	+	+	
	Phenyl-acetylene	Toluene-2-monooxygenase	+	+	+	+	+	+	+	
		Toluene-3-monooxygenase								
	Trans-cinnamionitrile	Toluene-2,3-dioxygenase	+	+	+	+	+	+	+	
FISH		<i>Archaea</i>	+	+	+	+	+	+	+	
		<i>Eubacteria</i>	+	+	+	+	+	+	+	
		<i>Dehalococcoides</i>	+	+		+		+	+	
	Methanogens									
		M825	<i>Methanosaetaceae</i>	+		+	+		+	+
		M1174	most <i>Methanobacteriales</i>		+	+	+		+	
		M1109	<i>Methanococcales</i>	+					+	
		M1200	most <i>Methanomicrobiales</i>	+		+	+		+	+
		MSMX 860	<i>Methanosarcina, Methansaeta</i>	+	+	+	+	+	+	+
	Methanotrophs									
		M450	<i>Methylocystis, Methylosinus</i>	+	+	+	+	+	+	+
		M84	<i>Methylococcus, Methylobacter</i>	+	+	+		+		
		M705	<i>Methylococcaceae, Methylomonas</i>	+	+				+	+

2.4 Deployment of Colonized FTISTRs (II)

Based on the promising results from analysis of the microbial community recovered from the first deployment of FTISTRs, the FTISTRs were deployed with basalt chips a second time to support objectives

of other researchers and to measure degradation kinetics. In the spring of 2009, FTISRs were placed into well TAN 35 and left to incubate for several months. An experiment in which methane and TCE would be injected into the influent of the FTISR columns was planned; however, this experiment was abandoned in the summer of 2009 due to equipment failure. The reactors were retrieved in September 2009 and the inoculated basalt chips were used to assess microbial populations (i.e., abundance, diversity, activity, potential), and to set up microcosm studies to analyze degradation potential for TCE and estimate the degradation half-life for TCE.

2.4.1 On-going Studies at INL: Microcosms

Each groundwater sample will be analyzed with a suite of enzyme probes, including phenylacetylene, 3-hydroxy-phenylacetylene, trans-cinnamionitrile, and coumarin. Three of the four probes target aromatic oxygenases, the other (coumarin) targets methane monooxygenase. FISH will be performed on samples and will specifically target either the particulate methane monooxygenase (pMMO) or sMMO. Molecular assessments will also be performed for each groundwater sample to quantify the presence of DNA. DNA will be extracted and amplified based on the targeted oxygenases; in addition, real-time polymerase chain reaction (RT-PCR) and qPCR methods will be used to specifically target the particulate and soluble forms of the methane monooxygenase. These more aggressive molecular approaches will also be used to target groups of methanotrophs known to be important in the metabolism of TCE. Labeled methane will be added at low concentrations to measure rates of attenuation.

Microcosm incubations are presently ongoing at the INL to determine a TCE half-life based on aromatic and methane monooxygenase enzymes. INL is extracting ribonucleic acid (RNA) and DNA from all of the reactors to identify activity of dominant microbial populations. To date, it appears that TCE is being aerobically degraded in the microcosm studies and control (inhibition and kill) studies are supporting these data. The studies have been ongoing for approximately 8 weeks. qPCR analyses on basalt chips and water collected after the incubation showed abundance of *Eubacteria* (pseudomonads, aerobic species) and very little *Archaea* (methanogens, DHC).

2.5 Evaluation of Aerobic Cometabolic Degradation of TCE at Other Sites

Enzyme probes have been used to evaluate TCE degradation potential at a number of DOE and DOD sites over the last 5 years (Table 2-3; Lee et al., 2005; Lee, 2007; Wymore et al., 2007). Based on these analyses of contaminated groundwater, with TCE concentrations ranging from <100 to over 10,000 µg/L, it appears that enzyme probes provide a direct and accurate estimate of aerobic cometabolic activity for subsurface populations. Data collected at these sites also indicate that measurable aerobic degradation is occurring naturally in many large aerobic chlorinated solvent plumes. Field-scale estimates and lab microcosm studies suggest intrinsic chlorinated solvent half-lives on the order of 5 to 30 years (e.g., Lee et al., 2008, Wymore et al., 2007; Table 2-4). While such half-lives are greater than half-lives typically observed in anaerobic settings in which TCE and other chloroethenes degrade, they are relevant for stabilization of large plumes. The widespread occurrence of measurable aerobic cometabolism of TCE suggests a fundamental basis in microbial ecology and implies that the process generally occurs in aerobic groundwater systems and is sustainable. In summary, cometabolic degradation of chlorinated solvents is occurring and the apparent rates are consistent with the observed sizes and shapes of typical aerobic plumes.

Table 2-3. Enzyme activity probe applications at various DOD, DOE, and private industry field sites.

Site	Area	Enzyme Probe Results		Maximum TCE Concentration* (µg/L)
		Toluene ⁺	Methane ⁺	
Hill AFB	OU-10	+	+	1,000
Hill AFB	OU-9	+	-	1,000
Hill AFB	OU-11	+	+	1,000
Tinker AFB	Building 3001	+	+	18,000
INL	TAN, Medial Zone	+	+	2,500
INL	TAN, Distal Zone	+	+	350
Sandia National Laboratory	TA-V	+	+	100
Sandia National Laboratory	TAG site	+	+	50
Paducah Gaseous Diffusion Plant	North West plume	+	+	20,000
SRNL	C-BURP	+	+	1,000
SRNL	A-14 Area	+	+	14,000
SRNL	P-Area	+	+	8,500
SRNL	T-Area	+	+	30
El Toro, Former Marine Base	IRP Site	+	-	180
Atlas, WY	Missile Site 12	+	-	4,800
Atlas, WY	Missile Site 1	+	-	1,200
BP, Industrial Site	X (anonymous)	+	+	1,800
BP, Industrial Site	Y (anonymous)	+	-	2,500

+ A positive means that at least one of the wells sampled showed activity with the probe.
 * Approximate maximum concentration of TCE in sampled wells.

AFB = Air Force Base
 BP = British Petroleum
 INL = Idaho National Laboratory
 IRP = Installation Restoration Program
 OU = Operable Unit
 SRNL = Savannah River National Laboratory
 TA-V = Test Area V
 TAN = Test Area North

Table 2-4. Sites where laboratory microcosms have been completed; calculated degradation half-life for TCE under field conditions; and relevant geochemical description.

Site	TCE Concentration* (µg/L)	Co-Contaminant	Geochemical Conditions	Positive Enzyme Probe Results*	Half Life (under field conditions) (years)
OU-10 Hill AFB	<5 – 170	PCE, MTBE	Generally aerobic; low carbon	3HPA, PA, Cinn, Coumarin	~ 22
Building 3001 Tinker AFB	<5 – 5,900	Chromium, acetone, benzene, toluene, xylene, lead, nickle, barium, cadmium	Multiple zones of contamination; aerobic and anaerobic conditions throughout. Some measurable carbon	PA, 3HPA, Cinn	~ 15
T-Area SRNL	<5		Generally aerobic; low carbon	PA, 3HPA, Cinn, Coumarin	~ 30
TAN Idaho National Laboratory	<5 – 6,000	PCE, strontium, sewage	Regions of anaerobic (source area) and aerobic (medial-distal). Measureable carbon throughout plume	PA, 3HPA, Cinn, Coumarin	TAN-55: ~19.7 TAN-29: ~6.7
TA-V Sandia National Laboratory	<5 - 30	PCE, nitrate	Aerobic; very little carbon	PA, 3HPA, Cinn, Coumarin	~ 18
3HPA – 3-hydroxyphenylacetylene PA phenylacetylene Cinn – trans-cinnamionitrile *TCE concentration range associated with measured rates					

3. MODELING COMETABOLISM AND TCE ATTENUATION

3.1 Introduction

Groundwater flow and transport models are commonly used to predict the evolution of contaminant plumes under various management scenarios, such as active remediation of high concentration portions of plumes and natural attenuation of lower concentration portions of plumes. This research project is primarily related to the natural attenuation application, in which TCE or other contaminants degrade without active intervention. Credible, defensible simulations of plume evolution are likely to be a substantial component of a line of evidence that natural attenuation is a suitable management alternative.

Groundwater simulations typically include a flow simulation and a contaminant transport simulation. Contaminant transport codes typically account for advection, dispersion, sorption, sources and sinks, reactions, and possibly other processes. The reaction components are of interest in this study, and can be used to account for a wide processes including biologically-mediated transformation of contaminants. An important aspect of simulating transport of a contaminant that undergoes transformation during transport is accounting for the kinetics of the transformation reaction.

One of the objectives of this project was to improve our ability to simulate transport of TCE in groundwater while undergoing cometabolic degradation. The approach included incorporating appropriate kinetic expression (competitive inhibition) for cometabolic degradation into a reactive transport code, parameterizing that expression, and then comparing plume evolution simulated using the enhanced code with plume evolution simulated using a more traditional description of degradation kinetics (first order decay). A result of this comparison is a basis for determining if the added difficulty in parameterizing the more complicated kinetic expression is warranted.

In this section, we describe some of the numerous kinetic models for cometabolic biodegradation of contaminants in groundwater, approaches for determining the values of parameters in the kinetic equations, and incorporation of the kinetic expression into flow and transport simulation software. We then present a parametric study of cometabolic TCE degradation via competitive inhibition kinetics in a batch reactor to determine the effect of various terms in the kinetic expressions. Next, we use the transport code with the competitive inhibition kinetics and with first order decay kinetics to simulate TCE plume evolution in a plume, and investigate the effect of changing parameter values on plume evolution.

The results of these activities include (1) a new competitive inhibition kinetic module for a widely-used reactive transport code, (2) an improved understanding of the effect of each term in the competitive inhibition model, (3) a rational basis for evaluating if the added difficulty in using the competitive inhibition model is justified.

3.2 Microbial Degradation Kinetic Models

Biologically-mediated transformation of groundwater contaminants are kinetically-controlled processes (i.e., they do not occur instantaneously). The ability to make reasonable predictions of how contaminant plumes in groundwater will evolve over time is based on the kinetic expressions embedded in a transport simulation code being a reasonable description of the actual degradation kinetics, and that those kinetic expressions can be defensibly parameterized (i.e., that numerical values can be specified for each parameter in the kinetic expressions, and that there is a defensible basis for those values).

3.2.1 Background

TCE is biodegraded by different mechanisms under anaerobic and aerobic conditions. Under anaerobic conditions, bacteria couple oxidation of organic carbon with reduction of TCE to obtain the energy they need for maintenance and growth. As TCE is reduced, a chlorine atom is replaced by a hydrogen atom, and the reaction product is DCE. The process, ARD, is beneficial to the responsible organism, which harvests energy from the reaction.

Under aerobic conditions, TCE is oxidized by bacteria, but the responsible organism does not derive energy from the reaction. Instead, TCE is oxidized by an enzyme that bacteria synthesize to derive energy by oxidizing a different compound to obtain energy (i.e., ammonia, toluene, phenol, or methane). The fortuitous transformation of a compound by an enzyme synthesized for another purpose, without yielding energy or other benefit to the organism that synthesized the enzyme is known as *cometabolism*. Hence, under aerobic conditions, TCE is said to be cometabolized or cometabolically degraded.

In order for TCE to be cometabolically degraded, the following conditions must occur.

- TCE must be present.
- Conditions must be aerobic. Measured dissolved oxygen (DO) concentrations in groundwater greater than 1 mg/L are typically considered to be aerobic.
- Bacteria capable of producing enzymes that can oxidize TCE must be present.
- In order for the bacteria to survive and produce enzymes that cometabolize, a primary substrate that can be utilized by the bacterial must be present at sufficient concentrations to sustain the community and to induce production of the TCE-cometabolic enzymes.
- Enzymes that can oxidize TCE must be present, and they must be active. Enzymes may require the presence of an additional compound, known as a co-enzyme or a co-factor, in order to react with a substrate. If all of the requisite compounds are present such that the enzyme does react with a particular substrate, the enzyme is said to be active.

It is assumed that if enzymes that cometabolize TCE are present and active in a bacterial community, then TCE will be cometabolized. Hence, if the EAP technique (Section 2) indicates that the targeted enzymes are active, then it is assumed that they will cometabolize TCE.

3.2.2 Kinetic Models

The following discussion of kinetic models is based primarily on Alvarez-Cohen and Speitel (2001).

3.2.2.1 Michaelis/Menton Kinetic Model

The Michaelis-Menton expression that describes kinetics of enzyme-based reactions is:

$$r_c = -\frac{k_c X S_c}{K_{sc} + S_c} \quad \text{Equation 3-1}$$

where

k_c = maximum specific rate of substrate degradation (mg substrate (mg cells)⁻¹ d⁻¹)

K_{sc}	=	half-saturation constant for the substrate (mg L^{-1})
r_c	=	rate of the reaction ($\text{mg L}^{-1} \text{d}^{-1}$)
S_c	=	substrate concentration (mg L^{-1})
X	=	the active microbial concentration (mg cells L^{-1}) (Alvarez-Cohen and Speitel, 2001; equation 1).

3.2.2.2 First Order Decay

A reaction with first-order kinetics is one in which the reaction rate is proportional to concentration:

$$r = \lambda S \quad \text{Equation 3-2}$$

where

r	=	reaction rate (mass/volume – time)
λ	=	reaction rate coefficient (1/time)
S	=	reactant concentration (mass/volume).

In the case where the substrate concentration is substantially less than the half-saturation constant, the S term in the denominator of Michaelis-Menton expression becomes insignificant, and the expression is approximately equal to the first order expression:

$$r_c = -k_1 X S_c \quad \text{Equation 3-3}$$

where

k_1	=	pseudo first-order cometabolic degradation rate coefficient ($\text{L (mg cells)}^{-1} \text{d}^{-1}$)
k_1	=	ratio k_c/K_{sc} (Alvarez-Cohen and Speitel, 2001; equation 3).

The attractiveness of the first-order decay model for application to field sites is its simplicity, in that the kinetic model can be parameterized using only two terms (k_1 and X). In cases where the coefficient is estimated from spatial concentration trends (e.g., Sorenson et al., 2000), the combined term $k_2 = k_1 X$ is typically estimated. In that case, the kinetic model is parameterized using only a single term, λ . Although a first-order model clearly does not account for a variety of factors in the microbial processes responsible for contaminant degradation (i.e., growth and death of cells, competition, inhibition and toxicity effects), it is unlikely that the values needed to parameterize more complicated kinetic models can be feasibly determined for in situ conditions, although it may be feasible to determine parameter values in laboratory or ex situ bioreactor conditions. Hence, a simpler model that can be parameterized may have more utility for simulating in situ processes than more complicated models that provide a more rigorous description of microbial processes but cannot feasibly be parameterized.

3.2.2.3 Competitive Inhibition Model

A feature of a cometabolic process is that an enzyme produced to interact with a growth substrate, such as a hydrocarbon, coincidentally also interacts with a non-growth substrate, such as a chlorinated

hydrocarbon. The growth substrate and non-growth substrate compete for active sites on the enzyme involved in the cometabolic process; hence, high concentrations of one substrate inhibit reactions of the other substrate with the enzyme. This interaction is referred to as competitive inhibition.

A practical implication of competitive inhibition is that high concentrations of the cometabolic substrate relative to growth substrate interfere with the enzyme-producing organism's ability to obtain energy from the growth substrate and subsequently to synthesize additional enzyme. Hence, the ratio of cometabolic substrate to growth substrate, and the relative affinity of the enzyme for each, is important with respect to the rate and long-term viability of a cometabolic process.

The Michaelis-Menton equation for transformation of a growth substrate and of a cometabolic substrate, modified to account for competitive inhibition, are shown below (Alvarez-Cohen and Speitel, 2002; equations 4 and 5).

$$r_g = - \frac{X k_g S_g}{K_{Sg} \left(1 + \frac{S_c}{K_{isc}} \right) + S_g}$$

Equation 3-4

$$r_c = - \frac{X k_c S_c}{K_{Sc} \left(1 + \frac{S_g}{K_{isg}} \right) + S_c}$$

where

- k_c = maximum specific rate of cometabolic substrate degradation (mg substrate (mg cells)⁻¹d⁻¹)
- k_g = maximum specific rate of degradation substrate degradation (mg substrate (mg cells)⁻¹d⁻¹)
- K_{isc} = inhibition coefficient for the cometabolic substrate (mg L⁻¹)
- K_{isg} = inhibition coefficient for the growth substrate (mg L⁻¹)
- K_{Sc} = half-saturation coefficient for the cometabolic substrate (mg L⁻¹)
- K_{Sg} = half-saturation coefficient for the growth substrate (mg L⁻¹)
- r_c = rate of the cometabolic substrate reaction (mg L⁻¹ d⁻¹)
- r_g = rate of the growth substrate reaction (mg L⁻¹ d⁻¹)
- S_c = concentration of cometabolic substrate (mg L⁻¹)
- S_g = concentration of growth substrate (mg L⁻¹)
- X = the active microbial concentration (mg cells L⁻¹).

The subscripts *g* and *c* refer to growth substrate (e.g. methane) and cometabolic substrate (e.g., TCE), respectively.

A common assumption is that $K_{isc} = K_{sc}$ and $K_{isg} = K_{sg}$, yielding the following expressions for competitive inhibition kinetics.

$$r_g = - \frac{X k_g S_g}{K_{Sg} \left(1 + \frac{S_c}{K_{Sc}} \right) + S_g}$$

Equation 3-5

$$r_c = - \frac{X k_c S_c}{K_{Sc} \left(1 + \frac{S_g}{K_{Sg}} \right) + S_c}$$

Numerical values for the following seven parameters are needed to parameterize this kinetic model:

- X
- k_c , K_{sg} , and S_g for the growth substrate
- k_c , K_{sc} , and S_c for the cometabolic substrate.

Hence, this kinetic model is more difficult to parameterize and apply than is the first order decay model.

3.2.2.4 Competitive Inhibition Kinetic Model with Low Dissolved Oxygen Inhibition

The expressions used to simulate utilization of methane as a growth substrate and cometabolism of TCE in a batch reactor were developed in Section 3.2.2.3, with the addition of a term that inhibits these aerobic processes at low concentrations of DO.

$$r_g = - \frac{X k_g S_g}{K_{Sg} \left(1 + \frac{S_c}{K_{Sc}} \right) + S_g} \times \frac{S_{ox}}{K_{S_{ox}} + S_{ox}}$$

Equation 3-6

$$r_c = - \frac{X k_c S_c}{K_{Sc} \left(1 + \frac{S_g}{K_{Sg}} \right) + S_c} \times \frac{S_{ox}}{K_{S_{ox}} + S_{ox}}$$

where

S_{ox} concentration of DO (mg/L)

$K_{S_{ox}}$ half-saturation coefficient for DO (mg/L).

Other terms are as defined previously.

The inhibition term varies from zero at DO concentration to one at some non-zero concentration. The value of the half-saturation coefficient controls how quickly the inhibition coefficient approaches one. The low oxygen inhibition coefficient is discussed in greater detail in Section 3.4.

3.2.2.5 Others

More complicated kinetic models that account for additional processes, including utilization of multiple substrates, non-competitive inhibition, degradation product toxicity, changes in population density, reductant limitation, and others have been developed (see Alvarez-Cohen and Speitler, 2001 and references cited therein). These more complicated kinetic models typically include additional parameters. Although these parameters may be quantifiable under laboratory conditions, the problem of parameterizing a model to describe field conditions becomes more difficult as the number of parameters required increases.

The current study is focused on natural attenuation of TCE in aerobic groundwater, not enhanced bioremediation. Under natural attenuation conditions, it is likely that the microbial community is at steady state, with relatively low concentrations of both the growth substrate and the cometabolic substrate (TCE). Under these conditions, the additional complexity of kinetic models that consider changes in microbial population is not warranted.

3.3 Compilation of Cometabolic Degradation Kinetic Parameter Values

3.3.1 Literature Values for Kinetic Parameters

Numerical values for kinetic parameters of the competitive inhibition model compiled from the literature are presented in Tables 3-1 through 3-3 (Alvarez-Cohen and Speitel, 2001). They compiled values for TCE cometabolism but not values for substrate utilization. In some cases, values for substrate utilization kinetic parameters were reported in the references cited by Alvarez-Cohen and Speitel, 2001; selected values for substrate utilization are included here.

TCE and other chlorinated ethanes are cometabolized by organisms that use a variety of growth substrates, including methane, propane, phenol, toluene, and ammonia (Anderson and McCarty, 1996, and references cited therein). For this study, we focus on TCE cometabolism by methanotrophs as a result of the conceptual model that methane is likely the growth substrate utilized by bacteria in groundwater at the TAN site at the INL, and the focus of other researchers involved in this project on methanotrophs.

Two methane-oxidizing enzymes are involved in TCE cometabolism: particulate methane monooxygenase (pMMO), and soluble methane monooxygenase (sMMO). All methanotrophs produce the particulate form, but only some produce the soluble form, and then only under copper-limited conditions. Hence, "typical conditions in nature are likely to favor pMMO expression" (Anderson and McCarty, 1996, and references cited therein). Rates of TCE cometabolism tend to be slower for pMMO than for sMMO (see Table 3-1). However, methanotrophs harvested from the aquifer at the TAN site have both pMMO and sMMO (Colwell, 2009), and hence both pMMO and sMMO are relevant to this study.

In their review of the literature related to kinetics of aerobic cometabolism of chlorinated solvents, Alvarez-Cohen and Speitel (2001) compiled kinetic parameter values for TCE cometabolism by methanotrophs and aromatic degraders, and other bacteria; their compilations are presented here as Tables 3-1 through 3-3. Of the cases compiled, the ones of most interest in this study are for either no additional substrate or methane as an additional substrate, and studies in which values are reported for k_c and K_{Sc} . For the cases that meet these criteria, the original references were examined to determine if kinetic values for methane consumption were also reported. Table 3-4 provides a compilation of these values.

The values included in Table 3-5 were selected for use in a parametric study of the competitive inhibition kinetics presented in subsequent sections.

Table 3-1. Kinetic coefficients for methanotropic cometabolism of TCE (Alvarez-Cohen and Speitel, 2001).

Table 1. Selected kinetic coefficients for methanotrophic cometabolism of TCE

Organism/condition	Initial TCE conc. (mg/L)	Additional substrate	Temperature (°C)	k_c (mg/mg-day) ¹	K_{Sc} (mg/L)	k_1 (L/mg-day) ¹	T_c (μg/mg)	T_y (μg/mg) ¹	Reference
<i>M. trichosporium</i> OB3b, sMMO	4–90	Formate	30	55	19	2.9	290	150	a
<i>M. trichosporium</i> OB3b, sMMO	2.6	None	30	3.8	7.2	0.53			b
<i>M. trichosporium</i> OB3b, sMMO	4	None		1.0	10	0.1	320		c
<i>M. trichosporium</i> OB3b, pMMO	0.13–8.5	None	24	0.24	4.7	0.05			d
<i>M. trichosporium</i> OB3b, pMMO	0.13–8.5	Formate	24	0.39	1.0	0.37			d
<i>M. trichosporium</i> OB3b, PP358, sMMO	0.06–8	Formate	23	21	11	1.4	150		e, f
Mixed culture	0.15	Methane	25			0.0052			g
Mixed culture	4	None	20			0.008		29	h
Mixed culture, biofilm	0.9	None	20–24			0.0029		34	i
Mixed culture, 0.06 μM Cu ²⁺	0.03–0.07	None	21			0.041			j
Mixed culture, no Cu ²⁺	0.03–0.07	None	21			0.62			j
<i>Methyomonas</i> sp. MM2, pMMO	0.03–0.07	None	21	0.046	1.4	0.033			j
<i>Methyomonas</i> sp. MM2, pMMO	0.03–0.07	EDTA	21	0.29	0.51	0.57			j
<i>Methyomonas</i> sp. MM2, pMMO	0.03–0.06	Formate	21			2.3	28		p
Mixed culture, sMMO	15	None	21	0.84	0.69	1.2	43	15	k
Mixed culture, sMMO	0.4–25	Formate	21	7.6	8.2	0.93	80	28	k
Mixed culture, sMMO, N ₂ fixing	2.2	None	20			0.28	56	21	l
Mixed culture, sMMO, N ₂ fixing	2.2	Formate	20			0.54	140	52	l
Mixed culture, sMMO	0.5–60	Formate	20	9.6	6.2	1.6	540	180	m
Mixed culture, sMMO	0.5–30	None	20	1.0	3.8	0.27	50	17	n
Mixed culture, sMMO	0.5–30	Formate	20	4.2	7.0	0.6	100	34	n
Mixed culture, sMMO	0.5–9	Methane	21	0.15	1.9	0.078	60		o
Mixed culture, sMMO	5.9	None	25			0.35	210		t
Mixed culture, pMMO	1	Methane	20	>0.012	0.13	>0.092	25	16	q, r
<i>Methyomonas methanica</i> 68-1, sMMO	6.6–66	Formate	25	3.7	30	0.12			s
Average ²				6.8	7.0	0.61	150	52	
Standard deviation				14	7.8	0.76	150	57	

a. Oldenhuis et al. 1991; b. Tsien et al. 1989; c. Tompson et al. 1994; d. Lontoh & Semrau 1998; e. Aziz et al. 1999; f. Fitch et al. 1996; g. Leeson & Bouwer 1989; h. Strand et al. 1991; i. Arvin 1991; j. Henry & Grbic-Galic 1990; k. Alvarez-Cohen & McCarty 1991b; l. Chu & Alvarez-Cohen 1996; m. Chang & Alvarez-Cohen 1996; n. Chang & Alvarez-Cohen 1995a; o. Chang & Criddle 1997; p. Henry & Grbic-Galic 1991; q. Anderson & McCarty 1996; r. Anderson & McCarty 1997; s. Koh et al. 1993; t. Smith et al. 1997.

¹ Biomass reported in mg dry cell mass; units conversions assume dry cell mass is 50% protein.

² Average and standard deviation computed by ignoring ">" signs and by assuming a range can be approximated by taking one sample value at the top and one at the bottom of the range.

Table 3-2. Kinetic coefficients for TCE cometabolism by aromatic degraders (Alvarez-Cohen and Speitel, 2001).

Table 2. Selected kinetic coefficients for TCE cometabolism by aromatic degraders

Organism/condition	Initial TCE conc. (mg/L)	Additional substrate	Temperature (°C)	k_c (mg/mg-day) ¹	K_{Sc} (mg/L)	k_1 (L/mg-day) ¹	T_c (μg/mg)	T_y (μg/mg) ¹	Reference
<i>Pseudomonas cepacia</i> G4, phenol	0.66–6.6	None	26–28	1.5	0.39	3.8	34		a, b
<i>Pseudomonas cepacia</i> G4, toluene	0–10	Toluene	28	0.94	0.79	1.2		14	h
<i>Pseudomonas putida</i> , toluene	2.6	Toluene	30			0.19	5.2		n
<i>Pseudomonas putida</i> B2 & TVA8, toluene	5	Toluene	28	1.3	6.4	0.20			o
Mixed culture, chemostat, phenol	0.1	None	23			0.012–0.48	>15		e
Mixed culture, chemostat, phenol	1–20	None	20	0.21	2.04	0.10	3.1	1.7	f
Mixed culture, chemostat, phenol	20	Phenol	20				3.4	1.9	f
Mixed culture, chemostat, phenol	27	None	21				240	110	j
Mixed culture, chemostat, phenol	1–25	None	20	0.33	11	0.030	82	52–222	m
Mixed culture, chemostat, toluene	1–30	None	20	0.17	8.64	0.020	7.3	2.1	f
Mixed culture, chemostat, toluene	30	Toluene	20				8.5	2.5	f
Mixed culture, biofilm, phenol	0.1–2	None	23	0.038–0.15	0.23–0.67	0.055–0.18	13–29		c, d
Mixed culture, biofilm, toluene	40–135	Toluene	20	0.38	0.17	2.2			g
Mixed culture, soil slurry, phenol	0.66	Phenol	20			0.08–0.13			i
Mixed culture, soil slurry, toluene	0.66	Toluene	20			0.07–0.15			i
Mixed culture, semi-batch, phenol	25	None	20	0.18			>510		k
Mixed culture, microcosm, phenol		Phenol	–					170	l
Average ²				0.52	3.4	0.56	86	64	
Standard deviation				0.53	4.2	1.0	160	84	

a. Folsom et al. 1990; b. Folsom & Chapman 1991; c. Segar 1994; d. Segar et al. 1995; e. Speitel et al. 1990; f. Chang & Alvarez-Cohen 1996; g. Arcanlegi & Arvin 1997; h. Landa et al. 1994; i. Jenal-Wanner & McCarty 1997; j. Hopkins et al. 1993; k. Bielefeldt et al. 1995; l. Tovanabootr et al. 1997; m. Shurtleff et al. 1996; n. Heald & Jenkins 1994; o. Kelly et al. 2000.

¹ Biomass reported in mg dry cell mass; units conversions assume dry cell mass is 50% protein. ² Average and standard deviation computed by ignoring “>” signs and by assuming a range can be approximated by taking one sample value at the top and one at the bottom of the range.

Table 3-3. Kinetic coefficients for TCE cometabolism by other bacteria (Alvarez-Cohen and Speitel, 2001).

Table 3. Selected kinetic coefficients for TCE cometabolism by other bacteria

Organism/condition	Initial TCE conc. (mg/L)	Additional substrate	Temperature (°C)	k_c (mg/mg-day) ¹	K_{Sc} (mg/L)	k_1 (L/mg-day) ¹	T_c (μg/mg)	T_y (μg/mg) ¹	Reference
Mixed culture, chemostat, propane	0.5–16	None	20	0.45	5.22	0.086	6.5	5.6	a
Mixed culture, chemostat, propane	16	Propane	20				13.9	11.9	a
<i>Mycobacterium vaccae</i> JOB5, propane		None	30	0.057	0.58	0.098			b
<i>Mycobacterium vaccae</i> JOB5, propane	0.03–5.4	Propane	25			0.014			c
Mixed culture, chemostat, propane	3	None	20	0.038	0.6	0.064			d
<i>Nitrosomonas europaea</i> , ammonia	0–3.3	Ammonia	22	1.0	1.4	0.74	8		e
<i>Nitrosomonas europaea</i> , ammonia	2.1	Ammonia	22	1.6	1.6	1.02	13		f
<i>Rhodococcus erythropolis</i> BD1, isopropylbenzene	3.3–26	None	30			0.018			g

a. Chang & Alvarez-Cohen 1995a; b. Wackett et al. 1989; c. Wilcox et al. 1995; d. Keenan et al. 1994; e. Ely et al. 1995b; f. Ely et al. 1997; g. Dabrock et al. 1992.

¹ Biomass reported in mg dry cell mass; units conversions assume dry cell mass is 50% protein.

Table 3-4. Kinetic parameter values for TCE and methane degradation.

Organism/Conditions	Initial TCE Concentration (mg/L)	Additional Substrate	Temperature (°C)	k_c (mg/mg-day)	K_{Sc} (mg/L)	k_g (mg/mg-day)	K_{Sg} (mg/L)	Reference
<i>M. Tricosporium</i> OB3b, pMMO	0.13-8.5	None	24	0.24	4.7	0.94-3.46	0.13-0.99	d
<i>Methylomonas</i> sp. MM2, pMMO	0.03-0.07	None	21	0.046	1.4	1.24-1.31	Not determined	j
Mixed culture, sMMO	15	None	21	0.84/0.53	0.69/0.37	Not determined	Not determined	k
Mixed culture, sMMO	0.5-30	None	20	1.0	3.8	1.03	3.8	n
Mixed culture, sMMO	0.5-9	Methane	21	0.15	1.9	3.77	6.85	o
Mixed culture, pMMO	1	Methane	20	>0.02	0.13	2.67	0.0156	q
Reference		Citation						
d	Lontoh, S., and J.D. Semrau, 1998. "Methane and trichloroethylene degradation by <i>Methylosinus trichosporium</i> OB3b expressing particulate methane monooxygenase." <i>Applied and Environmental Microbiology</i> 64: 1106-1114.							
j	Henry, S.M., and D. Grbic-Balic, 1990. "Effect of mineral media on trichloroethylene oxidation by aquifer methanotrophs." <i>Microbial Ecology</i> 20:151-169.							
k	Alvarez-Cohen, L., and P.L. McCarty, 1991. "A cometabolic biotransformation model for halogenated aliphatic compounds exhibiting product toxicity." <i>Environmental Science and Technology</i> 25:1381-1387.							
n	Chang, H-L., and L. Alvarez-Cohen, 1995. "Transformation capacities of chlorinated organics by mixed cultures enriched on methane, propane, toluene, or phenol." <i>Biotechnology and Bioengineering</i> 45:440-449.							
o	Chang, W-K., and C.S. Criddle, 1997. "Experimental evaluation of a model for cometabolism: prediction of simultaneous degradation of trichloroethylene and methane by a methanotrophic mixed culture." <i>Biotechnology and Bioengineering</i> 56:492-501.							
q	Anderson, J.E., and P.L. McCarty, 1996. "Effect of three chlorinated ethenes on growth rates for a methanotrophic mixed culture." <i>Environmental Science and Technology</i> 30:3517-3524.							

Table 3-5. Summary of literature values of kinetic parameters for methane oxidation and TCE cometabolism.

	k_c (mg/mg-day)	K_{Sc} (mg/L)	k_g (mg/mg-day)	K_{Sg} (mg/L)
Literature values for pMMO	>0.02 – 0.24	0.13 - 4.7	0.94 - 3.46	0.0156 - 0.99
Representative range for sensitivity study: pMMO case	0.02 – 0.3	0.1 - 5	1 - 4	0.01 – 1
Ratio Max/Min	15	50	4	100
Literature values for sMMO	0.15 - 1.0	1.9 - 3.8	1.03 - 3.77	3.8 - 6.5
Representative range for sensitivity study: sMMO case	0.1 - 1	1 - 5	1 - 4	3 - 7
Ratio Max/Min	10	5	4	2

3.3.2 Methane Concentrations

Methane concentrations measured in groundwater in the distal portion of the TAN TCE plume are approximately 0.1 to 1 µg/L. This range was selected for use in this study.

3.3.3 Biomass Concentration

Values of biomass concentration re needed to parameterize the competitive inhibition kinetic model. Methanotroph population density was measured (Radtke et al., 2008) in the distal portion of the TAN TCE plume. The measured population density reported in cells per mL were converted into biomass concentration (Table 3-6) using the conversion factor of 170 fg/cell (Balkwill et al., 1988).

A range of 1 E-3 to 1 E-2 mg/L was selected for use in this study.

Table 3-6. Methanotroph biomass concentration.

Well Sampled	Methanotroph Population Density (cells/mL)	Biomass Concentration (mg cells/mL)	Biomass Concentration (mg cells/L)
TAN-36	1.1 E+4	1.9 E-6	1.9 E-3
TAN-58	2.5 E+4	4.3 E-6	4.3 E-3

3.4 Parametric Study of Competitive Inhibition Kinetic Model

A parametric study of the competitive inhibition kinetic model developed in Section 3.2.2.4 is included in this section to illustrate the effect of each parameter on degradation rates as a function of substrate concentrations, and on changes in concentration over time. These simulations were performed for a batch reactor (e.g., a flask on a lab bench) to eliminate the complexities introduced by a flow and transport simulation, and because it is much more efficient in terms of computer and personnel resources to perform calculations for a batch reactor than for a groundwater flow system. The batch reactor calculations were performed using a Visual Basic routine in a Microsoft Excel spreadsheet. Groundwater flow and transport simulations mentioned in this section and described in greater detail in a subsequent section were performed using MODFLOW and RT3D in the Groundwater Modeling System (GMS) 6.5 environment.

Batch reactor simulations are presented in this section to illustrate the effect of each parameter in the competitive inhibition kinetic model on degradation rate as a function of substrate concentration, and on concentration as a function of time. Next, a series of simulations is presented to illustrate the range of degradation rates and concentration trends that might be expected based on the range of kinetic parameter values gleaned from the literature and microbial biomass, methane, and TCE concentrations measured at the TAN TCE plume. Finally, kinetic parameter values intermediate between the minimum and maximum literature values are selected that result in concentration trends that are roughly comparable to those observed in the TAN TCE plume. These parameter values are used in flow and transport simulations described in the following section.

Although biomass, methane, and TCE concentrations were derived from measurements made at the TAN TCE plume, and kinetic parameter values were selected to roughly mimic concentrations in the TAN TCE plume, the batch reactor simulations and the flow and transport simulations presented here are not intended to predict current or future conditions in the TAN TCE plume. The results of on-going remedial activities at the TAN site are not captured in these models, and hence these simulations do not predict expected concentration trends at TAN. Instead, information from TAN and an existing flow and transport model were used in this study due to their availability to the authors, and previous studies that show that aerobic cometabolism of TCE occurs in a large portion of the plume.

3.4.1 Low Dissolved Oxygen Inhibition Term

A term that slows the reaction rate at low DO concentrations was added to the conventional competitive inhibition expressions. Degradation rates for both the growth substrate and the cometabolic substrate are multiplied by the low oxygen inhibition coefficient. At DO concentrations well above the half-saturation coefficient (Figure 3-1), the inhibition coefficient value is close to one and therefore the inhibition coefficient has little effect. At DO concentrations below the half-saturation coefficient, the inhibition coefficient value approaches zero, and therefore the degradation rate approaches zero. Thus, this term essentially turns off both utilization of the growth substrate and degradation of the cometabolic substrate at low DO concentrations.

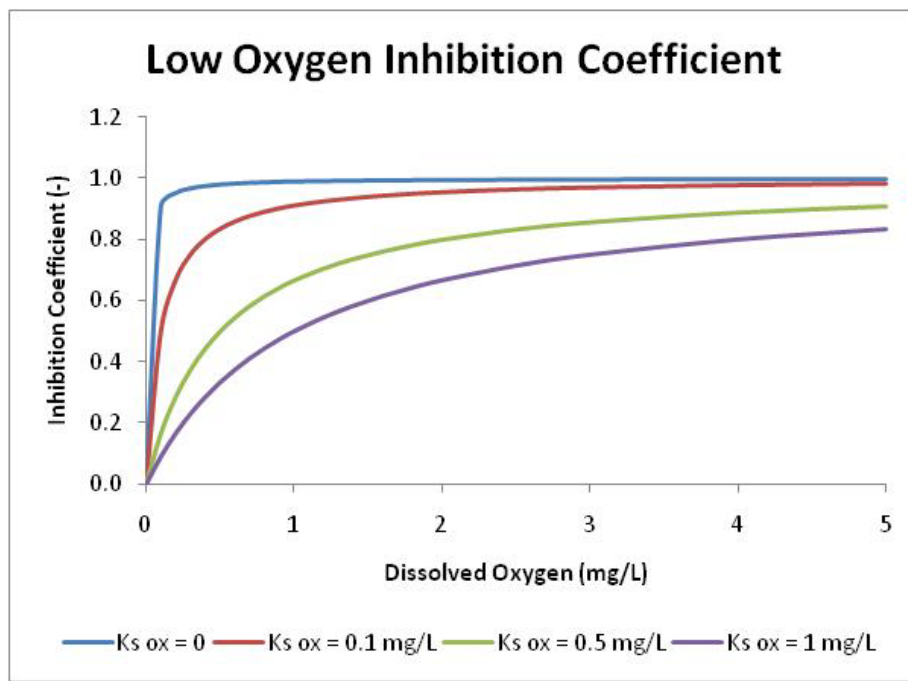


Figure 3-1. Effect of half-saturation coefficient on low-oxygen inhibition term.

The low oxygen inhibition term simply scales both the growth substrate rate and the cometabolic substrate rate by the same factor. Due to the simplicity of this effect, it is not investigated further in this parametric study. In the batch reactor simulation results presented here, DO and half-saturation coefficients were specified such that the low DO inhibition coefficient was equal to one, and thus the reaction rates were not inhibited by low DO concentrations.

3.4.2 Parametric Study of Competitive Inhibition Kinetics in a Batch Reactor

Reaction rates are proportional to the biomass concentration, X (mg cells/ L), and the same biomass concentration value is used in the rate expression for both the growth substrate and the cometabolic substrate. Given the linear relationship between biomass concentration and reaction rate, no figures are provided to illustrate this relationship.

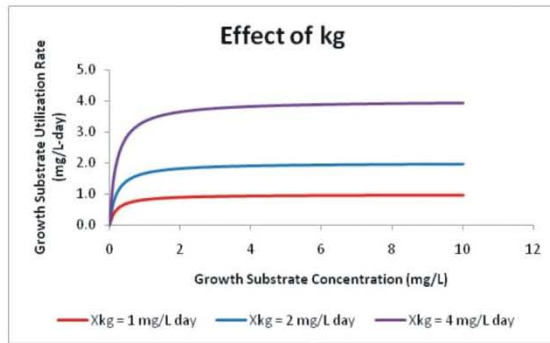
The effect of the maximum specific rate coefficient k (mg substrate/day per mg biomass/L), half-saturation coefficient K_s , (mg/L), and the competitive inhibition ration S/K_s (-) on reaction rate as a function of substrate concentration is illustrated for both the growth substrate and cometabolic substrate (Figure 3-2). The form of the reaction rate equation is the same for both substrates and therefore, the parameters applicable to each equation have the same effect on the reaction rate as a function of concentration curves.

The effects of each parameter on the reaction rate versus substrate concentration curve are summarized in Table 3-7.

Table 3-7. Summary of effect of increasing parameter values on reaction rates.

Parameter	Effect on Reaction Rate for Growth Substrate, r_g	Effect on Reaction Rate for Cometabolic Substrate, r_c
Low oxygen inhibition term, $S_{ox}/(K_{sox} + S_{ox})$	No effect for $S_{ox} \gg K_{sox}$. Rate reduced for smaller ratios of S_{ox} to K_{sox}	No effect for $S_{ox} \gg K_{sox}$. Rate reduced for smaller ratios of S_{ox} to K_{sox}
Biomass concentration, X	Larger X increases rate	Larger X increases rate
Maximum specific rate coefficient for growth substrate, k_g	Larger k_g increases rate. Plateau value is equal to k_g	No effect
Half-saturation coefficient for growth substrate, K_{sg}	Larger K_{sg} shifts curve to the right. At a given substrate concentration, r_g decreases with increasing K_{sg}	For a given S_g , increasing K_{sg} reduces the growth substrate inhibition ratio (see below)
Cometabolic substrate inhibition ratio, S_c/K_{sc}	Increasing ratio reduces rate due to competitive inhibition	For $S_c \ll K_{sc}$, the rate expression approaches a first-order expression
Maximum specific rate coefficient for cometabolic substrate, k_c	No effect	Larger k_c increases rate. Plateau value is equal to k_c
Half-saturation coefficient for cometabolic substrate, K_{sc}	For a given S_c , increasing K_{sc} reduces the cometabolic substrate inhibition ratio (see above)	Larger K_{sc} shifts curve to the right. At a given cometabolic substrate concentration, r_c decreases with increasing K_{sc}
Growth substrate inhibition ratio, S_g/K_{sg}	For $S_g \ll K_{sg}$, the rate expression approaches a first-order expression	Increasing ratio reduces rate due to competitive inhibition

Rate of Growth Substrate Utilization



Rate of Cometabolic Substrate Utilization

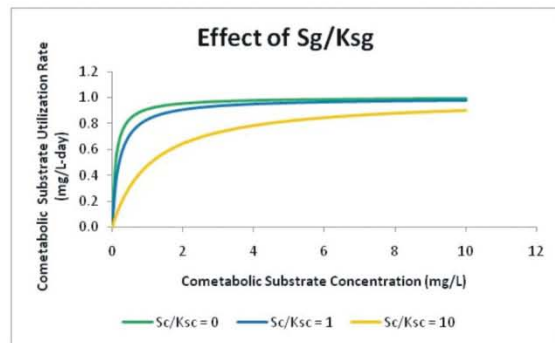
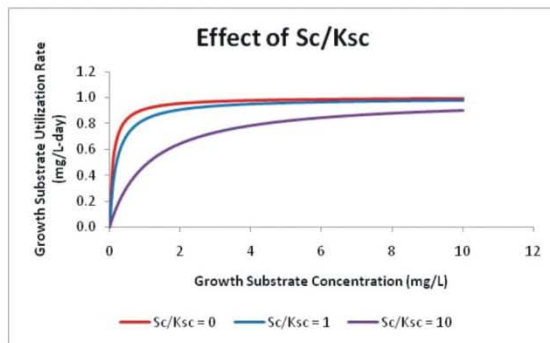
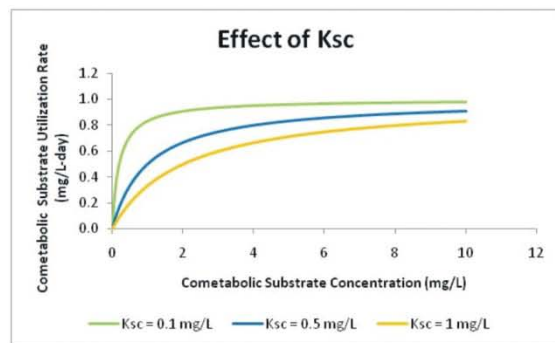
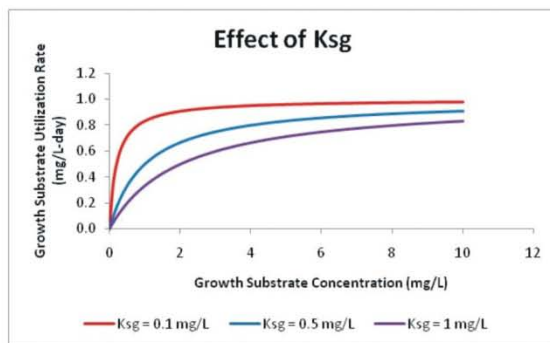
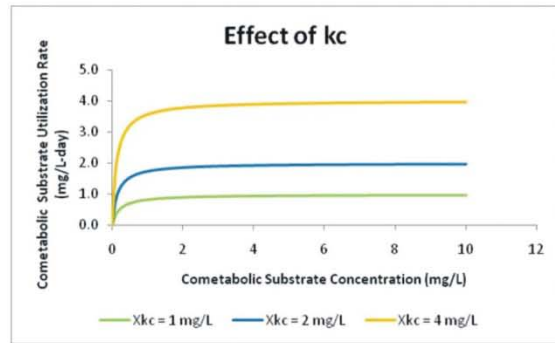


Figure 3-2. Effect of rate parameters and competitive inhibition ratio on reaction rate for 1 mg/L biomass concentration.

At substrate concentrations well below the half-saturation coefficient, $S \ll K_s$, the rate expression approaches a first order expression, which is defined as the reaction rate is proportional to concentration. The growth substrate rate equation, as an example and omitting the low oxygen inhibition term, is used to illustrate this point.

$$r_g = - \frac{X k_g S_g}{K_{sg} \left(1 + \frac{S_c}{K_{sc}} \right) + S_g}$$

$$\approx - \frac{X k_g}{K_{sg} \left(1 + \frac{S_c}{K_{sc}} \right)} S_g \quad \text{Equation 3-7}$$

$$= \text{constant} \times S_g$$

Hence, at $S \ll K_s$, the reaction rate is proportional to the substrate concentration, and the constant is the pseudo first-order rate coefficient.

Thus far in the parametric study, the effect of parameter values on reaction rates has been examined. The parametric study will be continued by examining the effect of parameter values on growth substrate and cometabolic substrate concentrations over time. A series of plots of concentration as a function time (Figures 3-3 and 3-4) are used to illustrate the effect of each parameter. These two composites are arranged with plots of growth substrate and cometabolic substrate concentration versus time for different values of K_{sg} in rows and different values of K_{sc} in columns. Curves for three values of k_c or k_g are provided on individual plots. A biomass concentration of 0.1 mg/L was specified, and the oxygen inhibition term was set to 1.0 by specifying $S_{ox} = 5$ mg/L and $K_{sox} = 0.01$ mg/L.

The trends in the composite figures (Figures 3-3 and 3-4) illustrated in Figure 3-5 show that, on an individual plot, faster reaction rates are shown as curves that decline more steeply with time. Increasing values of the maximum specific rate coefficient for growth substrate k_g and for cometabolic substrate k_c cause an increase in reaction rate of growth or cometabolic substrate, respectively. Comparing different plots, smaller values of the growth substrate half-saturation coefficient K_{sg} (moving down in a column) cause the growth substrate reaction rate to increase as well as competitive inhibition of cometabolic substrate reaction to increase. Smaller values of the cometabolic substrate half-saturation coefficient K_{sc} (moving to the left in a given row) cause the cometabolic substrate reaction rate to increase as well as competitive inhibition of growth substrate reaction to increase.

The effects of each parameter on rate of concentration decline were summarized previously in Table 3-7. Greater reaction rates correspond with faster decline in concentration of growth or cometabolic substrate.

3.4.3 Batch Reactor Kinetics Based on Literature and Observed Parameter Values

In the previous section, the effect of each parameter on reaction rate and concentration versus time plots was investigated. Parameter values used were reasonable, based on information in the published literature, but were primarily selected to illustrate the effect of varying each parameter.

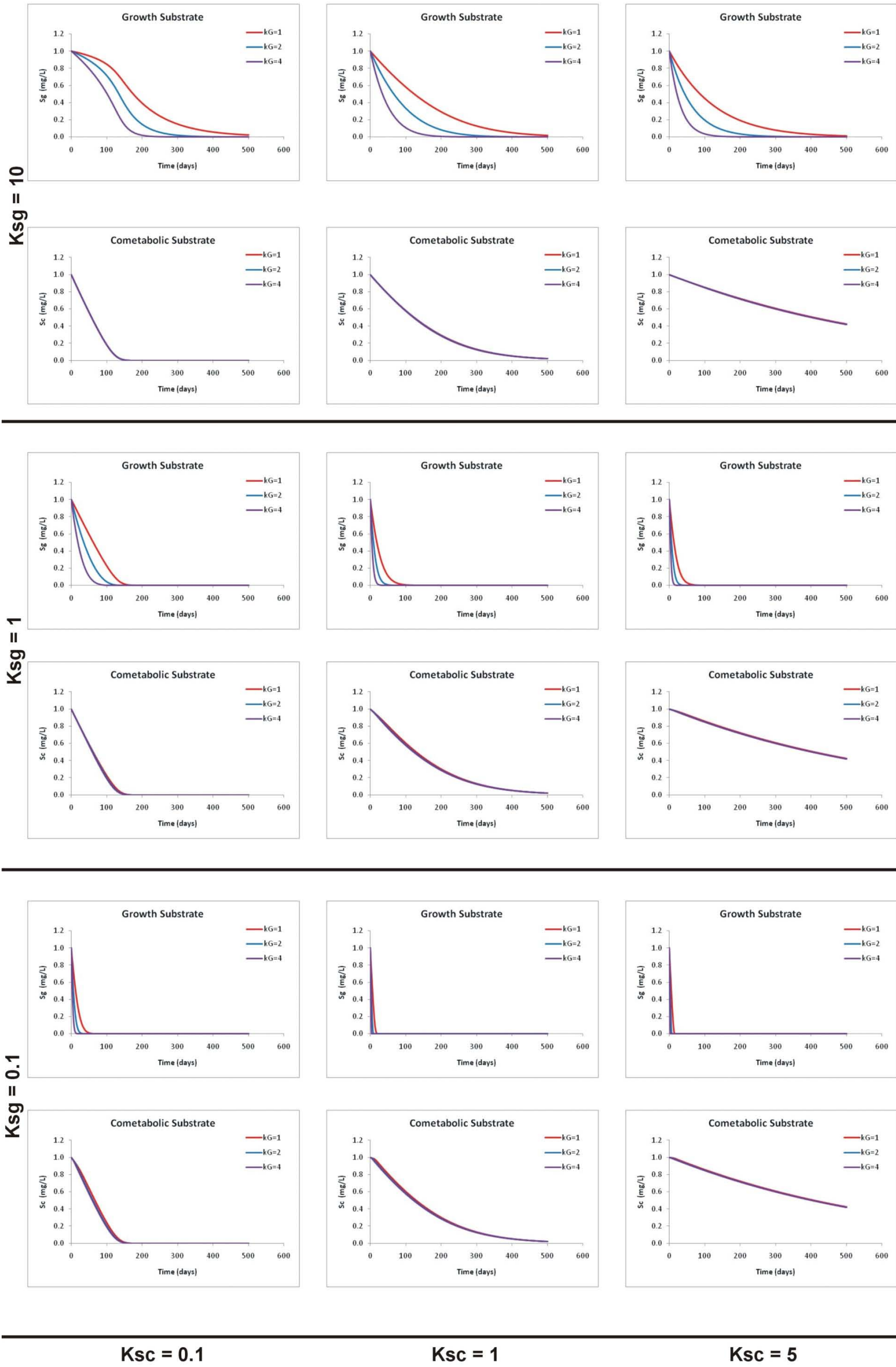


Figure 3-3. Effect of half-saturation coefficients and maximum growth rate coefficient k_g on substrate concentrations as a function of time.

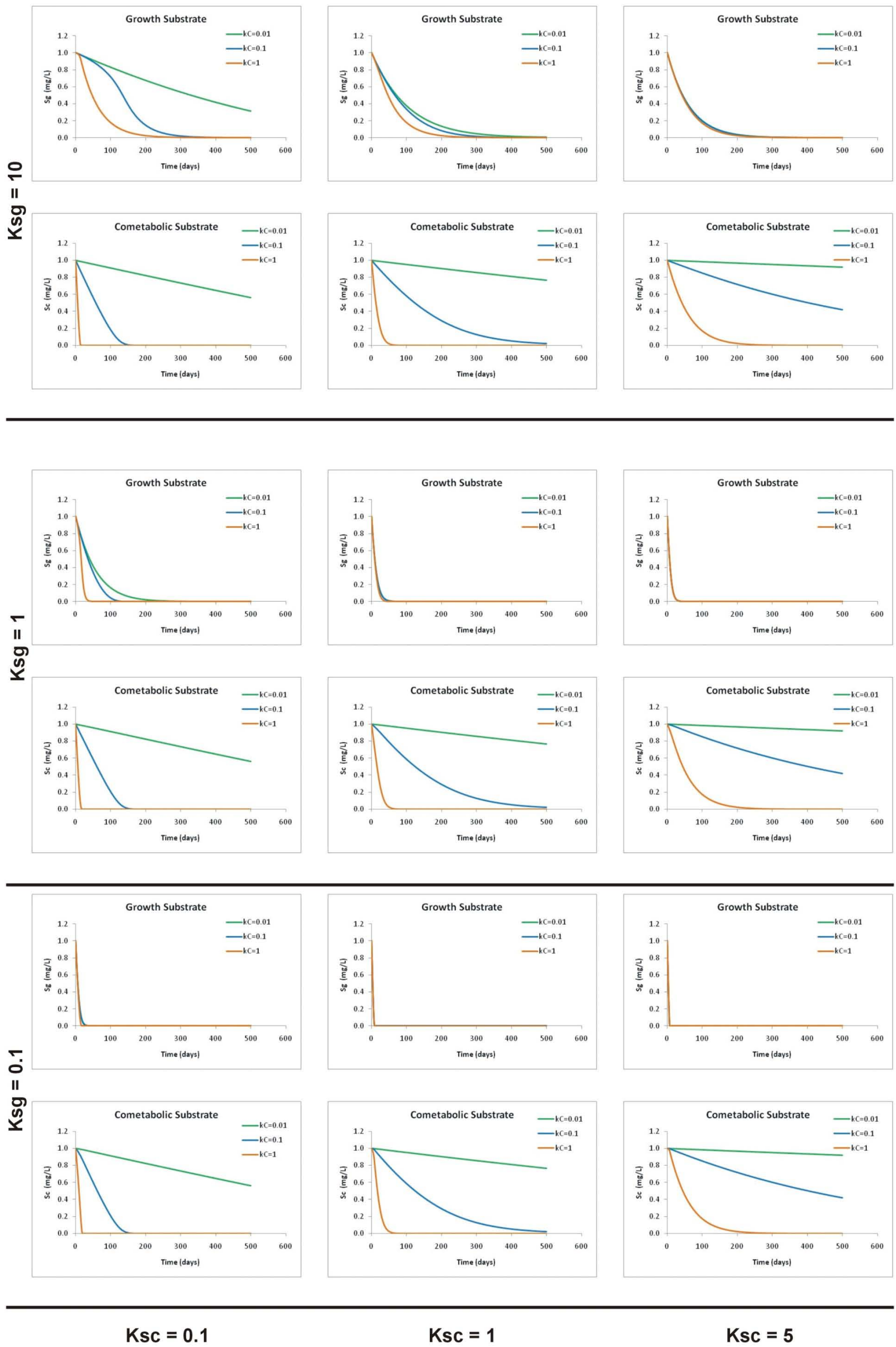


Figure 3-4. Effect of half-saturation coefficients and maximum cometabolic rate coefficient k_c on substrate concentrations as a function of time.

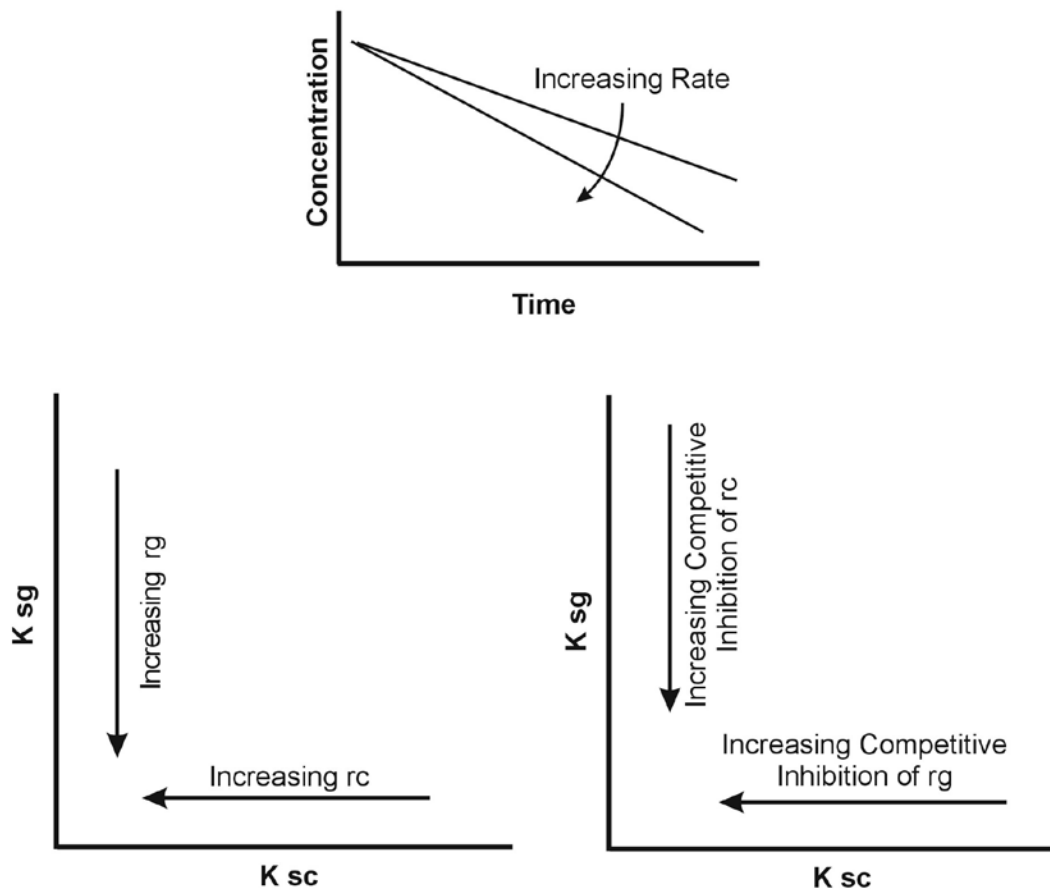


Figure 3-5. Summary of trends in individual concentration versus time plots and in composite figures.

In this section, combinations of kinetic parameter values (maximum specific rate coefficients and half-saturation coefficients, for methane and TCE oxidation) compiled from the literature and values for biomass, methane, and TCE concentration representative of the TAN TCE plume were used to calculate reaction rates and temporal concentration trends in a batch reactor. Calculations were performed with three sets of parameter values; one set yields the maximum degradation rate, another yields the minimum rate, and the third set is intermediate between the maximum and minimum sets. The parameter values used are provided in Table 3-8. The difference between parameter values in the maximum and minimum rate cases suggests that the reaction rates for both growth and cometabolic substrates will differ by orders of magnitude between the maximum and minimum rate cases.

The reaction rate curve for growth substrate at concentrations up to 10 mg/L (Figure 3-6) shows the typical shape presented earlier (Figure 3-2) for the maximum rate case. The curve for the minimum rate case plots along the horizontal axis at this scale. Concentrations of methane (the growth substrate) measured in groundwater in the distal portion of the TAN groundwater plume are on the order of 1 $\mu\text{g/L}$, and thus the extreme left portion of the rate curve is relevant. The growth substrate rate curve is shown at an expanded scale (Figure 3-7). The horizontal axis is presented with concentration units of $\mu\text{g/L}$ and the vertical axis has rate units of $\mu\text{g/L-year}$, which are more appropriate for the concentration and time scales relevant to a groundwater plume undergoing natural attenuation. Subsequent figures also use these units. The growth substrate reaction rate is approximately three orders of magnitude faster in the maximum rate case than in the minimum rate case. The linear form of both plots, in which reaction rate is proportional to concentration, indicates that first-order reaction kinetics apply to both cases at these substrate concentrations.

Table 3-8. Parameter values that yield maximum, minimum, and intermediate reaction rates.

Parameter	Maximum Rate Value	Minimum Rate Value	Intermediate Rate Value	Basis
X (mg cells/L)	0.01	0.001	0.001	Measured values
k_g (mg substrate/mg cells – day)	4	1	1	Literature values
K_{sg} (mg/L)	0.01	7	1	Literature values
k_c (mg substrate/mg cells day)	1	0.02	0.2	Literature values
K_{sc} (mg/L)	0.01	5	0.5	Literature values
S_g (mg/L)	0.001	0.001	0.001	Measured values in distal portion of TAN plume
S_c (mg/L)	0.25	0.25	0.25	Approximate maximum value in distal portion of TAN plume
S_{ox} (mg/L)	8	8	8	Typical value at TAN
K_{sox} (mg/L)	0.01	0.01	0.01	Selected to set low oxygen inhibition coefficient to 1

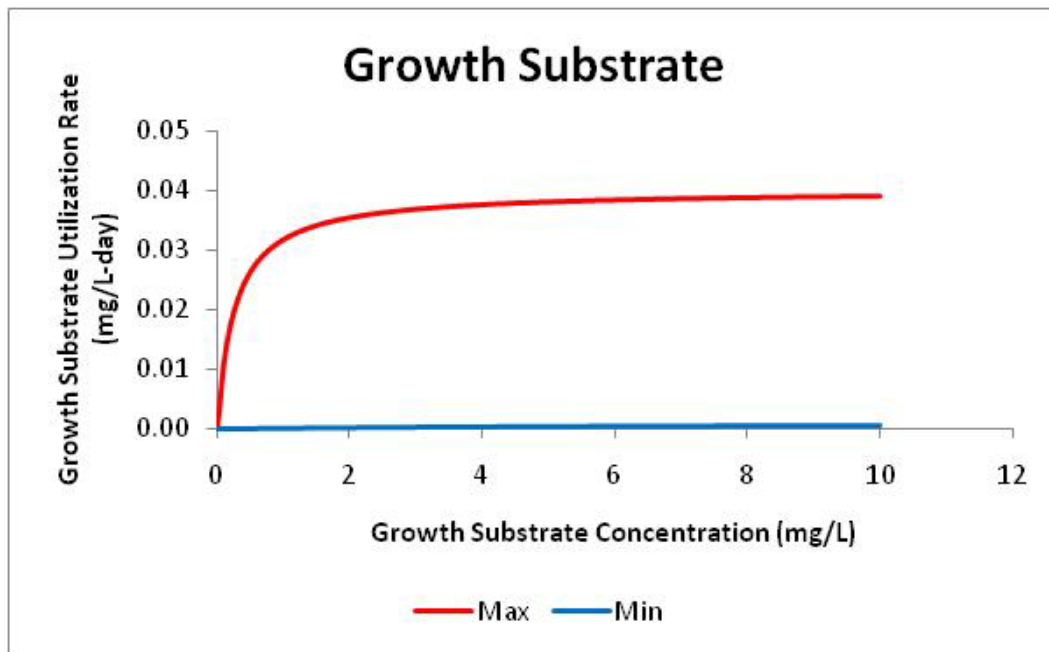


Figure 3-6. Growth substrate utilization rate versus concentration for maximum and minimum rate cases.

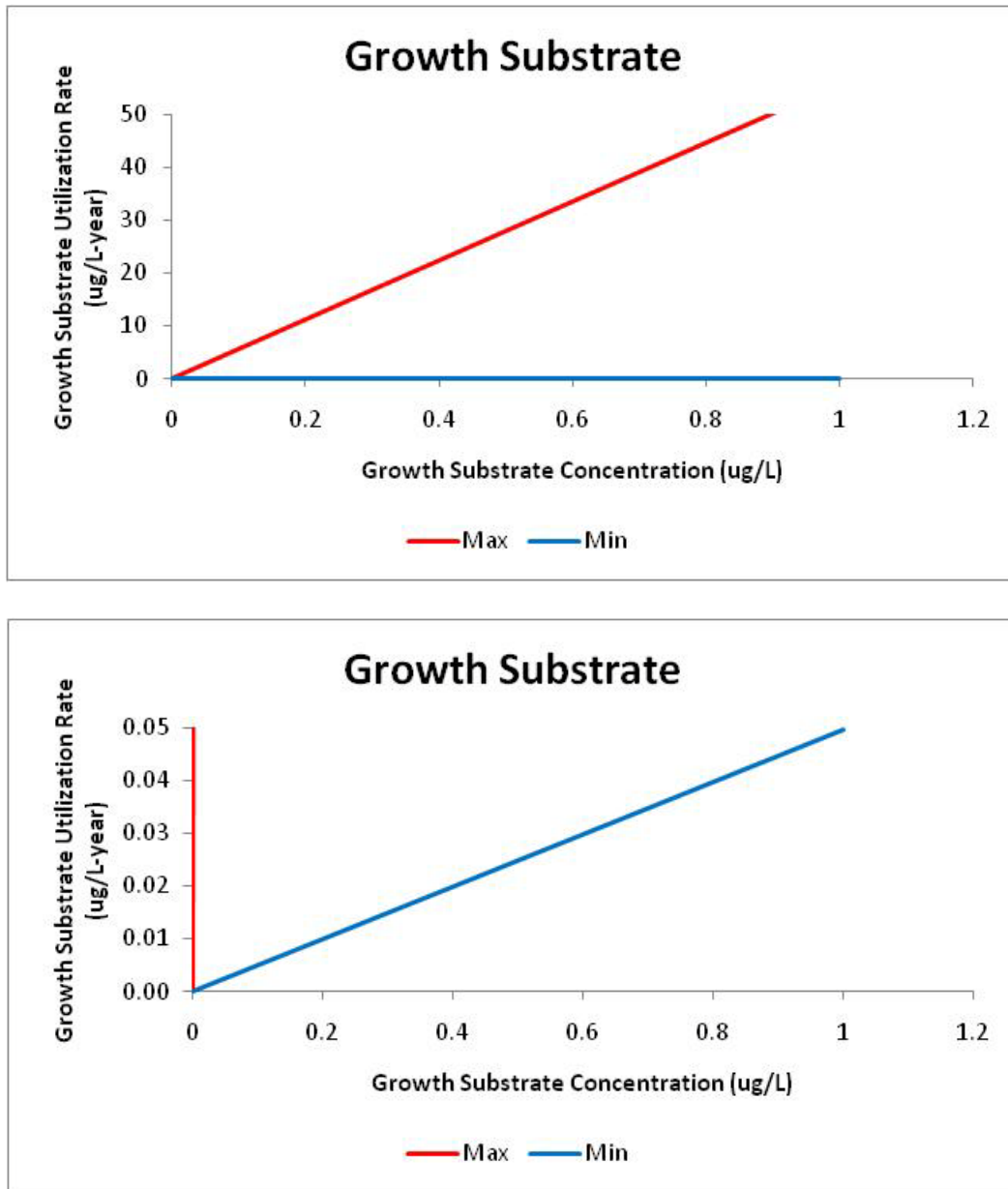


Figure 3-7. Growth substrate utilization rate for maximum (upper) and minimum (lower) rate cases.

The reaction rate curve for cometabolic substrate at concentrations up to 10 mg/L (Figure 3-8) also shows the typical shape presented earlier (Figure 3-2) for the maximum rate case, but the minimum rate case curve plots along the horizontal axis at this scale. Concentrations of TCE (the cometabolic substrate) measured in groundwater in the distal portion of the TAN groundwater plume are in the general range of 5 to 250 $\mu\text{g/L}$, and thus the low concentration portion of the rate curve is relevant. The cometabolic substrate rate curve is shown at an expanded scale (Figure 3-9) that covers TCE concentrations between 0 and 250 $\mu\text{g/L}$. The rate is approximately four orders of magnitude faster in the maximum rate case than in the minimum rate case. For the maximum rate case, the rate curve shows the characteristic break in slope, in this case at TCE concentration of approximately 30 $\mu\text{g/L}$, and thus TCE reaction kinetics are not first-order over much of the relevant concentration range. In contrast, reaction kinetics in the minimum rate case are first order.

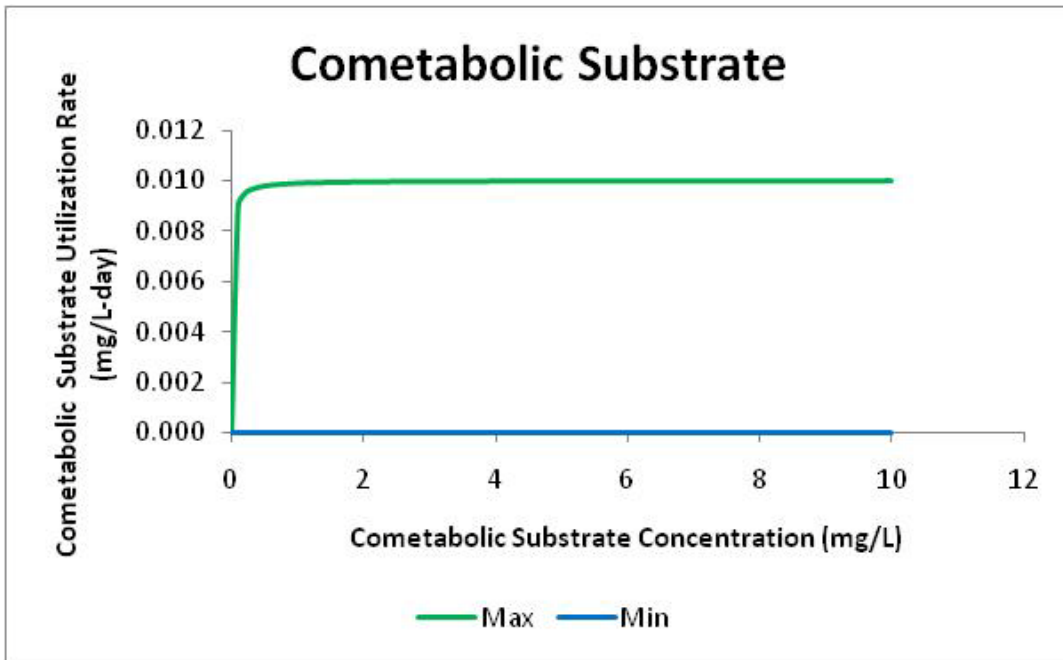


Figure 3-8. Cometabolic substrate utilization rate versus concentration for maximum and minimum rate cases.

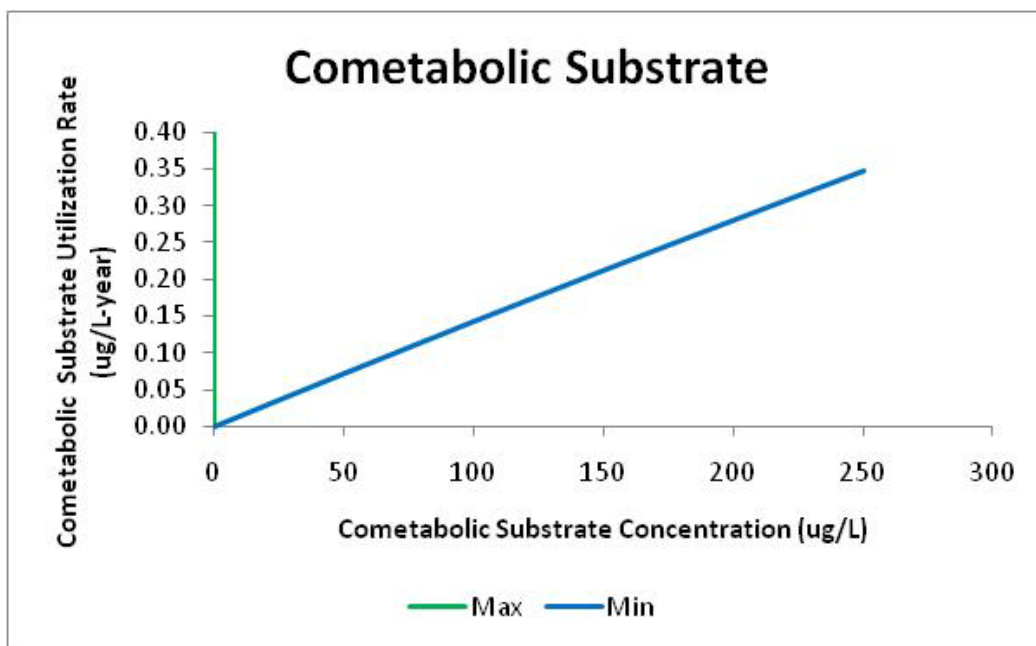
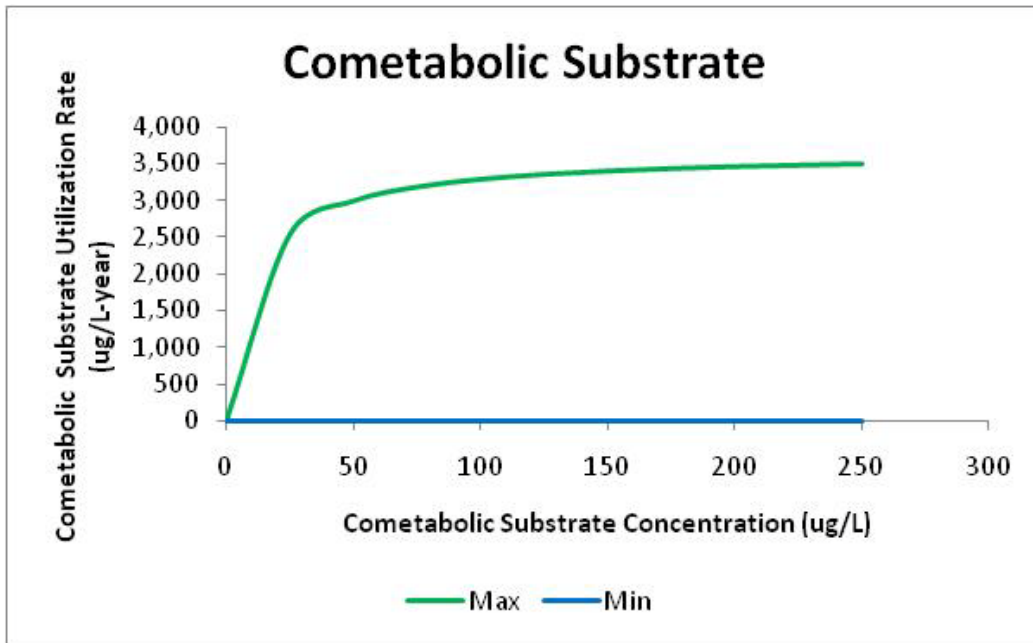


Figure 3-9. Cometabolic substrate utilization rate for maximum (upper) and minimum (lower) rate cases.

To put these reaction rates into context, the TAN TCE plume developed over approximately 50 years following disposal of TCE and other wastes into the aquifer. TCE concentrations in the distal part of the plume, in which natural degradation under aerobic conditions occurs, have ranged from 5 µg/L at the plume perimeter to a maximum of approximately 1,000 µg/L, although maximum concentrations have declined recently due to active remediation in the upgradient portions of the plume. TCE has persisted in the aquifer over the course of several decades, which establishes an upper limit on the degradation rate. Methane is present throughout the distal plume at concentrations on the order of 0.1 to 1 µg/L. Although it is not known if there is an ongoing input of methane, the presence and persistence of methane throughout the distal plume also establishes an upper bound on the methane utilization rate.

Trends in methane and TCE concentrations over time for the maximum and minimum rate cases (Figure 3-10). The concentration scales are the same in both plots, but the time scales are quite different. The plot for the maximum rate case shows that methane is depleted and TCE concentrations decline by approximately half within days. Under this scenario, methane would likely not exist throughout the plume and adjacent areas, TCE would not persist, and an extensive plume (like the 2-mile long TAN TCE plume) would not develop. This suggests that the maximum rate case likely overestimates reaction rates for the TAN plume. The plot for the minimum rate case shows that methane concentrations slowly decline over a decadal time scale, but that TCE is almost recalcitrant. The methane trend is credible, but the TCE concentration trend is inconsistent with an analysis by Sorenson et al. (2000) that concluded that TCE degrades with a half-life on the order of a decade. Over 3 decades with a 10-year half-life, TCE concentrations would decline by a factor of $1/2^3$ (i.e., an initial concentration of 250 µg/L would decline to about 30 µg/L). This suggests that the minimum rate case underestimates the rate of TCE reaction in a plume similar to the TAN plume.

A set of intermediate parameter values was selected that yield methane and TCE concentration trends that are roughly similar to trends that might be expected in a slowly attenuating plume, although no claim is made that these values are applicable to the TAN plume. The growth substrate rate curve (Figure 3-11) is linear, indicating that methane degradation in this case would be via first-order kinetics, and the cometabolic substrate rate curve is only slightly curved, and hence degradation kinetics would be approximately first order. This contrasts sharply with the two-slope rate curve in the maximum rate case. Comparison to Figure 3-7 shows that the growth substrate rate in the intermediate rate case is almost two orders of magnitude slower than in the maximum rate case and about one order of magnitude faster than in the minimum rate case. The cometabolic rate curve in the intermediate case is about two orders of magnitude slower than in the maximum case and about two orders of magnitude faster than in the minimum rate case (Figure 3-9).

Growth and cometabolic substrate concentration trends for the intermediate rate case (Figure 3-12) show that methane concentrations decline to 1 ng/L over the course of 22 years, and that TCE concentrations decline to 7 µg/L over the 27-year (10,000-day) time period. Although no claim is made that these parameter values are applicable to the TAN plume, batch reactor simulations using these values provide results that are, at least in a general sense, consistent with conditions observed in the TAN plume. As discussed in a subsequent section, the intermediate case parameter values were used in a flow and transport simulation that utilizes competitive inhibition kinetics.

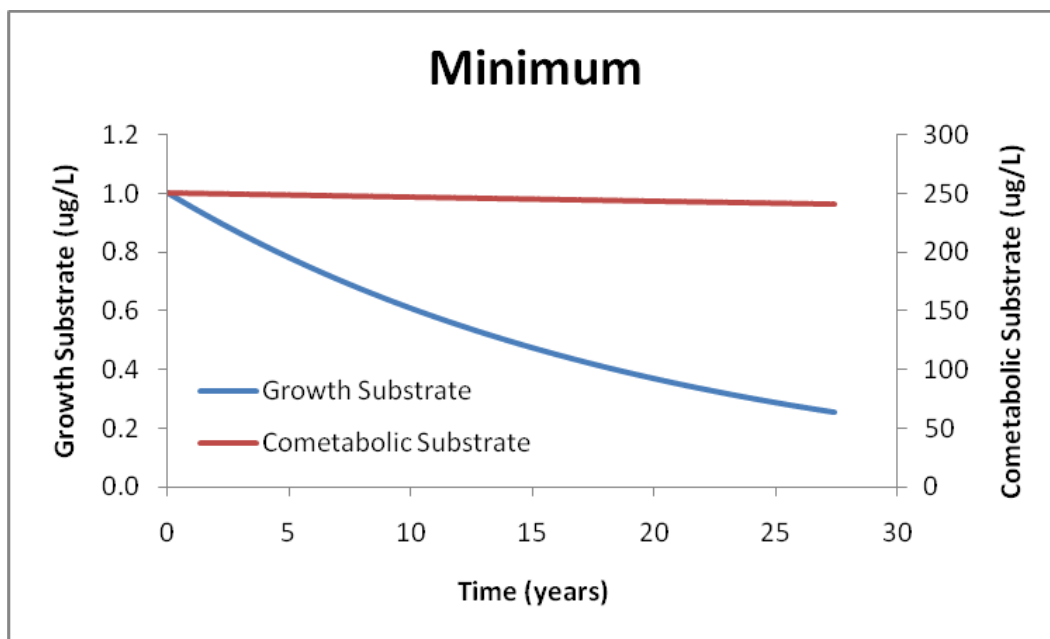
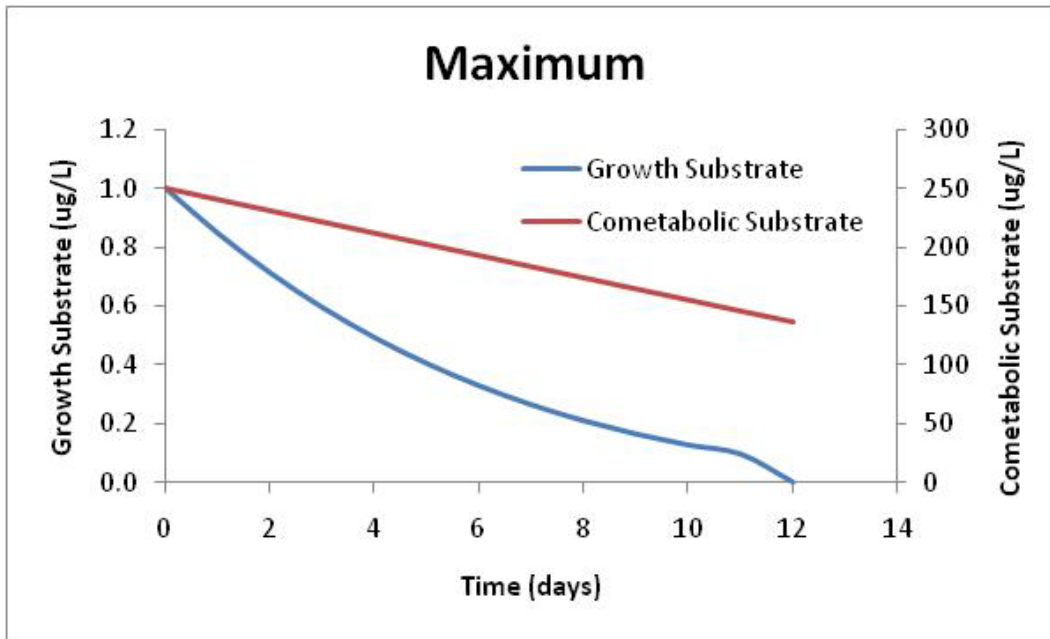


Figure 3-10. Growth and cometabolic substrate concentration trends for maximum (upper) and minimum (lower) rate cases.

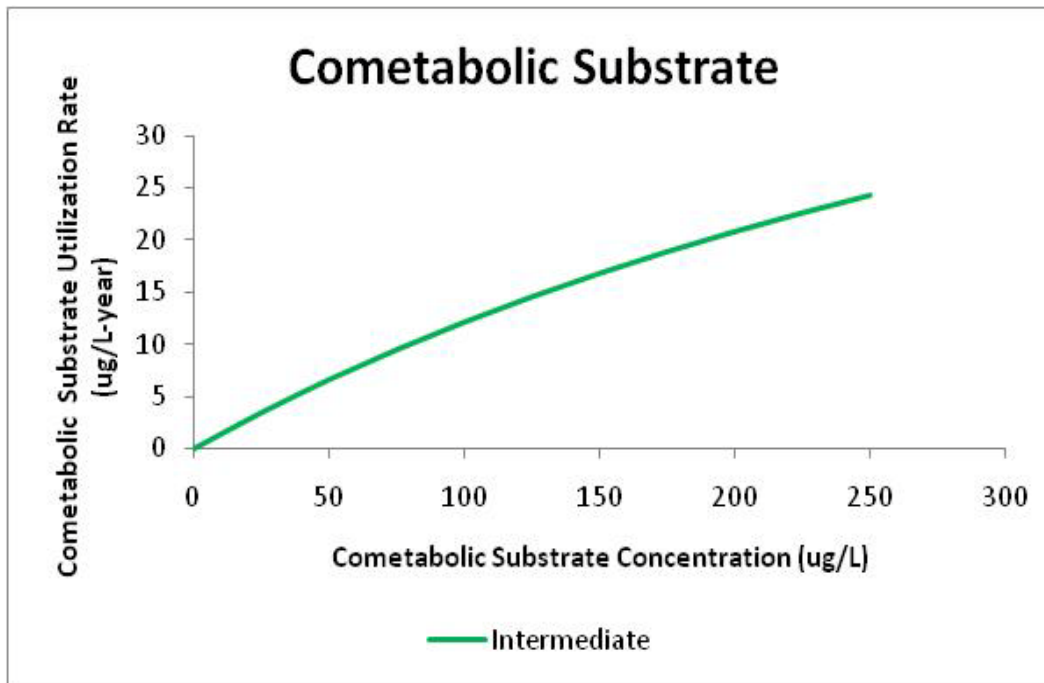
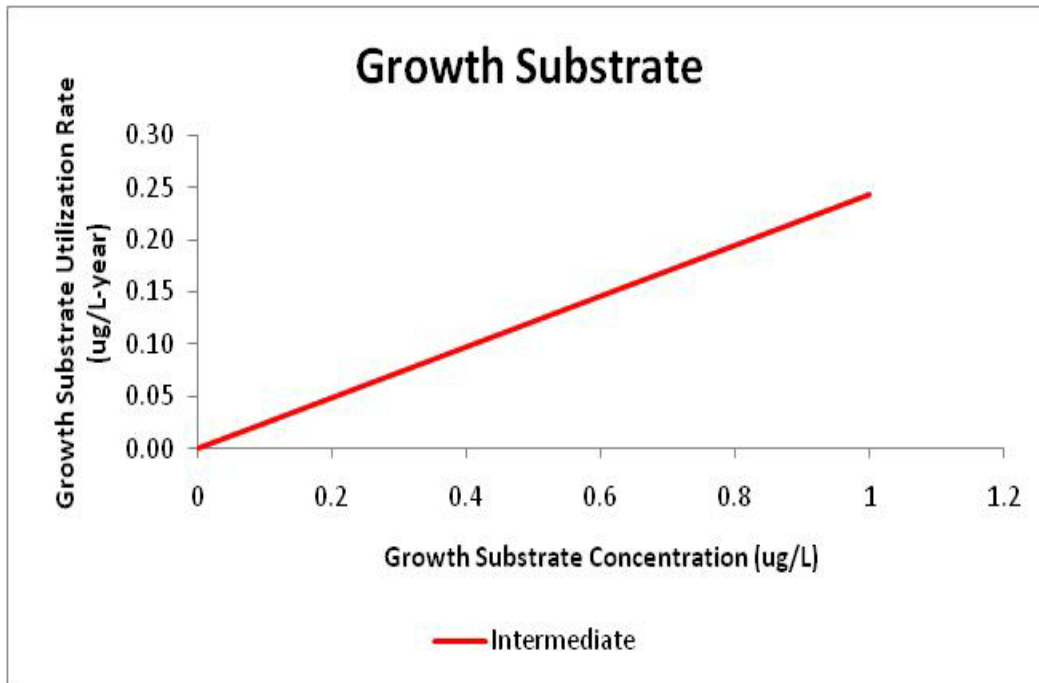


Figure 3-11. Growth (upper) and cometabolic (lower) substrate utilization rate for intermediate rate case.

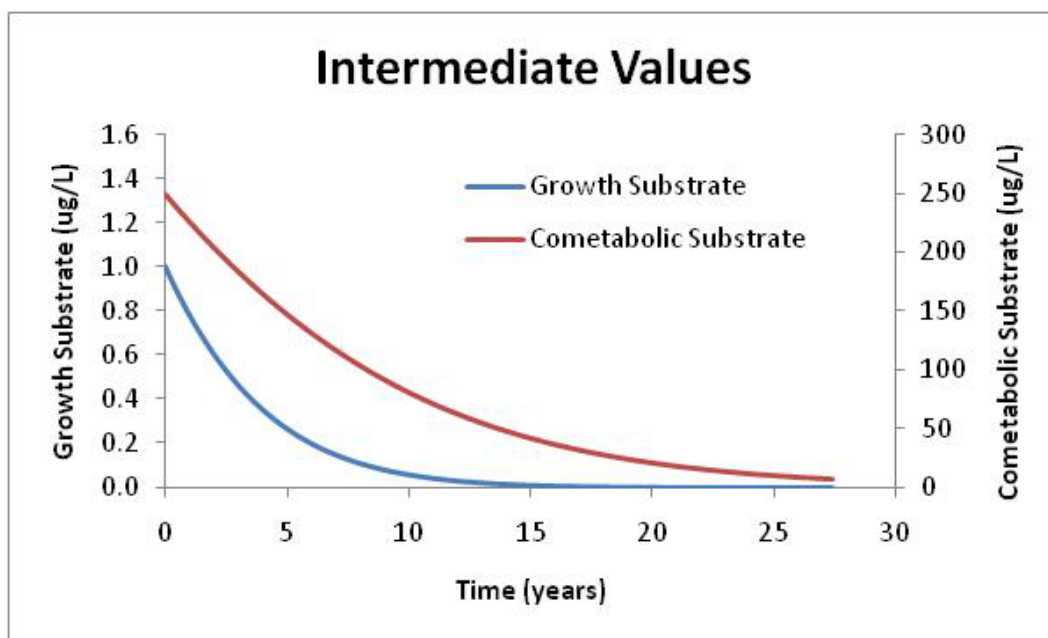


Figure 3-12. Growth and cometabolic substrate concentration trends for intermediate rate case.

Comparison of the reaction rate curves for growth and cometabolic substrates for the maximum and minimum rate cases, which may represent the extremes of likely behavior based on published literature values and selected measure values, shows that there are approximately three to four orders of magnitude difference between the estimated rates in these cases. This large range makes it difficult to select appropriate values for predictive purposes, and suggests that site-specific values would be needed to perform meaningful predictions.

3.4.4 Conclusions from the Parametric Study

The following conclusions can be drawn from this parametric study:

1. Values for kinetic parameters in the competitive inhibition model available from the literature provide a starting point for estimating values for use in calculations.
2. Literature values span such a wide range that estimated reaction rates vary over orders of magnitude, and consequently predicted temporal concentration trends also vary greatly. The wide range of literature parameter values leads to considerable uncertainty in predicted reaction rates and concentration trends.
3. This suggests that use of site-specific parameter values instead of literature values may lead to improved predictions of reaction rates and concentration trends.
4. Growth substrate reaction kinetics, based on literature parameter values and methane concentrations measured in the distal portion of the TAN TCE plume, are in the first-order kinetics portion of the rate curve.
5. The cometabolic substrate rate curve for the maximum rate case extends above the first-order kinetics portion of the rate curve; however, the maximum rate case appears to result in unrealistically rapid degradation and hence is not a reasonable combination of parameter values, at least for a plume

undergoing natural attenuation similar to the TAN plume. The reaction kinetics for the minimum and intermediate rate cases are in the first-order kinetics portion of the rate curve. The intermediate rate case yields concentration trends that are similar to those expected for a slowly attenuating plume.

6. The competitive inhibition kinetic model requires numerical values for five parameters (X , k_g , K_{sg} , k_c , K_{sc}), and thus it is inherently more difficult to parameterize than a first order kinetic model.
7. The relatively slow reaction rates for TCE cometabolism in aerobic groundwater (half-life of years to a decade or more) suggests that measuring kinetic parameters in a short-term lab or field test that replicate in situ conditions would be difficult, due to the slow rate of change in concentration. The difficulty in parameterizing the more complicated kinetic model and the observation that first order kinetics may be applicable for combinations of parameter values applicable to a slowly-attenuating plume lead to the conclusion that a first-order kinetic model is more appropriate than a competitive inhibition kinetic model for simulating concentration trends in a slowly attenuating plume.

3.5 Simulation of TCE Transport Using Competitive Inhibition Kinetics

This section describes the development of a new competitive inhibition kinetic module for the transport simulation code RT3D, and simulations of a TCE plume using that modified code.

3.5.1 Development of a Competitive Inhibition Kinetics Module for RT3D

Modeling software that simulates groundwater flow and contaminant transport is well developed and readily available. A commonly used modeling package is the GMS, which was developed by researchers at Brigham Young University using support provided by the DOE, DOD, and the Environmental Protection Agency, and is presently distributed by *Aquaveo Inc.* (South Jordan, Utah). GMS includes a variety of software codes for preparing input data, simulating groundwater flow and transport, and interpreting/presenting simulation results, and provides a convenient interface between different software modules.

Codes included in GMS that simulate contaminant transport in GMS include MT3D (Mass Transport in Three Dimensions) and RT3D. RT3D includes a variety of modules for contaminant transformation subject to several kinetic models, including first order decay, Michaelis-Menton or Monod kinetics, and sequential anaerobic degradation of chloroethenes. However, it does not include competitive inhibition kinetics, which is at least one kinetic model that is likely applicable to cometabolic degradation of TCE. RT3D allows user-defined kinetic modules to be added, which allows considerable flexibility in adapting the code for additional applications.

A user-defined kinetic module for competitive inhibition kinetics was prepared by Prabhakar Clement (Auburn University), one of the developers of RT3D. This module is freely available at the RT3D website maintained by Pacific Northwest National Laboratory at <http://bioprocess.pnl.gov/rt3d.htm>. Appendix A provides program documentation and instructions for downloading and installing the software.

The notation used in that module differs slightly from the notation used in this report. The notation in this report uses the subscripts g and c to refer to growth and cometabolic substrates, respectively. The notation in the RT3D module uses M (for methane) instead of g to refer the growth substrate, and T (for TCE) instead of c to refer to the cometabolic substrate. Otherwise, the equations are the same. The RT3D module includes the low oxygen inhibition term.

3.5.2 Numerical Modeling Approach

A flow and transport model, developed previously for the TAN plume, was used to evaluate the capability of the RT3D competitive inhibition module to effectively simulate degradation of growth and cometabolic substrates. The numerical modeling approach required installation of the RT3D competitive inhibition module, assignment of chemical reaction package parameters, and representation of growth and cometabolic substrate source terms. Subsequently, sensitivity runs were made to evaluate the effect of key competitive inhibition parameters.

3.5.2.1 RT3D Code

The RT3D competitive inhibition module can be applied to any pair of growth and cometabolic substrates subject to competitive inhibition. The notation used in this module refers to methane as the growth substrate and TCE as the cometabolic substrate.

3.5.2.2 Chemical Reaction Package Parameters

A simulated batch reactor study was used to identify a set of parameter values that would produce observable TCE and methane degradation within a reasonable time scale. Table 3-9 presents model parameters, definitions, and intermediate values that should result in contaminant degradation roughly comparable to that observed in the TAN plume. However, this simulation is not intended to be used for predicting future evolution of the TAN plume.

3.5.2.3 Source Term Representation

Initial RT3D runs utilized the TCE source term as used in the MT3D model but without a specified half-life. A methane concentration was added at the point source representing well TSF-05. These runs did not converge because of the variability in TCE source term concentrations from one stress period to another. In subsequent runs, the TCE disposal concentrations were simplified to promote model convergence. These models did run, but did not provide easily observable TCE and methane degradation. A simplistic model was then constructed that introduced a single TCE pulse (250 µg/L) at the source term representing well TSF-05 during one stress period and permitted that pulse to attenuate throughout subsequent stress periods. A conservative tracer also was added at the same concentration. A constant concentration of methane (1 µg/L) was added during stress periods 7 through 97.

3.5.3 Modeling Results

Figure 3-13 presents the TCE plume and conservative tracer plume distribution for layer 15 during stress period 15. Although the same masses of TCE and conservative tracer were added to the model, the areal distribution of TCE was smaller than that of the conservative tracer. Both TCE and the conservative tracer have the same transport characteristics, except that TCE degrades.

Figure 3-14 presents comparison of breakthrough curves for TCE and the conservative tracer for cell row 23, column 34, layer 15. In this comparison, TCE concentrations went to zero after 31 years. Concentrations of the conservative tracer remained through the end of the modeled period. Figure 3-15 presents the ratio of TCE to conservative tracer concentrations. This figure indicates that the ratio drops to zero in approximately 10,000 days. Both figures illustrate that the RT3D simulation is capable of representing cometabolic degradation.

Table 3-9. RT3D Chemical Reaction Package parameters.

Parameter	Model Parameter	Definition	Intermediate Values for TAN Model	Units
X	X	Biomass Concentration	0.001	mg cells/L
k_g	km	Growth substrate specific rate coefficient	1	mg growth substrate/mg cells-day
K_{sg}	Kst	Growth substrate half-saturation coefficient	1	mg growth substrate/L
S_g	Methane source term concentration	Growth substrate concentration	0.001	mg growth substrate/L
k_c	kT	Cometabolic substrate specific rate coefficient	0.2	mg cometabolic substrate/mg cells-day
K_{sc}	Kst	Cometabolic substrate half-saturation coefficient	0.5	mg cometabolic substrate/mg cells-day
S_c	TCE source term concentration	Cometabolic substrate concentration	0.25	mg cometabolic substrate/L
oxy	O	Oxygen concentration	8	mg DO/L
K_{so}	Kso	Oxygen half-saturation coefficient	0.01	mg DO/L

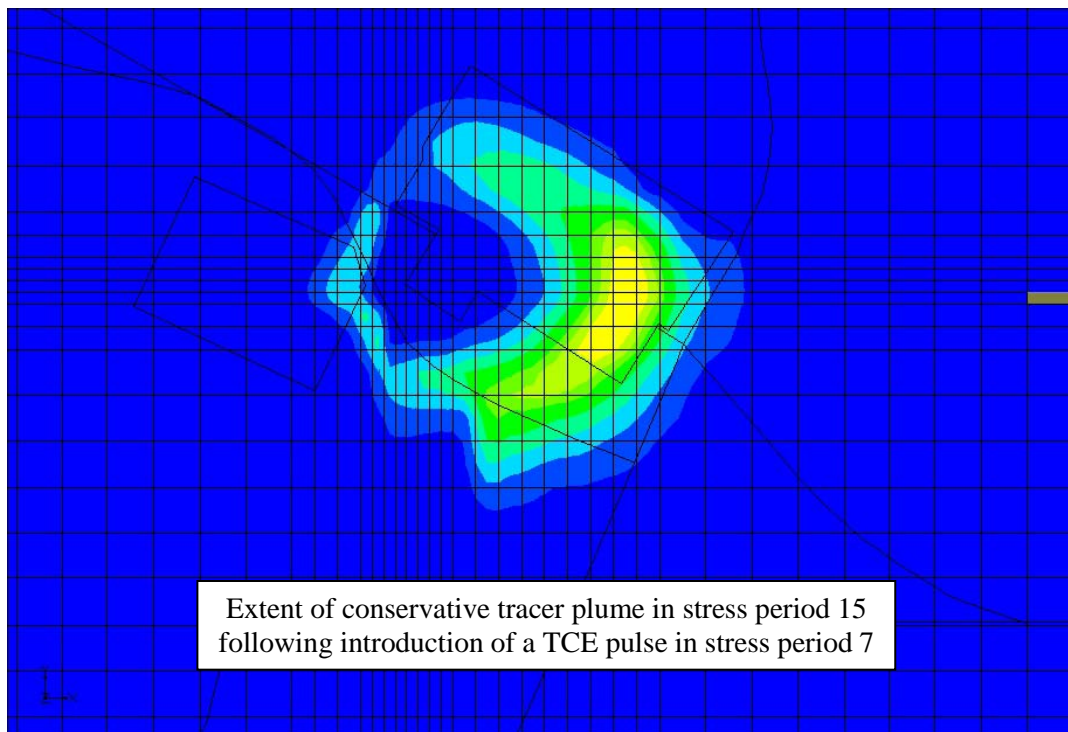
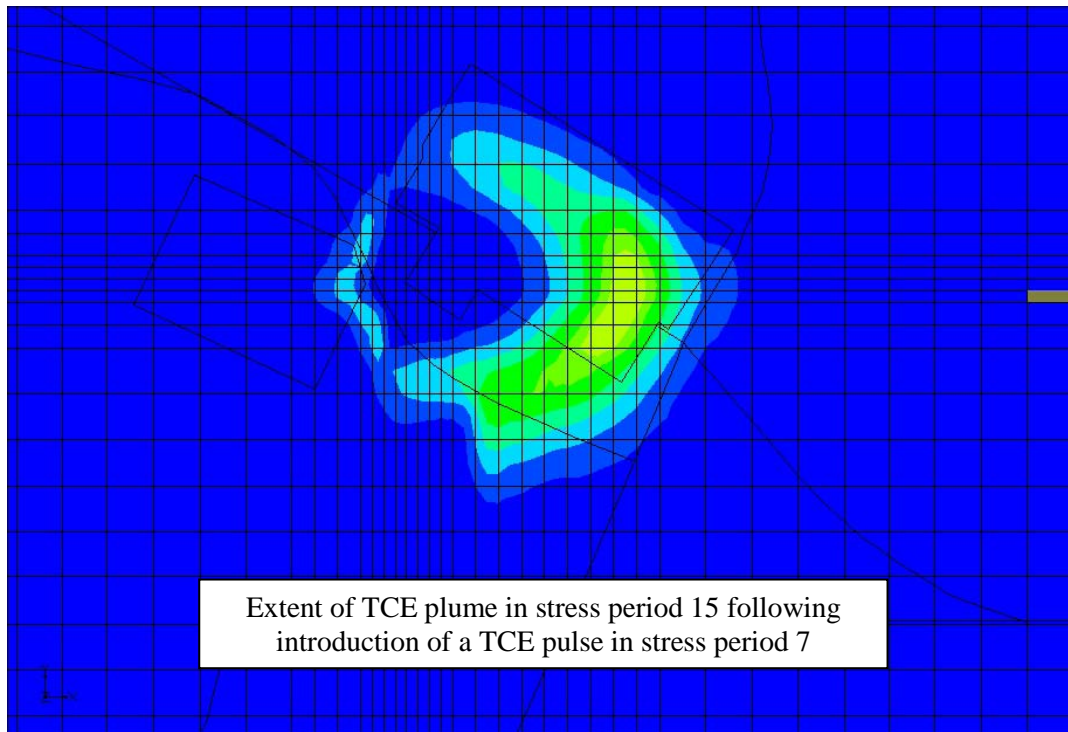


Figure 3-13. Comparison of the extent of TCE and conservative tracer in stress period 15 following addition of identical pulses of TCE and tracer in stress period 7.

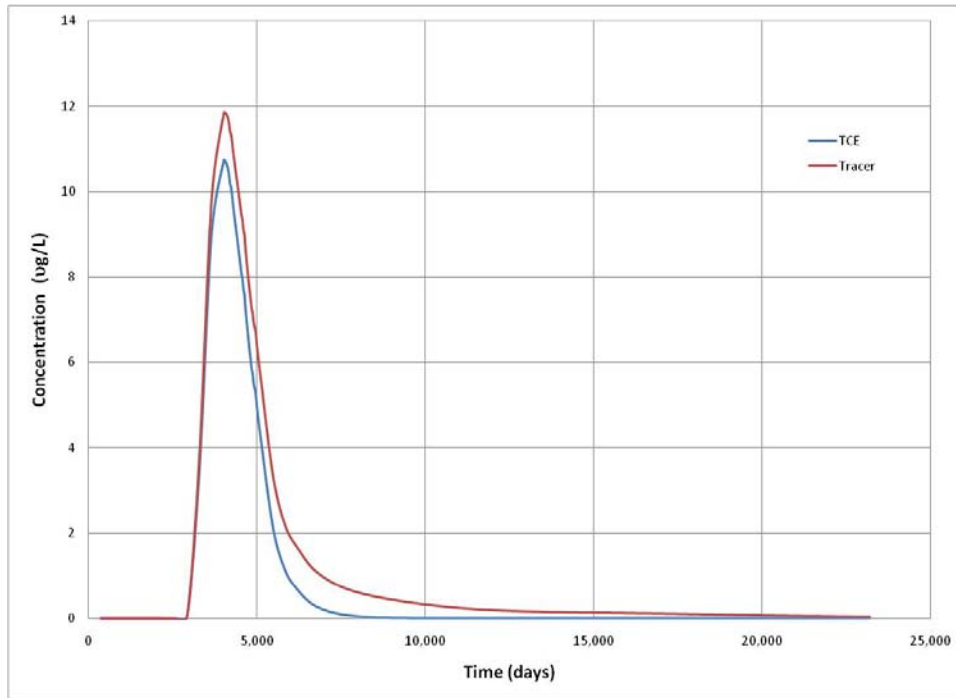


Figure 3-14. Comparison of breakthrough curves for cell row 23, column 34, layer 15 for TCE (blue) and conservative tracer (red).

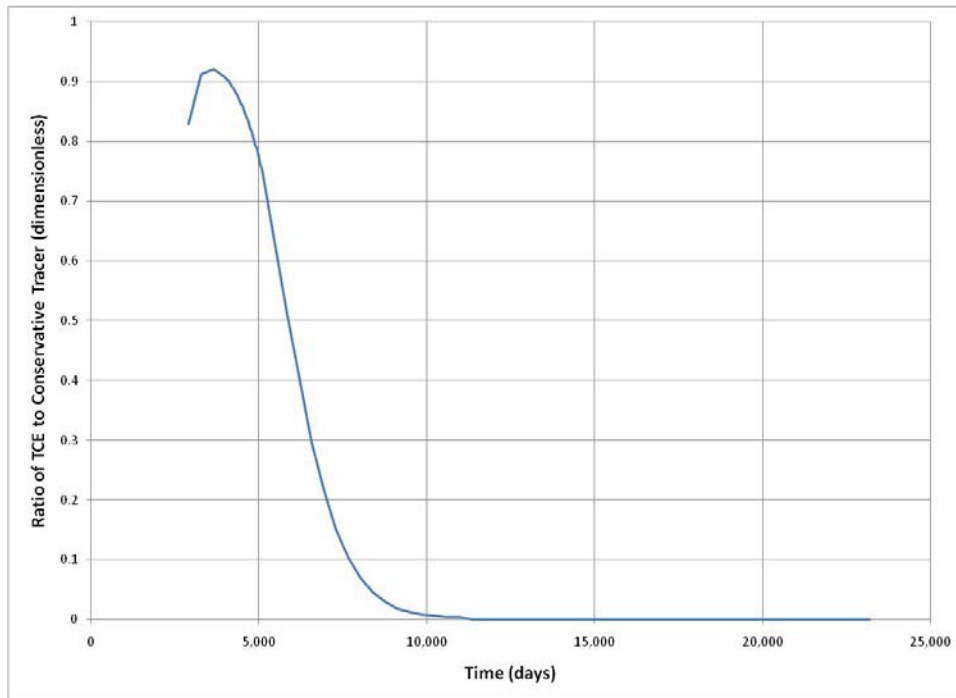


Figure 3-15. Ratio of TCE to conservative tracer concentrations

Figure 3-16 presents simulated masses of TCE and a conservative tracer with time as simulated in the RT3D model. This plot demonstrates that the RT3D competitive inhibition module is capable of effectively simulating the degradation of the cometabolic substrate. In this simulation, total masses of approximately 5,700 g of TCE and conservative tracer were added to the model in stress period 7. Simulated TCE mass dropped to near zero between 10,000 and 12,000 days. Simulated mass of the conservative tracer decreased to approximately 4,200 g. This apparent decrease is attributed to numerical dispersion.

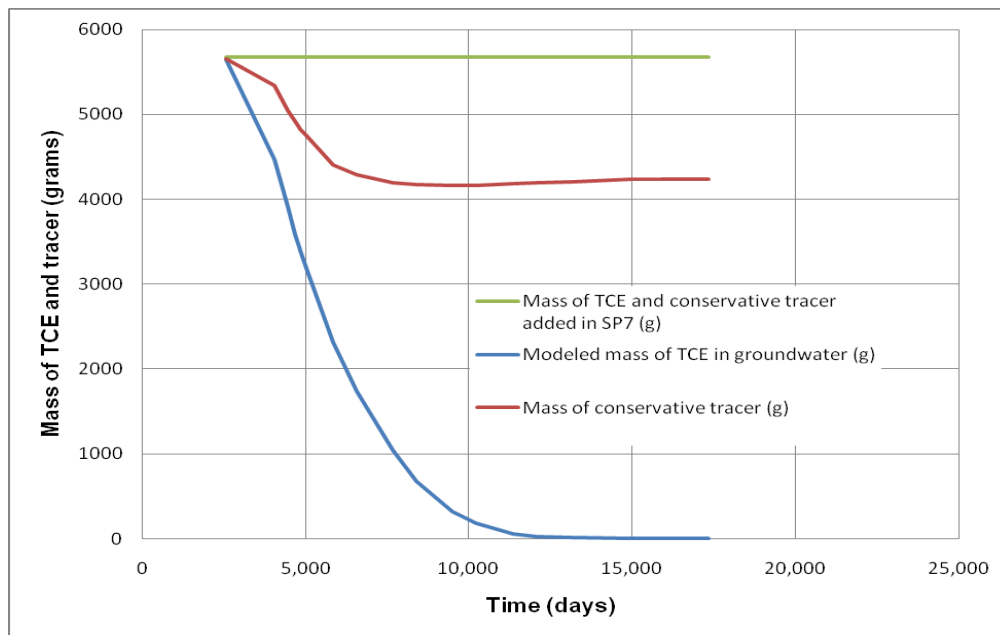


Figure 3-16. Mass of TCE and conservative tracer added to the RT3D model in stress period 7 and simulated TCE and tracer masses with time.

Two simulation runs were made to evaluate the sensitivity of TCE and methane degradation to changes in specific rate coefficients. In the first run, the TCE specific rate coefficient was increased from 0.2 to 1.0 mg growth substrate/mg cells-day. This rate increase was expected to result in relatively rapid methane degradation. Figure 3-17 presents plots of TCE mass changes with time for both specific rate coefficients. These plots indicate that the modeled mass of TCE degraded only slightly faster using a specific rate coefficient that was five times larger than the initial value of 0.2 mg/mg.

Figure 3-18 presents the ratio of TCE mass for cometabolic substrate specific rate coefficients of 0.2 and 1.0 mg growth substrate/mg cells-day. This plot shows that degradation of TCE increases with time by as much as 30% with a specific rate coefficient that is five times larger.

A second sensitivity simulation was run in which the biomass concentration was increased by an order of magnitude (from 0.001 to .01 mg cells/L). This increase resulted in reasonably complete degradation of TCE mass in less than 5,000 days. In contrast, TCE was completely degraded in approximately 13,000 days in the original simulation. Figure 3-19 contrasts TCE mass changes for the two simulations.

A third sensitivity simulation was run in which the growth substrate half-saturation coefficient (K_{sg}) was increased by five times. In this simulation, TCE degradation was slowed and the mass of TCE had not completely degraded by the end of the model run at approximately 23,000 days (Figure 3-20).

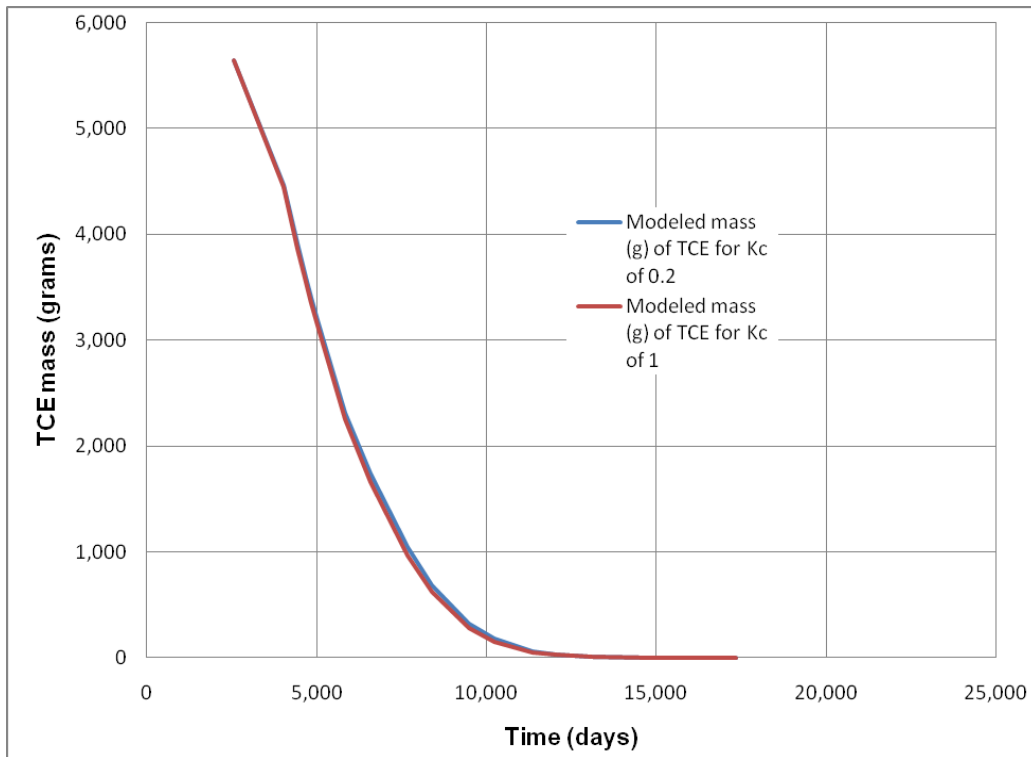


Figure 3-17. Simulated changes with time of TCE mass for cometabolic substrate specific rate coefficients of 0.2 and 1.0 mg growth substrate/mg cells-day.

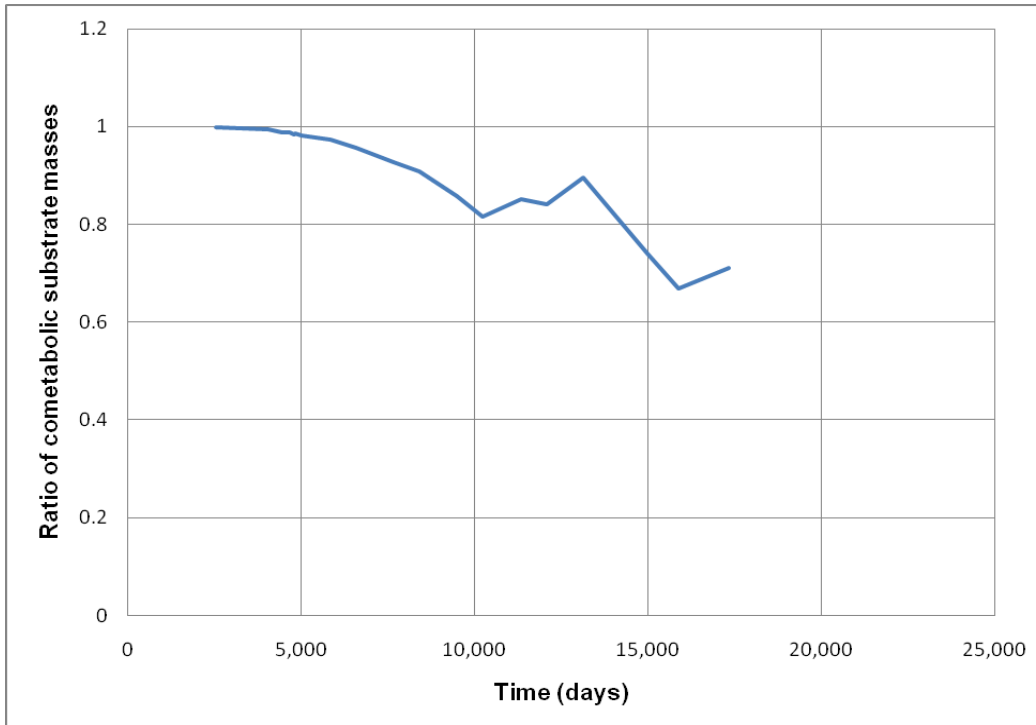


Figure 3-18. Ratio of the TCE mass for a k_C of 0.2 to the mass for a k_C of 1.0 for the modeled interval, in days.

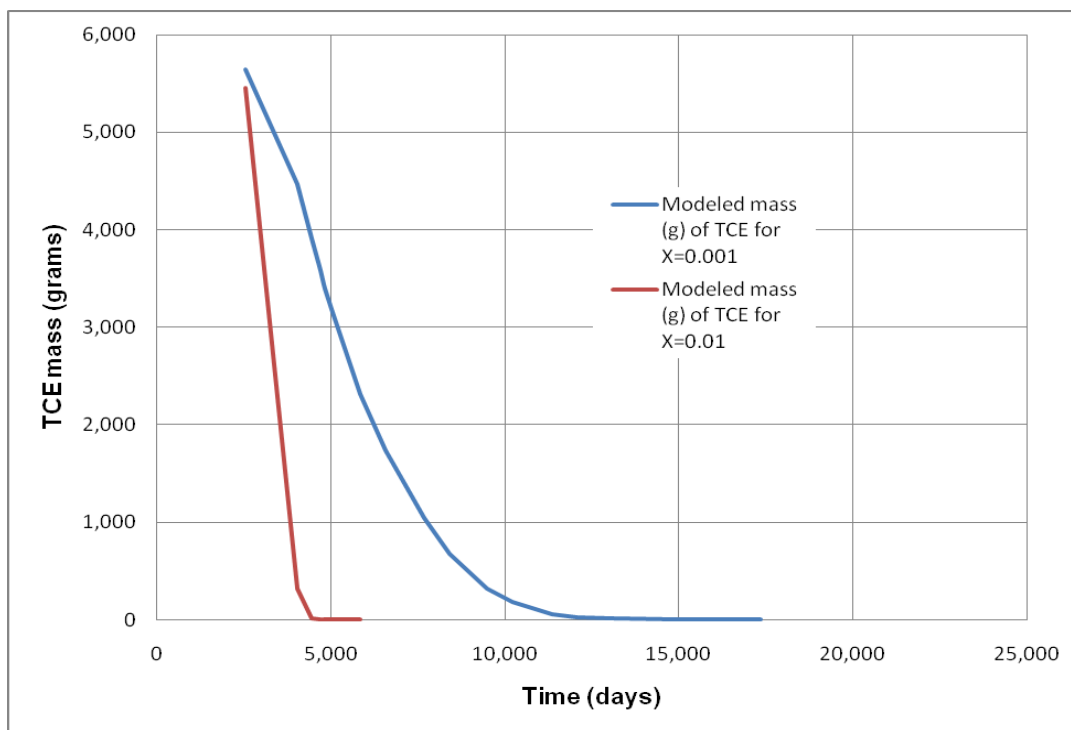


Figure 3-19. Simulated changes with time of TCE mass for biomass concentration (X) values of 0.001 and 0.01 mg cells/L.

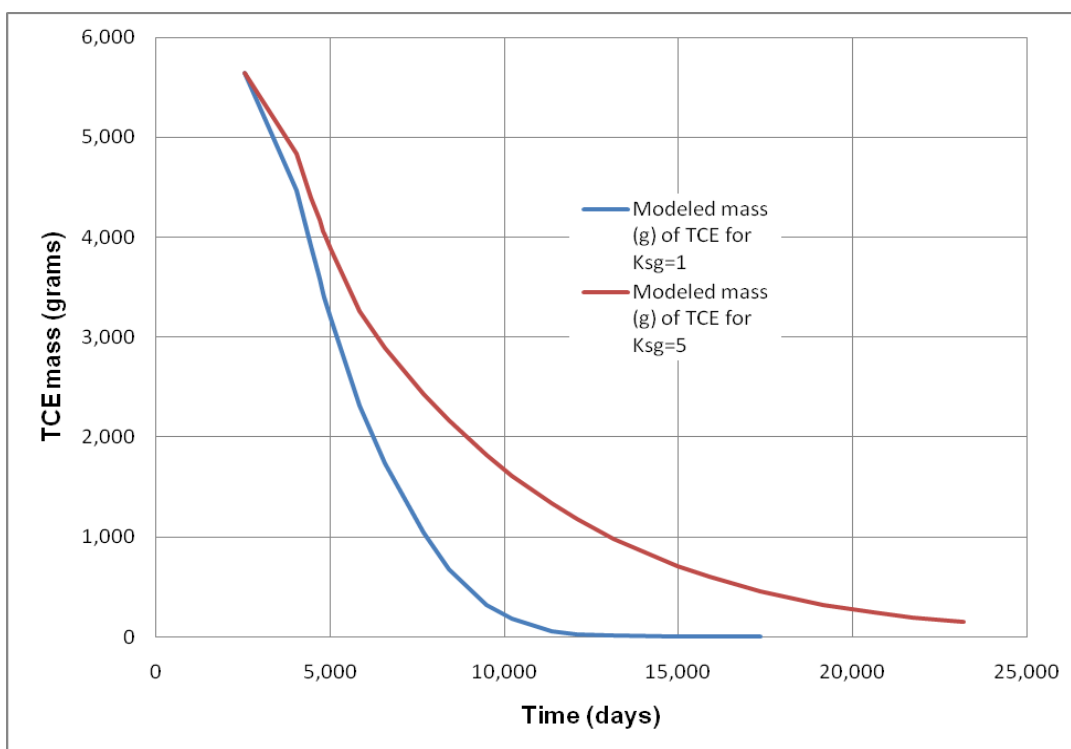


Figure 3-20. Simulated changes with time of TCE mass for growth substrate half-saturation coefficient (K_{sg}) values of 1 and 5 mg growth substrate/L.

A simulation run was made in which the methane specific rate coefficient was increased from 1 to 5 mg growth substrate/mg cells-day. Figure 3-21 compares methane masses for the two specific rate coefficients. Based on this plot, methane was significantly degraded with the larger specific rate coefficient. Mass fluctuations were derived from changes in injection rate from stress period to stress period for the methane source term.

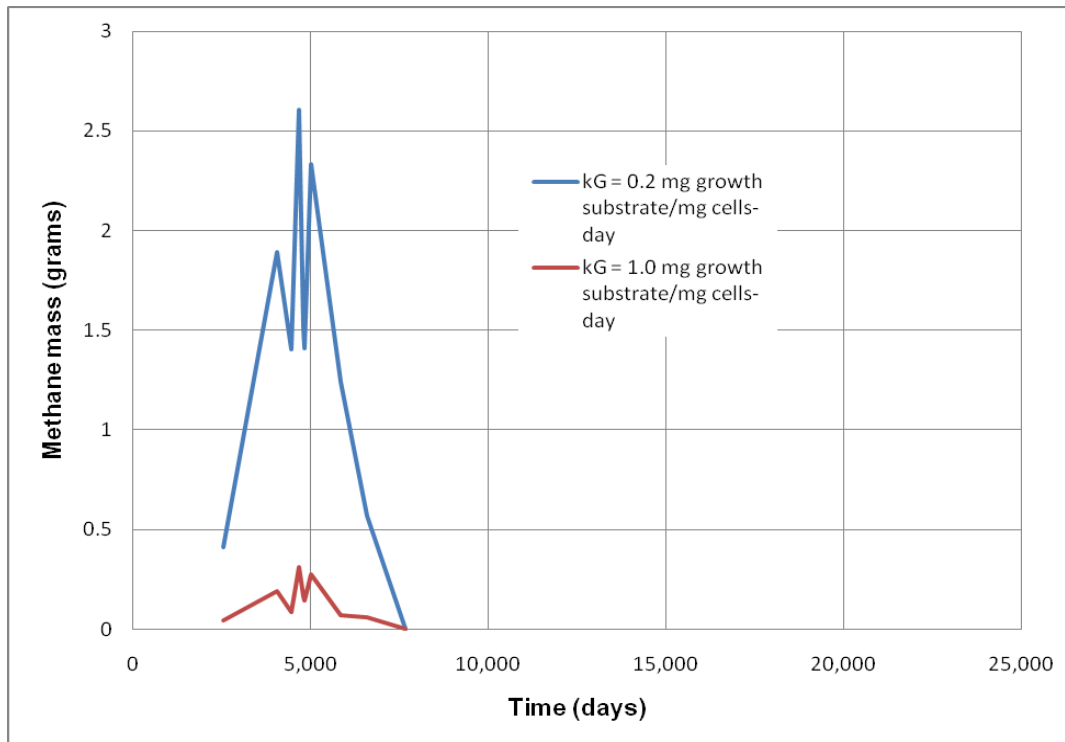


Figure 3-21. Simulated methane mass for growth substrate specific rate coefficients of 0.2 and 1.0 mg growth substrate/mg cells-day.

3.5.4 Conclusions from the Competitive Inhibition Kinetics Simulations

The RT3D competitive inhibition kinetics module was applied to an existing numerical model to demonstrate the effectiveness of this tool in representation of degradation of growth and cometabolic substrates. The flow and transport model, originally developed to represent TCE transport at the INL TAN in these simulations, was utilized.

Kinetics parameters in batch simulations were identified that produced reasonable reaction patterns; these parameters were applied to the TAN model to evaluate the capability of this tool to effectively represent degradation of growth and cometabolic substrates. These simulations were not intended to represent actual contaminant transport or concentration trends at TAN.

A simplistic TCE pulse model was used to demonstrate that the model was capable of representing degradation of TCE and methane over time. In this model, TCE was added as a concentration to all layers through a simulated injection well during a year-long stress period (SP7). Methane was also added throughout the simulation stress periods to the same simulated injection well. The distribution of TCE was compared to the distribution of a conservative tracer in a subsequent stress period (SP15) to show the relative degradation of the cometabolic substrate. In these simulations, the total mass of TCE decreased to zero after 10,000 days.

Subsequent sensitivity runs were made to evaluate the effect of variations in growth and cometabolic substrate specific rate coefficients. A five-fold increase in the TCE specific rate coefficient resulted in up to a 30% decrease in mass of TCE. A five-fold increase in the methane specific rate coefficient resulted in an order of magnitude decrease in the mass of methane. A 10-fold increase in biomass concentration resulted in a large increase in TCE degradation, with the mass totally degraded within 5,000 days. A five-fold increase in the growth substrate half-saturation coefficient (K_{sg}) resulted in a much reduced degradation rate, with TCE remaining at the end of the 23,000-day modeling run.

In this study, the RT3D competitive inhibition kinetics module produced observable TCE degradation. Based on these results, this module appears to be capable of representing simulation of competitive inhibition kinetics in a three-dimensional transient transport model.

3.6 Simulation of TCE Transport at TAN Using First-Order Kinetics

This section describes simulation of a TCE plume using a first-order kinetic model. The first part of this section describes estimation of a TCE degradation half-life based on recent monitoring data from the TAN plume. The second part discusses simulation of a TCE plume using a range of half-life values.

3.6.1 Recalculation of TCE Half-Life

3.6.1.1 *Tracer-Corrected Method*

The tracer-corrected method (Sorenson et al., 2000) was used to recalculate the half-life of TCE in groundwater at TAN using recently collected water-chemistry data. Tritium was selected as the tracer for the tracer-corrected method because it is transported conservatively in water and measured tritium concentrations in groundwater can be corrected to account for radioactive decay that occurred after disposal.

Tritium and TCE concentration data were available from six monitoring wells at TAN during 2009. These wells consisted of TAN-44, TAN-33, TAN-51, TAN-54, TAN-52, and GIN-4. A total of 11 tritium and TCE samples were collected and analyzed from these wells during several 2009 sampling events.

3.6.1.2 *Tritium Decay Correction*

In the tracer-corrected method, measured tritium concentrations were first corrected to account for radioactive decay. Decay-corrected tritium concentrations were calculated using the following equation:

$$C_o = C / \text{EXP}(DF_{\text{trit}} \times T_T), \quad \text{Equation 3-8}$$

where

- C_o = corrected tritium concentration
- C = measured tritium concentration in a downgradient well
- DF_{trit} = Tritium decay factor of -1.55E-04
- T_T = estimated travel time.

Groundwater travel time was estimated by dividing the distance from the TSF-05 source term to the downgradient monitoring well by the groundwater velocity (V_{gw}). For this problem, travel time was calculated using three velocity estimates. The first estimate of 0.11 m/d was calculated by Sorenson et al. (2000). Two bounding estimates were based on the assumptions that the tritium plume extent in 2009 was located between wells TAN 52 and TAN IDHW-7 and that first tritium release to TSF-05 occurred in 1953. The lower velocity estimate of 0.098 was estimated assuming that tritium had just reached well TAN 52 in 2009. The higher estimate of 0.125 m/d was estimated assuming that the tritium breakthrough had reached well TAN IDHW-7 in 2009. The distance of monitoring wells downgradient from well TSF-05, estimated time of travel from the source term to the well for the range of assumed groundwater velocities, measured 2009 tritium concentrations, and decay-corrected tritium concentrations are shown in Table 3-10.

3.6.1.3 Determination of Decay Coefficient and TCE Half-Life

The ratio of the TCE concentration to the decay-corrected tritium concentration was then calculated for each of the analytical results in the data set. Table 3-11 presents measured 2009 TCE concentrations in groundwater from TAN wells, the ratio of concentrations of TCE to decay-corrected tritium, and the natural log of the concentration ratios for the assumed range of groundwater velocities.

The natural logs of concentration ratios were then plotted arithmetically against the distance from the source term and a best-fit trend line was constructed. The data set included concentration data that were flagged as UJ, indicating that concentrations were not detected in the sample above the reporting limit and that the estimated value was between the method detection limit and the reporting limit. Consequently, plots were constructed to include the entire data set and a data set that excluded those UJ flagged concentrations. Plots and linear trend lines constructed for the range of reasonable groundwater velocities are shown on Figures 3-22 through 3-24. Trend lines for the range of groundwater velocities are similar, with slopes changing slightly, as noted in the trend-line equations.

The TCE half-life was determined using the following equation:

$$\text{TCE } \frac{1}{2} \text{ life} = \ln 2 / \lambda \quad \text{Equation 3-9}$$

where

$$\lambda = \text{TCE decay coefficient.}$$

The TCE decay coefficient (λ) was calculated by multiplying the negative slope of the trend lines shown in Figure 3-22 by the groundwater velocity. Table 3-12 presents the trend-line slope, TCE decay coefficient, and TCE half-life for each of the velocity estimates and for each of three the data sets.

Table 3-10. Determination of the decay-corrected tritium concentration for the range of groundwater velocities, 2009 data set.

Date	Well	Distance (m)	Time (days)			Tritium Concentration (pCi/L)	Decay-Corrected Tritium Concentration (pCi/L)		
			Groundwater Velocity = 0.098 m/d	Groundwater Velocity = 0.11 m/d	Groundwater Velocity = 0.125 m/d		Groundwater Velocity = 0.098 m/d	Groundwater Velocity = 0.11 m/d	Groundwater Velocity = 0.125 m/d
1/14/2009	TAN 44	381	3,888	3,464	3,048	1,270	2,324	2,176	2,039
4/15/2009	TAN 44	381	3,888	3,464	3,048	1,610	2,946	2,758	2,585
1/14/2009	TAN 33	381	3,888	3,464	3,048	849	1,553	1,454	1,363
4/15/2009	TAN 33	381	3,888	3,464	3,048	830	1,519	1,422	1,333
1/14/2009	TAN 33	381	3,888	3,464	3,048	1,050	1,921	1,799	1,686
4/15/2009	TAN 33	381	3,888	3,464	3,048	1,020	1,866	1,747	1,638
5/19/2009	TAN 51	1,402	14,307	12,746	11,217	682	6,300	4,943	3,898
5/18/2009	TAN 54	1,402	14,307	12,746	11,217	725	6,697	5,255	4,143
5/18/2009	TAN 54	1,402	14,307	12,746	11,217	834	7,704	6,045	4,766
5/18/2009	TAN 52	2,012	20,527	18,288	16,093	288	6,995	4,939	3,512
5/19/2009	GIN 4	2,560	26,126	23,276	20,483	239	13,855	8,897	5,764

Table 3-11. Computation of the natural log of the ratio of TCE to tritium concentrations, 2009 data set.

Date	Well	Distance (m)	TCE Concentration (µg/L)	Ratio of TCE to Tritium Concentrations			Natural Log of the Ratio of TCE to Tritium		
				Groundwater Velocity = 0.098 m/d	Groundwater Velocity = 0.11 m/d	Groundwater Velocity = 0.125 m/d	Groundwater Velocity = 0.098 m/d	Groundwater Velocity = 0.11 m/d	Groundwater Velocity = 0.125 m/d
1/14/2009	TAN 44	381	122	5.24E-02	5.60E-02	5.97E-02	-2.948418264	-2.882510212	-2.817920321
4/15/2009	TAN 44	381	101	3.43E-02	3.66E-02	3.90E-02	-3.373908776	-3.308000724	-3.243410833
1/14/2009	TAN 33	381	120	7.71E-02	8.24E-02	8.79E-02	-2.562292796	-2.496384744	-2.431794853
4/15/2009	TAN 33	381	83	5.49E-02	5.86E-02	6.26E-02	-2.902128669	-2.836220618	-2.771630727
1/14/2009	TAN 33	381	120	6.24E-02	6.66E-02	7.11E-02	-2.774779053	-2.708871001	-2.644281111
4/15/2009	TAN 33	381	84	4.52E-02	4.83E-02	5.15E-02	-3.095919096	-3.030011044	-2.965421153
5/19/2009	TAN 51	1,402	104	1.65E-02	2.10E-02	2.67E-02	-4.103937044	-3.861395413	-3.623704615
5/18/2009	TAN 54	1,402	182	2.72E-02	3.46E-02	4.39E-02	-3.605463253	-3.362921622	-3.125230824
5/18/2009	TAN 54	1,402	189	2.45E-02	3.13E-02	3.97E-02	-3.707784673	-3.465243042	-3.227552243
5/18/2009	TAN 52	2,012	45.7	6.53E-03	9.25E-03	1.30E-02	-5.030811897	-4.682817382	-4.341782758
5/19/2009	GIN 4	2,560	11.9	8.59E-04	1.34E-03	2.06E-03	-7.059861152	-6.616959043	-6.182914976

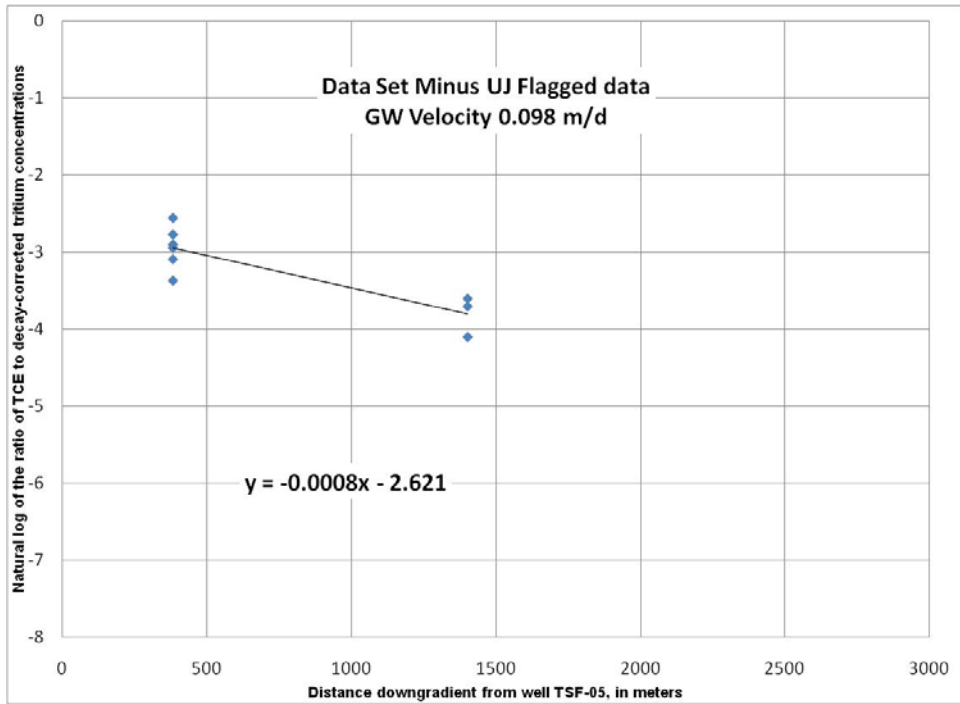
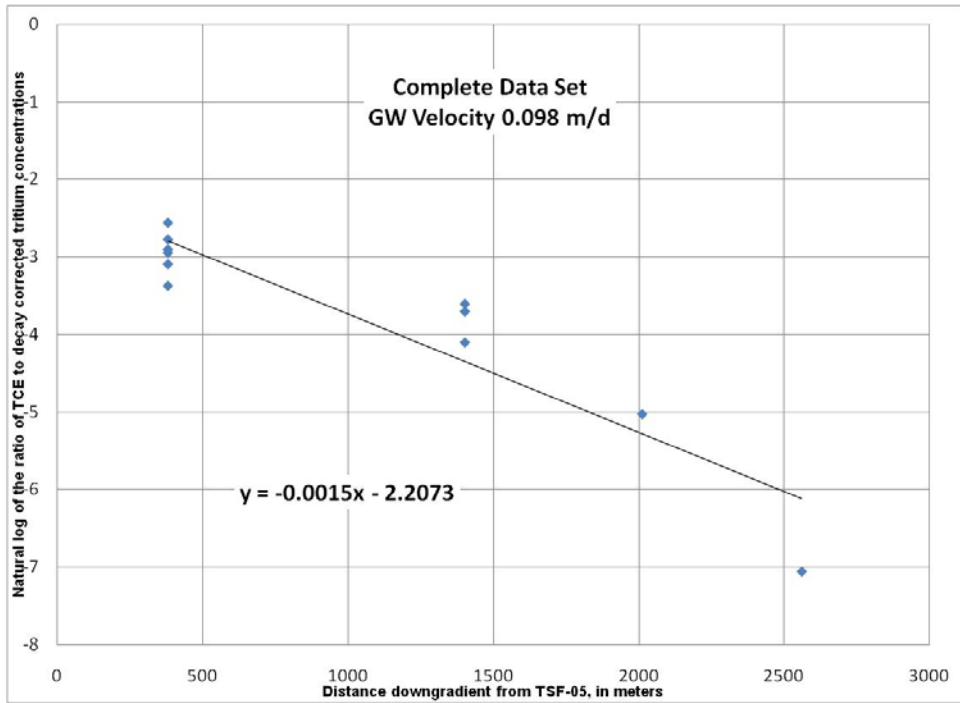


Figure 3-22. Plots of the natural log of the ratio of TCE to tritium concentrations with distance downgradient from the TSF-05 injection well for an assumed groundwater velocity of 0.098 m/d for the complete data set and the data set minus samples with UJ flags.

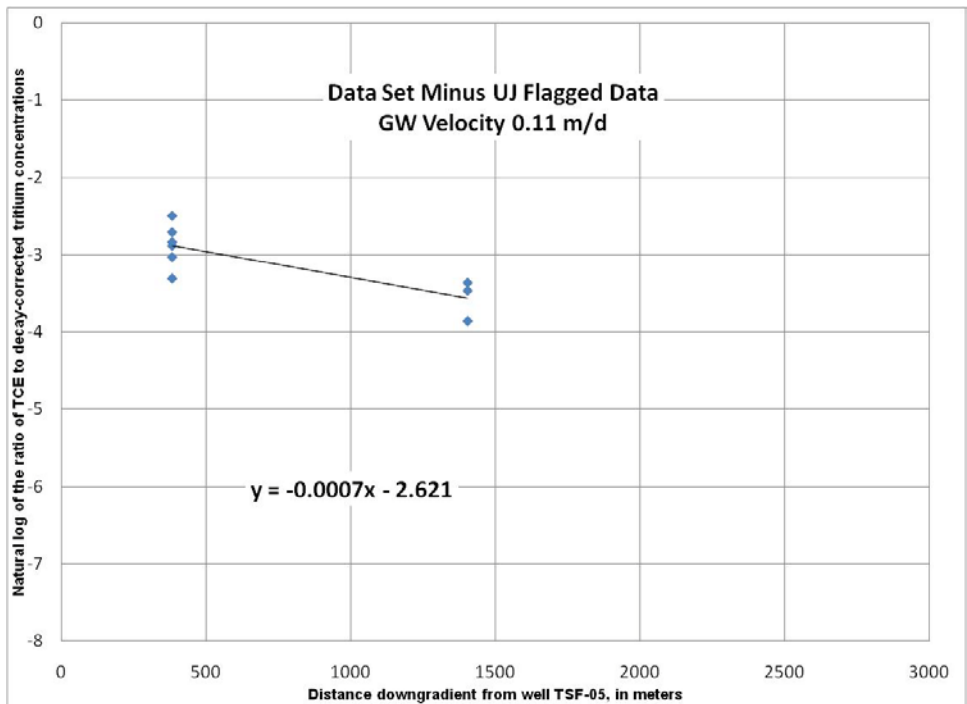
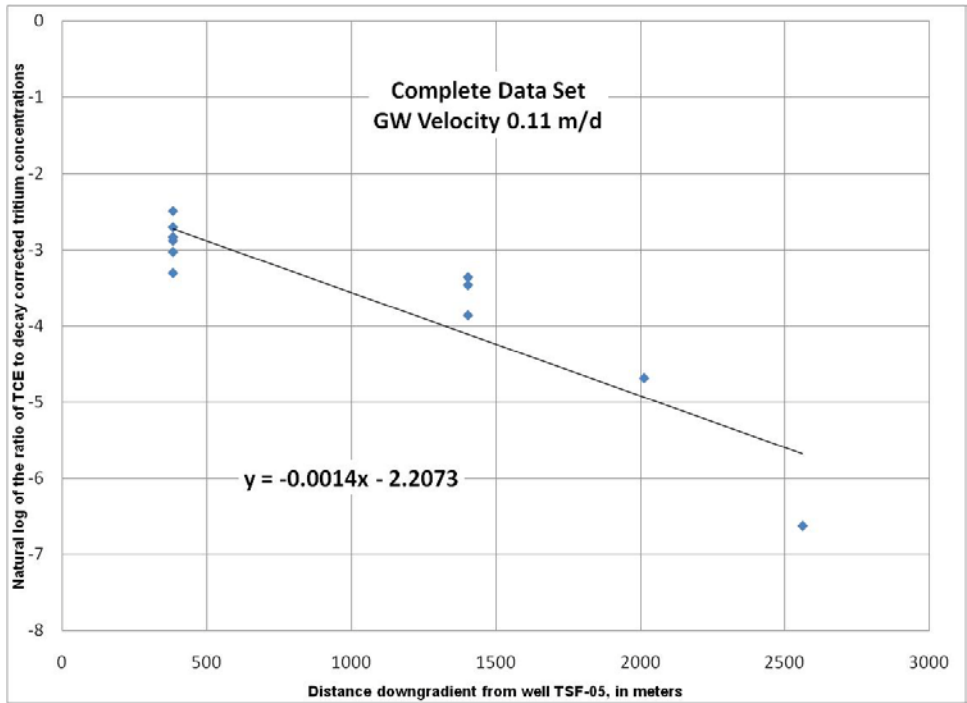


Figure 3-23. Plots of the natural log of the ratio of TCE to tritium concentrations with distance downgradient from the TSF-05 injection well for an assumed groundwater velocity of 0.11 m/d for the complete data set and the data set minus samples with UJ flags.

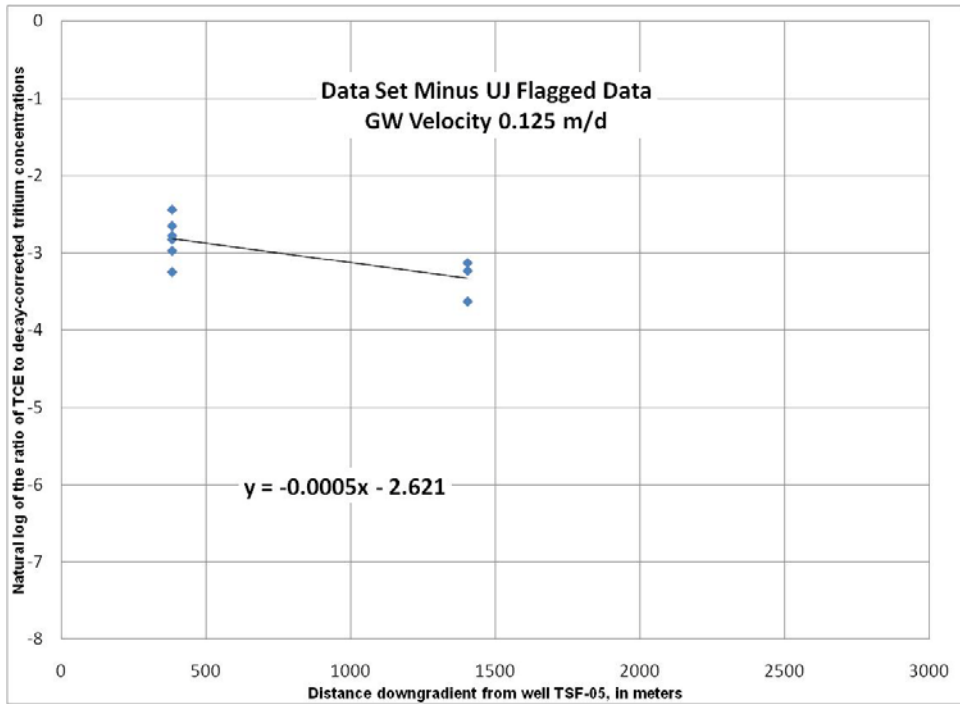
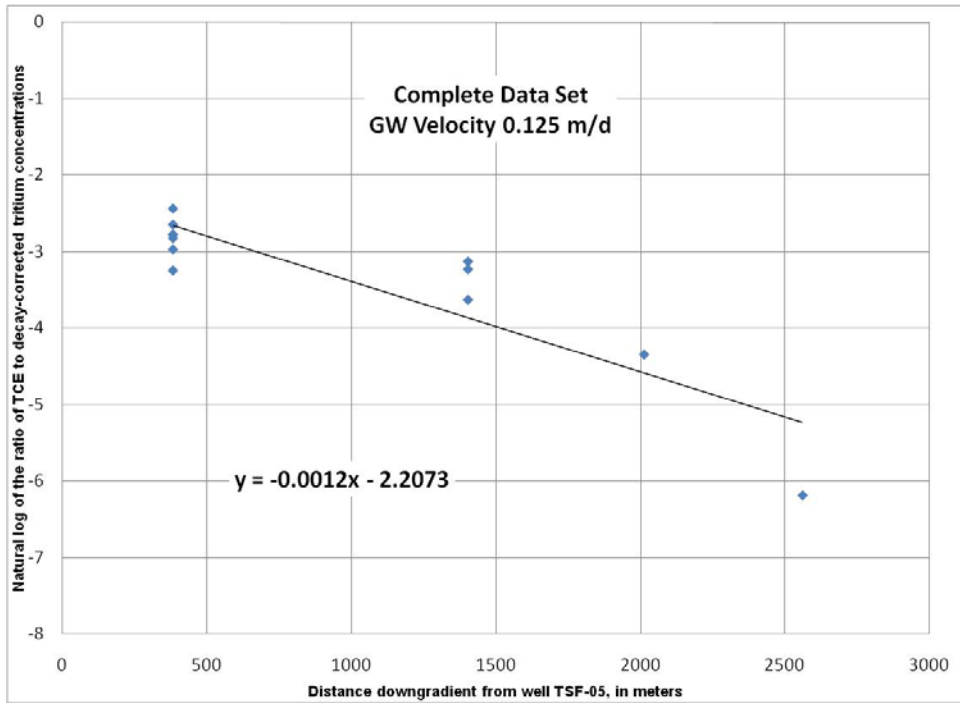


Figure 3-24. Plots of the natural log of the ratio of TCE to tritium concentrations with distance downgradient from the TSF-05 injection well for an assumed groundwater velocity of 0.125 m/d for the complete data set and the data set minus samples with UJ flags.

Table 3-12. Determination of TCE half-life for the range of acceptable groundwater flow velocities.

	Slope of Concentration Distance Plots (1/m)	Groundwater Velocity (m/d)	TCE Decay Coefficient, λ (negative slope times velocity) (1/days)	TCE Half-Life (days)	TCE Half-Life (years)
Velocity of 0.098 m/d					
Complete 2009 TCE and tritium data set	-0.0015	0.098	1.47E-04	4,715	12.9
TCE and tritium data set minus UJ flagged data	-0.0008	0.098	7.84E-05	8,841	24.2
Velocity of 0.11 m/d					
Complete 2009 TCE and tritium data set	-0.0014	0.11	1.54E-04	4,501	12.3
TCE and tritium data set minus UJ flagged data	-0.0007	0.11	7.70E-05	9,002	24.7
Velocity of 0.125 m/d					
Complete 2009 TCE and tritium data set	-0.0012	0.125	1.50E-04	4,621	12.7
TCE and tritium data set minus UJ flagged data	-0.0005	0.125	6.25E-05	11,090	30.4

The TCE decay coefficient (λ) was calculated by multiplying the groundwater velocity by the negative slope of the concentration ratio plot trend lines. The TCE half-life was then determined by dividing the natural log of 2 by λ . Table 3-12 presents the calculated half-life for TCE for the range of estimated groundwater velocities at TAN. The half-life estimates for the complete data set range from 12.3 to 12.9 years.

3.6.2 Simulation of TCE Transport with First-Order Decay Kinetics

A numerical model of groundwater flow and contaminant transport was constructed using (INEEL 1999) as part of remediation activities at the INL TAN. The original numerical transport model was constructed using the TETRAD code (ADA International Consulting Ltd., Calgary, Canada). This model subsequently was converted to MODFLOW and MT3D codes on the GMS platform.

The TAN model grid consisted of 66 rows, 62 columns, and 16 layers and represented an area of approximately 70 km² of the eastern Snake River Plain surrounding TAN. The numerical model was bounded by specified head boundaries. Recharge cells were used to represent infiltrating wastewater disposed to the TSF-07 pond. A point source was used in row 21, column 21 and layers 1 through 15 to represent wastewater and TCE injections to the aquifer during 1955-1972 from well TSF-05. The transient model was run for 97 stress periods to represent the 63-year time interval beginning in 1949. Disposals to the well were represented by transient flow rates and TCE concentrations.

This numerical model was used in the current study to evaluate sensitivity of TCE transport and distribution to a range of TCE half-lives, as determined from the 2009 data set. Model simulations were not intended to accurately represent distribution of TCE in TAN groundwater. The purpose of these runs was solely to evaluate the sensitivity of numerically derived TCE concentrations to the reasonable range of TCE half-life estimates. Numerical model runs were made for TCE half-lives of 12.3, 12.7, and 12.9 years, respectively.

Figure 3-25 presents the extent of the TCE plume in model layer 15 after 20, 40, and 60 years for each of the simulated TCE half-lives. These half-lives were determined using a reasonable range of groundwater velocities that were derived from the probable first arrivals of tritium at the downgradient plume margin. The narrow range of TCE half-lives resulted in small differences in areal distribution. For example, for the 60-year distribution, the difference in longitudinal extent of the TCE plume was approximately half of a cell width (50 m) between the 12.3-year half-life and the 12.9-year half-life simulations.

The narrow range of TCE half-lives as determined from 2009 TCE and decay-corrected tritium data resulted in a limited assessment of the simulation sensitivity to changes in TCE half-life. To better evaluate this sensitivity, a wider range of half-life values was derived from Sorenson et al (2000). TCE half-life determined using decay-corrected tritium concentrations from that more extensive data set was 13 years, with a 95% confidence interval that ranged from 11 to 17 years. Simulations were run for this larger range.

The extents of the resulting TCE plume in layer 15 after 20 years, 40 years, and 60 years as derived from 11-, 12.3-, and 17-year TCE half-lives are presented in Figure 3-26. In this figure, the blue shaded area represents concentrations between 0.0005 and 1 mg/L, the yellow shaded area represents concentrations between 1 and 20 mg/L, and the red shaded area represents concentrations exceeding 20 mg/L. The plume extent after 60 years for the 17-year half-life is approximately 150 m longer than that for the 11-year half-life. The plume area exceeding 20 mg/L is significantly elongated for the 17-year half-life. After 60 years, the total simulated mass in the 11-year half-life TCE plume (45 kg) was approximately 39% of the simulated TCE mass in the 17-year half-life plume (114 kg).

3.6.3 First-Order Decay Kinetics Conclusions

The tracer-corrected method was used to calculate the half-life of TCE from 2009 TAN analytical data. This calculation was based on the groundwater velocity of 0.11 m/d as determined from Sorenson et al (2002) and on bounding groundwater velocities of 0.98 and 0.125 m/d. Based on the range of estimated groundwater velocities, the TCE half-life ranged from 12.3 to 12.9 years.

Numerical simulations of the TAN model were run using the calculated half-lives. These simulations resulted in small changes in TCE plume extent (approximately 50 m).

A wider range of half-lives was used to more clearly demonstrate the effect of first-order kinetics rates on the TCE plume extent. This range was derived from previous studies and represented a 95% confidence interval that ranged from 11 to 17 years. This range of half-lives resulted in easily observable differences in plume extent and in simulated contaminant mass. After 60 years, the estimated mass of TCE for the 11-year half-life simulation was approximately 39% of the mass for the 17-year half-life simulation.

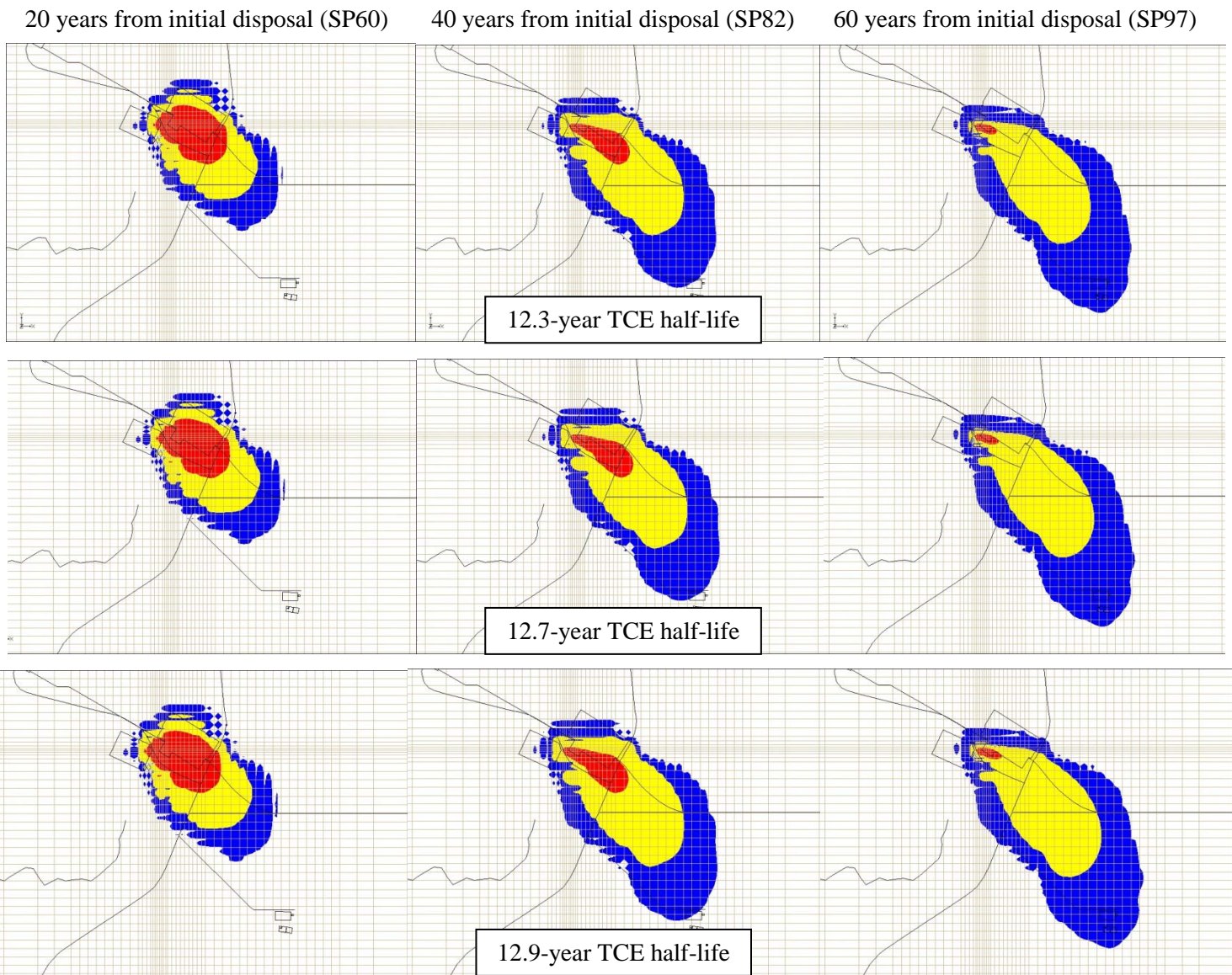


Figure 3-25. Extent of TCE plume in layer 15 after 20 years (SP60), 40 years (SP82), and 60 years (SP97) using 12.3-, 12.7-, and 12.9-year TCE half-lives.

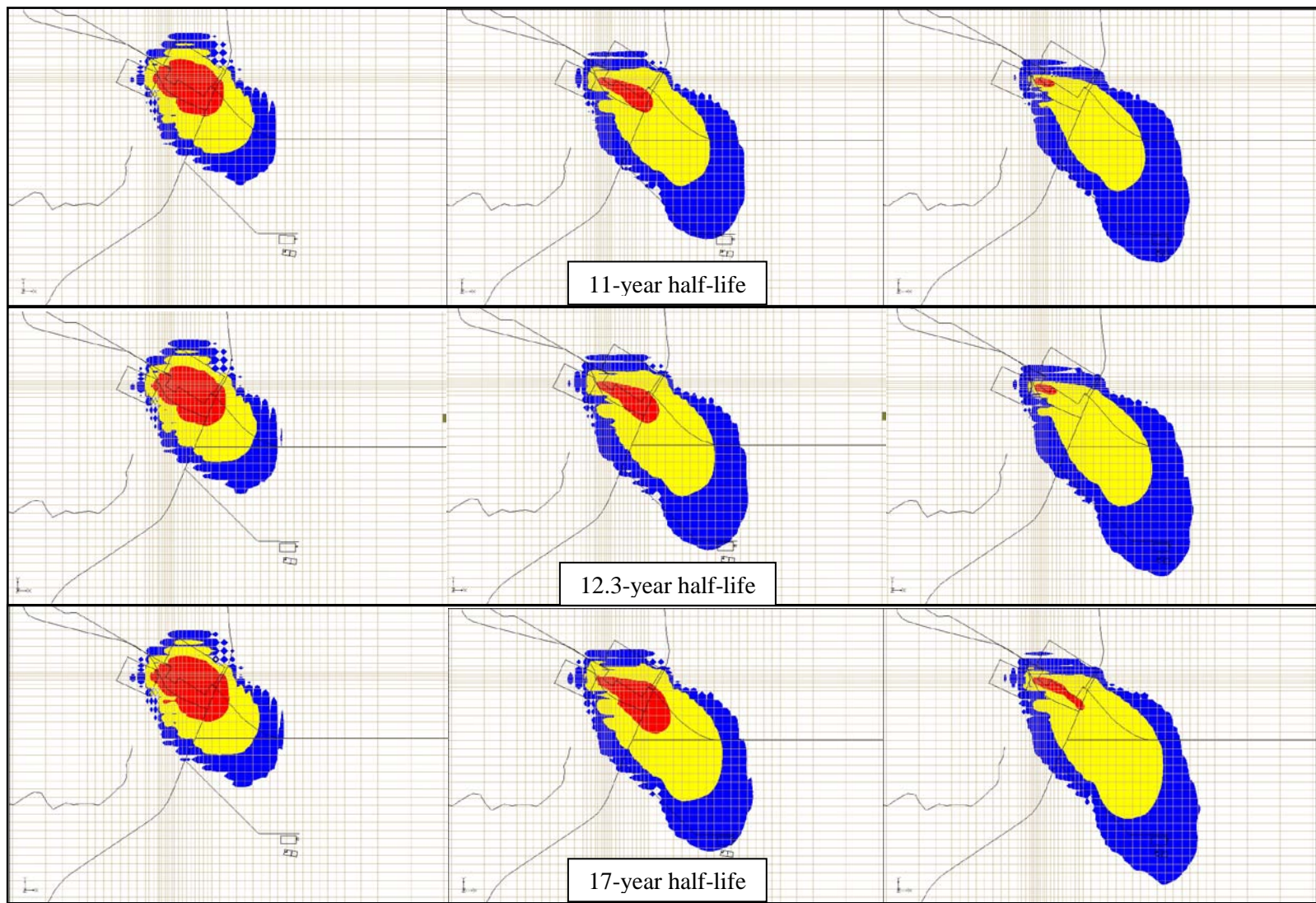


Figure 3-26. Comparison of the TAN TCE plume extent after 20, 40, and 60 years simulated using 11-, 12.3-, and 17-year TCE half-lives.

3.7 Summary and Conclusions

The results of the modeling study can be summarized as follows:

- A competitive inhibition kinetic model with a low DO inhibition term was studied.
- A wide range of numerical values for parameters is available in the published literature.
- A parametric study for a batch reactor illustrates the effect of each parameter on reaction rate as a function of concentration, and on temporal concentration trends.
- Selecting parameter values from the literature and measured biomass, methane, and TCE concentrations that result in maximum and minimum reaction rates produces a range of reaction rates and temporal concentration trends that span several orders of magnitude. This indicates that the range of literature values is so wide that site-specific values will be needed to perform meaningful predictions of plume evolution.
- For some reasonable combination of parameter values, the competitive inhibition kinetic model is approximately equivalent to a first-order model.
- Given that a competitive inhibition model is much more difficult to parameterize than a first order model, and that plumes in which natural attenuation is an important process may be in the first order kinetic range, it is not clear that the added complexity of the competitive inhibition model is justified for simulating naturally-attenuating plumes. Nevertheless, a competitive inhibition kinetics module was developed for the reactive transport code, RT3D, and has been made publically available.
- Simulations of plume behavior using the competitive inhibition kinetics module show that the module works as expected.
- First order half-life values for TCE degradation in a plume where TCE is naturally attenuating estimated using recent water chemistry data are similar to values estimated by previous workers.
- Plume simulations using the range of half-life values estimated here and by previous workers show a moderate range in plume evolution, more so in the portions of the plume where concentrations are higher than in the low concentration portion of the plume.
- Defensible methods for determining in situ degradation half-life values would improve our ability to make credible and defensible predictions of plume evolution.

4. INCIDENTAL SUPPORT OF FLOW-THROUGH IN SITU REACTOR STUDIES

A system of FTISRs was designed for testing hypotheses regarding microbial transformation of chlorinated solvents in the contaminant plume at TAN. The system was designed to provide controlled circulation of ground water through containers of crushed basalt, and was subsequently modified to allow introduction of electron donors and acceptors into the liquid stream, and to provide for liquid and gas sampling. Conceptually the system was to mimic actual in situ conditions as closely as possible. Initially it was to be mounted at land surface near the chosen study well (TAN 35), water would be circulated out of the well, through the system, and back into the ground or into an air stripper according to the environmental space (ft below land surface [bls]) regulations governing that site. However, due to regulatory constraints, the difficulty of controlling reactor temperature at land surface, and other logistical obstacles, it was decided to design a system for installation entirely within the well. TAN 35 is a 12-in. borehole with 8 in. casing to 195 ft, and below that 8 in. uncased bore to a total depth of 420 ft bls. At the start of in situ experiments, water level was 218 ft bls and when the system was removed in September of 2009, water stood at 226 ft bls. According to tests completed after this well was completed in 1997, the bore penetrates basalt formations that are fairly impermeable and have a zone of high permeability at 310 ft bls.

Over the course of the program, two FTISR systems were used; one that was installed in 2006 to 2007 and the second from 2008 to 2009. Both systems used type 3041 stainless steel reactors 5.95 cm inside diameter \times 100 cm long with internal volume of 2,800 cc (Figure 4-1). Both employed a simple pneumatic pumping system for circulating water through reactors; otherwise, to accommodate changes in experimental plans, plumbing configurations of the two systems differed significantly.

4.1 Construction and Operation

The loop pumping system used in both years is illustrated in Figure 4-2. It consists of a pneumatic line that extends from compressed nitrogen cylinders and cycle timer at land surface to the top of each reactor. Below water on each line and above each reactor is a large diameter section of tubing to provide increased volume above a tee branch that extends back up the well bore out of the water. Below the tee is a check valve oriented to allow circulation up through the reactor. During a pump cycle, pressure is provided through the cycle timer. Gas pressure downward pushes water out of the expanded loop volume. The check valve prevents movement down through the reactor, so water is forced through the tee and back up the well bore to discharge just above water. When pressure is released by the cycle timer the loop and expanded volume hydrostatically refill through the reactor inlet.

The first year system (Figure 4-3) consisted of a string of six FTISR vessels connected together like a string of sausages and suspended on a steel cable. Each reactor had its own pneumatic line and loop pump. Discharge from the pumps terminated 2 ft above water. All plumbing was flexible 1/4-in. polyethylene tubing. This system had no provision for delivering water to land surface. Two cycle timers were used, three reactors connected to one and three to the other. This allowed for two different flow rates in order to test a hypothesis that flow rate is a significant factor in microbial colonization of basalt in the system. Based on the expanded pump loop volume and cycle frequency, groundwater circulated through three reactors at 0.1 m/d (low flow) and at 1 m/d through the other three (high flow). The first year system was suspended with pump loops bundled and the tee's 10 ft (high flow) and 5 ft (low flow) below the water level (218 ft bls), the top reactor was situated at 233 ft bls, and the bottom at 260 ft bls. System inlet for all six reactors was situated in the higher permeability zone at 310 ft bls.

The second year system (Figure 4-4) was significantly modified from the first year system in an attempt to expand functionality: To provide for sampling during operation each reactor was fitted with a line returning from the loop tee to land surface; each reactor was fitted with a separate line for making additions, such as electron donor, from land surface; and a separate loop was added for taking water samples directly from the aquifer without passing through a reactor. Only one cycle timer and three reactors were used, so all reactors operated at the same flow rate of 1 m/d. Because the intention for the second installation was to directly monitor TCE and its derivatives, which very readily penetrate plastics, all sample and pump loop tubing had to be stainless steel. Also, because the second year experimental plan proposed introduction of xenic compounds to the reactors, due to regulatory considerations manually operated shut-off valves were required on each reactor and on the aggregate system inlet from the aquifer. A pneumatic valve system had to be provided to switch circulating pump loop water from discharge just above water level to delivery at land surface. These second year modifications required additional hardware for valve operation and routing: A fourth FTISR shell was modified to hold the shut-off valve mechanism, and a pneumatic valve carrier was mounted above the reactor string so that it would be suspended out of the water and just below the bottom of the 8-in. casing. The modified system was many times heavier than that of year one, and a boom truck and crew, in place of a hydraulic pump reel, had to be used for installation and removal.

4.2 Discussion

The first year system worked flawlessly. After 8 months, the reactors were recovered and their contents distributed to the participating labs for analyses. The second year system also functioned well on basic function, and basalt chips were recovered as in year one. However, sampling and additive injection were not completed. Although all parts of the system seemed to function as designed, water delivered to the surface was badly mixed with nitrogen gas used for pneumatic operation thus rendering samples useless for the purposes they were intended. The cause of this failure is not known. Although sampling was not part of year one operation, the same system as year one had been used on another project unrelated to this one. The pumping and sample system worked very well in that application. It may be that the greater depth to water at TAN (220 ft compared with 145 ft in the other) allowed more time gasification of water as it rose to the surface. Possibly metal surface effects are at fault; only plastic tubing was used in the other project. Also, water level dropped significantly during the second year (220 to 226 ft). This was not unanticipated, and the second system was installed with several feet of margin. Nevertheless, it did appear as though some if not all of the added volume loops were at least partially dry. Given the procedural delays involved, winter weather conditions, and considerable cost of mobilizing a second rig, repositioning the system after installation was not an option.

The FTISR assembly was removed from Well TAN 35 in October 2009, and the basalt chips were colonized by microorganisms from groundwater pumped through the columns. The colonized basalt chips were used in a microcosm study (described in Section 2) designed to measure TCE and methane kinetics.

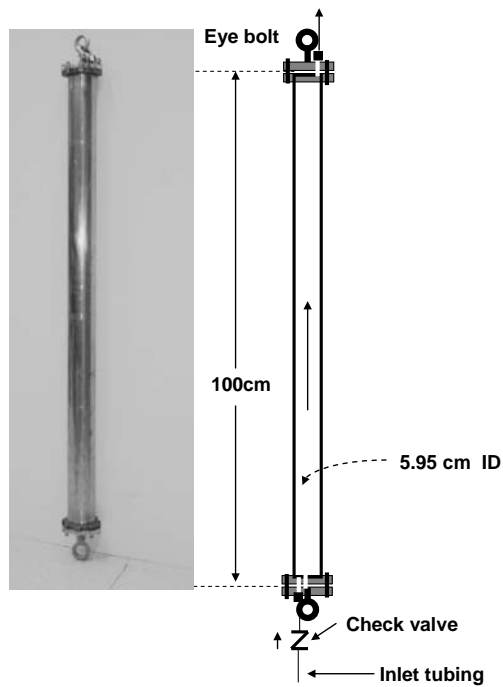


Figure 4-1. FTISR design and dimensions.

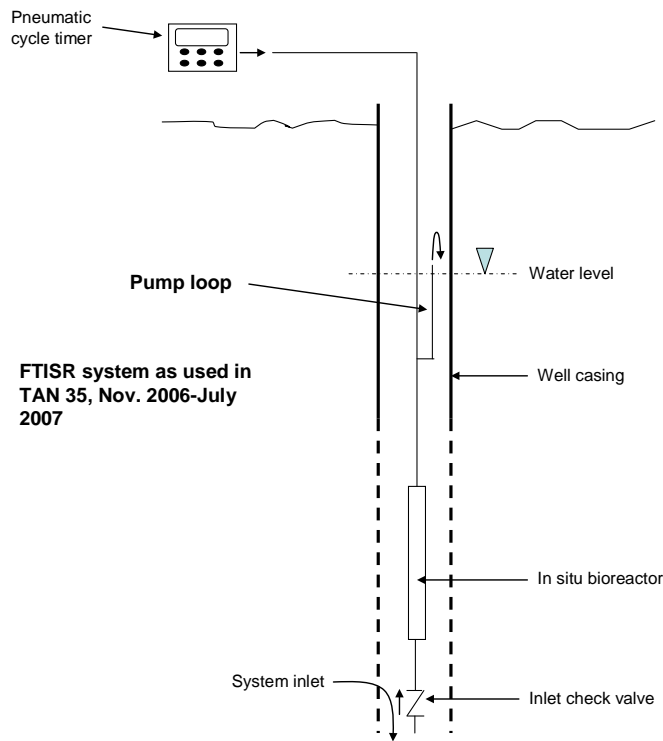


Figure 4-2. Schematic of pneumatic pump system used in both years.

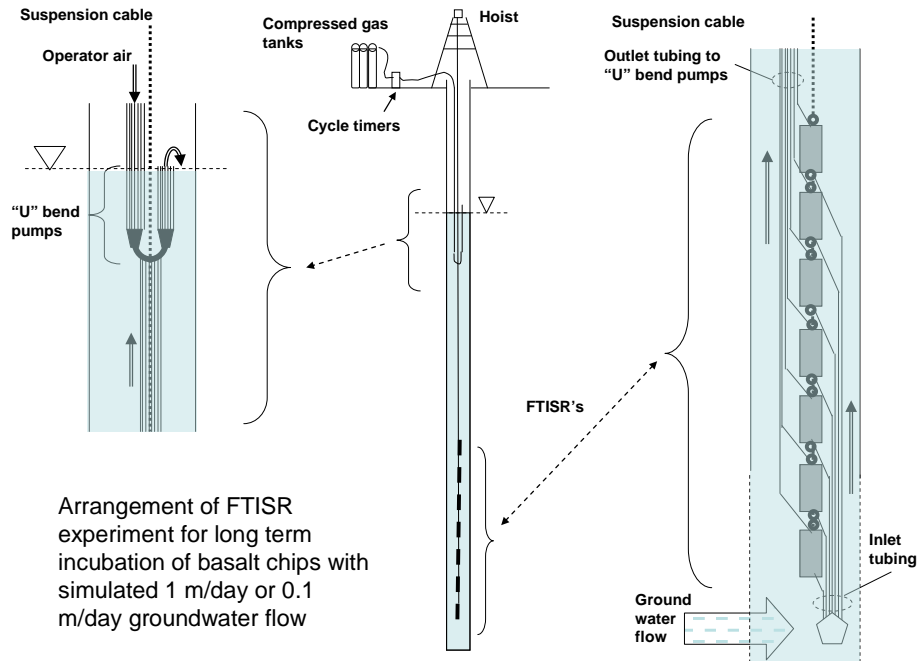


Figure 4-3. Operation schematic for first year system.

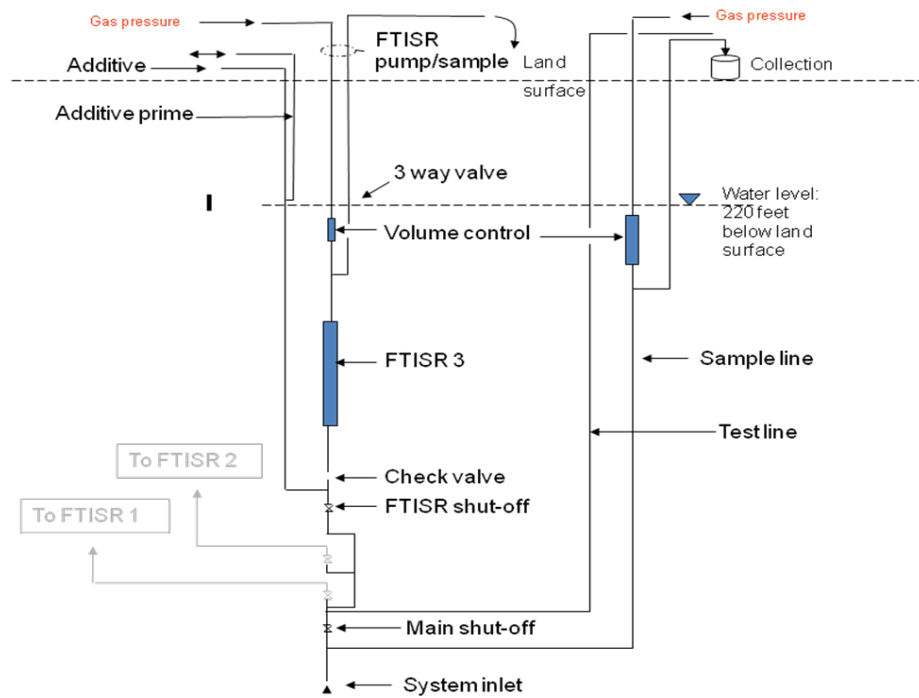


Figure 4-4. Operation schematic for second year system.

5. REFERENCES

- Alvarez-Cohen, L., and P.L. McCarty, 1991, "A Cometabolic Biotransformation Model for Halogenated Aliphatic Compounds Exhibiting Product Toxicity," *Environmental Science and Technology*, 25:1381-1387.
- Alvarez-Cohen, L., and G.E. Speitel Jr., 2001, "Kinetics of Aerobic Cometabolism of Chlorinated Solvents," *Biodegradation*, 12:105—126.
- Anderson, J.E., and P.L. McCarty, 1996, "Effect of Three Chlorinated Ethenes on Growth Rates for a Methanotrophic Mixed Culture," *Environmental Science and Technology*, 30:3517-3524.
- Arp, D.J., C.M. Yeager, and M.R. Hyman, 2001, "Molecular and Cellular Fundamentals of Aerobic Cometabolism of Trichloroethylene," *Biodegradation*, 2:81-103.
- Balkwill, D. L., F. R. Leach, J. T. Wilson, J. F. McNabb, and D. C. White, 1988, "Equivalence of Microbial Biomass Measures Based on Membrane Lipid and Cell Wall Components, Adenosine Triphosphate, and Direct Counts in Subsurface Aquifer Sediments," *Microbial Ecology*, 16:73–84.
- Chang, H-L., and L. Alvarez-Cohen, 1995, "Transformation Capacities of Chlorinated Organics by Mixed Cultures Enriched on Methane, Propane, Toluene, or Phenol," *Biotechnology and Bioengineering*, 45:440-449.
- Chang, W-K., and C.S. Criddle, 1997, "Experimental Evaluation of a Model for Cometabolism: Prediction of Simultaneous Degradation of Trichloroethylene and Methane by a Methanotrophic Mixed Culture," *Biotechnology and Bioengineering*, 56:492-501.
- Clingenpeel, S.R., W.K. Keener, C.R. Keller, K. De Jesus, M.H. Howard, and M.E. Watwood, 2005, "Activity-Dependent Fluorescent Labeling of Bacterial Cells Expressing the TOL Pathway," *Journal of Microbiological Methods*, 60:41-46.
- Colwell, F.S. (Oregon State University), personal communication with R.C. Starr (North Wind), August 6, 2009, "Methanotropic and Other Bacteria."
- DOE et al., 1995, *Record of Decision – Declaration for the Technical Support Facility Injection Well TSF-05) and Surrounding Groundwater Contamination (TSF-23) and Miscellaneous No Action Sites – Final Remedial Action*, U.S. Department of Energy, U.S. Environmental Protection Agency, and Idaho Department of Health and Welfare – Division of Environmental Quality, August 4.
- DOE et al., 2001, *Record of Decision Amendment – Technical Support Facility Injection Well TSF-05) and Surrounding Groundwater Contamination (TSF-23) and Miscellaneous No Action Sites – Final Remedial Action*, U.S. Department of Energy, U.S. Environmental Protection Agency, and Idaho Department of Environmental Quality, September.
- Goltz, M.N., E. J. Bouwer, and J. Huang, 2001, "Transport Issues and Bioremediation Modeling for the In Situ Aerobic Cometabolism of Chlorinated Solvents," *Biodegradation*, 12: 127-140.

- Gossett, J.M., C.E. Cameron, B.P. Eckstrom, C. Goodman, and A.F. Lincoff, 1985, *Mass Transfer Coefficients and Henry's Constants of Packed-Tower Air Stripping of Volatile Organics: Measurements and Correlations*, Engineering and Services Laboratory, U.S. Air Force Engineering and Services Center: Tyndall AFB, FL, Report No. ESL-TR-85-18.
- Henry, S.M., and D. Grbic-Balic, 1990, "Effect of Mineral Media on Trichloroethylene Oxidation by Aquifer Methanotrophs," *Microbial Ecology*, 20:151-169.
- Howard-Jones, M.H., V.D. Ballard, A.E. Allen, M.E. Frischer, and P.G. Verity, 2002, "Distribution of Bacterial Activity in the Marginal Ice Zone of the Central Barents Sea During Summer," *Journal of Marine Systems*, 38:77-91.
- INEEL, 1999, *Numerical Modeling Support of the Natural Attenuation Field Evaluation for Trichloroethene at the Test Area North, Operable Unit 1-07B, Idaho National Engineering and Environmental Laboratory*, INEEL/EXT-97-01284, Lockheed Martin Idaho Technologies Company, Idaho Falls, Idaho.
- Kauffman, M.E., W.K. Keener, S.R. Clingenpeel, M.E. Watwood, D.W. Reed, Y. Fujita, and R. M. Lehman, 2003, "Use of 3-Hydroxyphenylacetylene for Activity-Dependent, Fluorescent Labeling of Bacteria That Degrade Toluene Via 3-Methylcatechol," *Journal of Microbiological Methods*, 55:801-805.
- Keener, W.K., and M.E. Watwood, 1997, Probes for Enzyme-Dependent Fluorescent Labeling of Bacteria Degrading Trichloroethylene, in Alleman, B.C. and A. Leeson (eds), *In Situ and On-Site Bioremediation Volume 5*, Proceedings of the *Fourth International In Situ and On-Site Bioremediation Symposium*, Battelle Press, Columbus, Ohio, pp 327-332.
- Keener, W.K., M.E. Watwood, and W.A. Apel, 1998, "Activity-Dependent Fluorescent Labeling of Bacteria that Degrade Toluene Via Toluene 2,3-Dioxygenase," *Applied Microbiology and Biotechnology*, 49:455-462.
- Keener W.K., M.E. Watwood, K.D. Schaller, M.R. Walton, J.K. Partin, W.A. Smith, and S.R. Clingenpeel, 2001, "Use of Selective Inhibitors and Chromogenic Substrates to Differentiate Bacteria Based on Toluene Oxygenase Activity," *Journal of Microbiological Methods*, 46:171-185.
- Lee, M. H., 2007, "Application of Enzyme Activity Probes to Characterize Aerobic Microorganisms in Groundwater at PGDP, INL, and Elsewhere," *Kentucky Research Consortium for Energy and the Environment 2007 Scientific and Technical Symposium*, University of Kentucky, October 30-31 2007.
- Lee, M.H., S.C. Clingenpeel, O.P. Leiser, and M.E. Watwood, 2005, "Molecular and Physiological Characterization of Aerobic TCE Degradation Potential," *Eighth International In Situ and On-Site Bioremediation Symposium*, Battelle Press, Columbus, OH.
- Lee, M.H., S.C. Clingenpeel, O.P. Leiser, R.A. Wymore, K.S. Sorenson, Jr., and M.E. Watwood, 2008, "Activity-Dependent Labeling of Oxygenase Enzymes in a Trichloroethene-Contaminated Groundwater Site," *Environmental Pollution*, 153:238-246.

- Lontoh, S., and J.D. Semrau, 1998, "Methane and Trichloroethylene Degradation by *Methylosinus Trichosporium* OB3b Expressing Particulate Methane Monooxygenase," *Applied and Environmental Microbiology*, 64: 1106-1114.
- Miller, A.R., W.K. Keener, M.E. Watwood, and F.F. Roberto, 2002, "A Rapid Fluorescence-Based Assay for Detecting Soluble Methane Monooxygenase," *Applied Microbiology and Biotechnology*, 58:183-188.
- Radtke et al., 2008, "Coupled Biogeochemical Process Evaluation for Conceptualizing Trichloroethene Cometabolism," 7th International Symposium for Subsurface Microbiology, Shizuoka, Japan, November 16-21.
- Semprini, L., and P.L. McCarty, 1992, "Comparison Between Model Simulations and Field Results for In Situ Bioremediation of Chlorinated Aliphatics: Part 2. Cometabolic Transformations," *Ground Water*, 30:37-44.
- Sorenson, K.S. Jr., L.N. Peterson, R.E. Hinchee, and R.L. Ely, 2000, "An Evaluation of Aerobic Trichloroethene Attenuation Using First-Order Rate Estimation," *Bioremediation Journal*, 4:337-357.
- Speitel, G.E. Jr., R.C. Thompson, and D. Weissman, 1993, "Biodegradation Kinetics of *Methylosinus trichosporium* OB3b at Low Concentrations of Chloroform in the Presence and Absence of Enzyme Competition by Methane," *Water Research*, 27:15-25.
- Starr, R.C., M.C. Koelsch, and K.S. Sorenson, Jr., 2004, *EMSP Annual Report: Coupling of Realistic Rate Estimates with Genomics for Assessing Contaminant Attenuation and Long-Term Plume Containment – Task 4 – Modeling*, NW-ID-2004-062, North Wind Inc., Idaho Falls, ID.
- Wiedemeier, T.H., M.A. Swanson, D.E. Moutous, E.K. Gordon, J.T. Wilson, B.H. Wilson, D.H. Kampbell, P.E. Haas, R.N. Miller J.E. Hansen, and F.H. Chapelle, 1998, *Technical Protocol for Evaluating Natural Attenuation of Chlorinated Solvents in Ground Water*, United States Environmental Protection Agency, Office of Research and Development, Washington, D.C., EPA/600/R-98/128.
- Wymore, R.A., M.H. Lee, A.R. Miller, F.S. Colwell, M.E. Watwood, and K.S. Sorenson, Jr., 2007, "Field Evidence for Intrinsic Aerobic Chlorinated Ethene Cometabolism by Methanotrophs Expressing Soluble Methane Monooxygenase," *Bioremediation Journal*, 11:125-139.

Appendix A

Cometabolic Kinetic Reaction Package for RT3D

Reaction Package to Simulate a Cometary Bioremediation Process

This document describes the details of a RT3D-reaction package that can be used to simulate competitive reactions between methane and TCE. The purpose of the reaction model is to describe a two-species (both mobile species) reactive transport to simulate a cometary bioremediation system that uses methane as the substrate and co-metabolically degrades TCE. The set of two coupled reaction equations solved by the module are:

Growth substrate (methane) reaction equation:

$$\frac{dM}{dt} = r_M = \frac{-k_M [X] [M]}{K_{S_M} \left(1 + \frac{[T]}{K_{S_T}} \right) + [M]} \left[\frac{[O]}{K_{S_O} + [O]} \right] \quad (\text{Equation A-1})$$

Co-metabolic substrate (TCE) degradation reaction equation:

$$\frac{dT}{dt} = r_T = \frac{-[X] k_T [T]}{K_{S_T} \left(1 + \frac{[M]}{K_{S_M}} \right) + [T]} \left[\frac{[O]}{K_{S_O} + [O]} \right] \quad (\text{Equation A-2})$$

where

- r_{Me} = rate of growth substrate (methane) reaction (mg L⁻¹ day⁻¹)
- r_{TCE} = rate of cometary substrate (TCE) reaction (mg L⁻¹ day⁻¹)
- $[X]$ = active cell concentration at a node (mg active cells L⁻¹)
- $[M]$ = Methane (growth substrate) concentration (mg L⁻¹)
- $[T]$ = TCE (cometary substrate) concentration (mg L⁻¹)
- k_M = maximum specific reaction rate for methane degradation (mg growth substrate (mg cells)⁻¹ day⁻¹)
- k_T = maximum specific reaction rate for TCE degradation (mg TCE (mg cells)⁻¹ day⁻¹)
- K_{S_M} = half saturation coefficient for methane (mg L⁻¹)
- K_{S_T} = half saturation coefficient for TCE (mg L⁻¹)
- K_{S_O} = dissolved oxygen concentration at which the relative rate of methane utilization is one half of the maximum rate (mg L⁻¹)
- $[O]$ = dissolved oxygen concentration at node (mg L⁻¹).

Review of literature data indicates that these reactions can be facilitated via two distinct pathways that use to type of enzymes namely particulate methane monooxygenase (pMMO) and soluble methane monooxygenase (sMMO). The reaction rates would depend on the choice of the pathway. Our preliminary simulation results indicate that that pMMO pathway seemed to be faster for the given reaction parameters. Typical reaction parameters used are summarized in Table A-1.

Table A-1. Mean values of biodegradation parameters for PMMO and SMMO pathways.

Parameters	SMMO	PMMO
Kt (day⁻¹)	1	0.15
KSt (mg/L)	2	2.5
km (day⁻¹)	2.5	2.5
KSm (mg/L)	3	0.05
Kso (mg/L)	0.5	0.5

```

c Reaction package for cometabolic reactions (assume fixed amount of biomass)
c Please refer to the RT3D user manual for further details
      SUBROUTINE Rxns(ncomp,nvrndata,j,i,k,y,dydt,
        &      poros,rhob,reta,rc,nlay,nrow,ncol,vrc)
C*Block 1:*****
c List of calling arguments
c ncomp - Total number of components
c nvrndata - Total number of variable reaction parameters to be input via RCT file
c J, I, K - node location (used if reaction parameters are spatially variable)
c y - Concentration value of all component at the node [array variable y(ncomp)]
c dydt - Computed RHS of your differential equation [array variable dydt(ncomp)]
c poros - porosity of the node
c reta - Retardation factor [ignore dummy reta values of immobile species]
c rhob - bulk density of the node
c rc - Stores spatially constant reaction parameters (can dimension up to 100 values)
c nlay, nrow, ncol - Grid size (used only for dimensioning purposes)
c vrc - Array variable that stores spatially variable reaction parameters
C*End of Block 1*****
C*Block 2:*****
c* *Please do not modify this standard interface block*
      !MS$ATTRIBUTES DLLEXPORT :: rxns
      IMPLICIT NONE
      INTEGER ncol,nrow,nlay
      INTEGER ncomp,nvrndata,j,i,k
      INTEGER, SAVE :: First_time=1
      DOUBLE PRECISION y,dydt,poros,rhob,reta
      DOUBLE PRECISION rc,vrc
      DIMENSION y(ncomp),dydt(ncomp),rc(100)
      DIMENSION vrc(ncol,nrow,nlay,nvrndata),reta(ncomp)
C*End of block 2*****
C*Block 3:*****
c *Declare your problem-specific new variables here*
c   INTEGER
c     DOUBLE PRECISION m,t
c     DOUBLE PRECISION x,o,km,kt,ksm,kst,kso
c     DOUBLE PRECISION oxyterm,methterm,tceterm
C*End of block 3*****

```

```

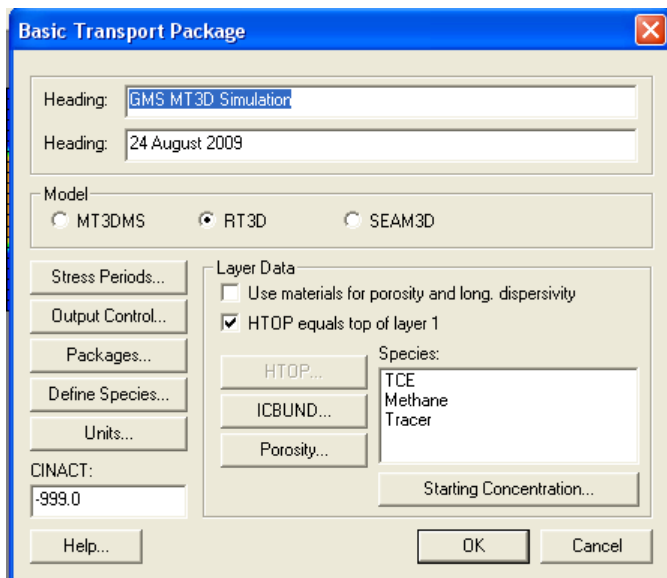
C*Block 4:*****
c  *Initialize reaction parameters here, if required*
c  IF (First_time .EQ. 1) THEN
c    x = .01 !mg/L of biomass
c    o = 0.3 !mg/L of oxygen
c    kso = 0.5 ! mg/L (Oxygen half saturation constant)
c    km = 2.5 ! 1/(mg cells - day) (methane max specific deg. rate)
c    kst = 0.5 ! mg/L (TCE half saturation constant)
c    kt = 0.05 !1/(mg cells - day) (TCE max specific degradation rate)
c    ksm = 0.5 ! mg/L (methane half saturation constant)
c    First_time = 0 !reset First_time to skip this block later
c  END IF
C*End of block 4*****

C*Block 5:*****
c  *Assign or compute values for new variables, if required*
c  m = y(1) !methane
c  t = y(2) !TCE
c  x = vrc(j,i,k,1) !mg/L of biomass
c  o = vrc(j,i,k,2) !mg/L of oxygen
c  kso = vrc(j,i,k,3) ! mg/L (Oxygen half saturation constant)
c  km = vrc(j,i,k,4) !1/mg cells - day) (methane max spec deg. rate)
c  kst =vrc(j,i,k,5) !mg/L(TCE half saturation constant)
c  kt =vrc(j,i,k,6) !1/(mg cells - day) (TCE max specific deg. rate)
c  ksm =vrc(j,i,k,7) ! mg/L (methane half saturation constant)
C*End of block 5*****
C*Block 6:*****
c  *Differential Reaction Equations*
c  oxyterm = o/(kso+o)
c  methterm = 1+(m/ksm)
c  tceterm = 1+(t/kst)
c  dydt(1) =-km*x*m*oxyterm/((ksm*tceterm) + m)
c  dydt(2) = -x*kt*t*oxyterm/((kst*tceterm) + t)
C*End of block 6*****
RETURN
END

```

How to use the new user defined package using GMS

- 1) First copy the special version of the RT3D executable with the new user-defined code, or the general RT3D version with appropriate DLL the folder from where RT3D is run from, typically C:\Program Files\GMS 6.5\models\rt3d\.
- 2) Go to GMS' Edit pull down menu (second one) and select Preferences, Models and point your RT3D to this executable file. Note you can also place the executable at another place of your choice and then appropriately set the preferred location.
- 3) Develop your MODFLOW model for the site.
- 4) After testing your flow simulations, start creating the RT3D input files in GMS. Select user defined package as your reaction package, after clicking the packages button. Then click on "define species" button to create three species namely, TCE, Methane, and Tracer (as shown below). Continue inputting relevant information.



- 5) Under chemical reaction package module, click on define parameters and then name seven parameter as shown in the screen (keep them in the same order). Make sure you check on the spatially variable option button when you create the parameter names (this will allow you to vary the parameter on a cell by cell basis and you must select this option). Continue inputting the relevant data and save your file and you are then ready to run.

